UDC 624.071.2 : 624.916.3

Paper to be read before the Institution of Structural Engineers at 11 Upper Belgrave Street, London SW1X 8BH, on Thursday 10 April 1975

Timber lattice roof for the Mannheim Bundesgartenschau

E. Happold, BSc, CEng, FIStructE, FICE, FIOB

W. I. Liddell, MA, DIC, CEng, MIStructE, MICE

Ove Arup & Partners

Mr. Edmund Happold is the Executive Partner of Structures 3, which is one of the structural divisions of Ove Arup & Partners. Educated at Leeds Grammar School, Bootham School, York, and Leeds University, he worked with Severud, Elstad and Krueger, New York, in the early days of cable roofs and pneumatic structures. The first cable roofs worked on with Ove Arup & Partners were in 1967, for the Conference Centre in Mecca, Saudi Arabia. Since then he has been engaged on many lightweight roof schemes, being a director of the Lightweight Structures Laboratory which Ove Arup & Partners share with Frei Otto. He is a corresponding member of SFB 64, the German Government-sponsored grouping of university departments interested in long span roofs, is the Institution representative on the organizing committee for the Conference on Tension Structures which held its meetings in London in 1974, and is a representative on the BS Code Committee for Air Supported Structures. He is a member of the Council of the Institution.

Mr. Ian Liddell joined Ove Arup & Partners as an assistant engineer working on the Sydney Opera House, after graduating from Cambridge in 1960. In 1962 he did a post-graduate course at Imperial College and subsequently spent four years with Holst & Company Limited as a design engineer, estimator and site engineer on a cooling tower contract. He returned to Ove Arup & Partners in 1967 to work with Mr. Edmund Happold as project engineer in charge of a prestige building in Saudi Arabia, and is now an associate partner in Structures 3, responsible for a number of projects at home and abroad. He is involved in a structural design course at Cambridge University and is a member of the Institution's ad hoc committee investigating "Criteria for the structural adequacy of buildings".

Synopsis

Shells constructed by lifting a flat square lattice into a doubly curved shape are a recent form of construction. Such a shell of four times' greater span than any previous examples had to be completed in 18 months for an exhibition. This paper describes the engineering design. It attempts to show how the loads were defined, how the structure was modelled and tested both physically and mathematically, and how these models were used to determine the construction details. The design process had to be evolved to derive sufficient understanding so that the decisions could be made by the critical dates.

INTRODUCTION

Background

Linear Arches or Ribs. 'Conceive a cord or chain to be exactly inverted, so that the load applied to it, unchanged in direction, amount and distribution, shall act inwards instead of outwards; suppose, further, that the cord or chain is in some manner stayed or stiffened, so as to enable it to preserve its figure and to resist a thrust; it then becomes a linear arch, or equilibrated rib; and for the pull at each point of the original cord is now substituted an exactly equal thrust along the rib at the corresponding point.' William John MacQuorn Rankine, 1858.[1]

Since 1946 Professor Frei Otto of Stuttgart University has been using hanging chain nets to define possible structures in which, when inverted, the self-weight produces direct force only[2] (Fig 1). Fine chains cannot transmit moment and a suspended chain net can easily be used, provided it is a shear-free mechanism, to determine the statically most favourable dome shape under gravity loading for any continuous boundary condition. Such a direct force structure can theoretically be extremely thin but its thickness will be determined by the stiffness required to withstand buckling and asymmetrical loading.

With this technique, Professor Otto was using the same method employed by the Spanish architect, Antoni Gaudi, at the end of the nineteenth century.[3] Methods of graphical analysis were popular with the engineers at that time, and Gaudi developed their two-dimensional modelling into three dimensions (Fig 2). For the Guell Colony chapel he made wire models hung with appropriate weights to achieve in reverse a logical structure which he could amend until it satisfied him architecturally (Fig 3(a) and (b)). This method of visualising more complex forms gave him a buildable sculptural freedom which conventional simulation methods, such as drawing, could never have allowed.

Professor Otto went on to develop an erection method from the fact that the shape of a hung quadrangular chain net can be recreated in the initial shape by a flexurally semi-rigid lattice of steel or wooden rods in a uniform mesh provided that the lattice is rotatable at the inter-section points. The lattice can be prefabricated as an equal grid, pulled or pushed up and then fixed against collapse by the edge forces. Such a lattice has no in-plane shear stiffness and there are differing angular displacements at various points, the largest at the diagonal edges and the smallest near the principal axes. Shear stiffness can, to a limited extent, be provided by fixing

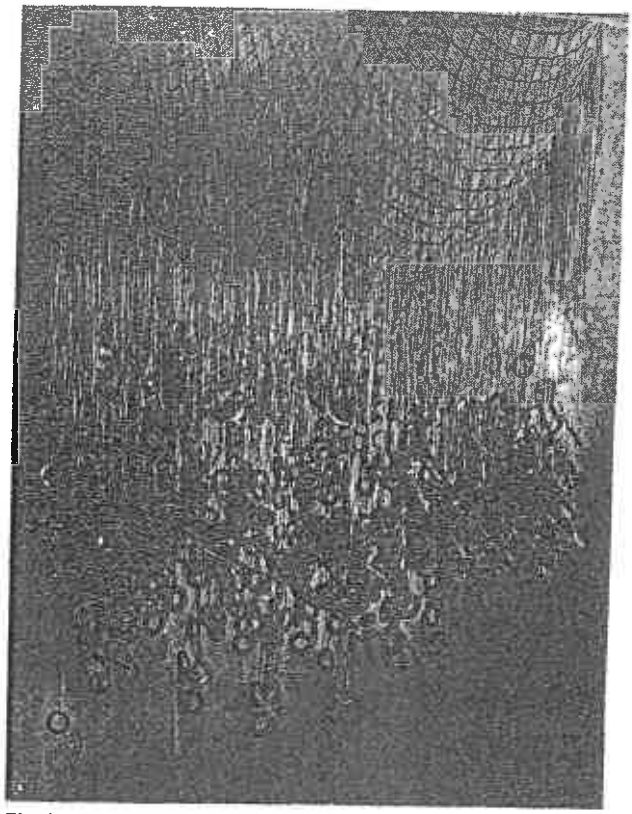

Fig 1. Early hanging chain model

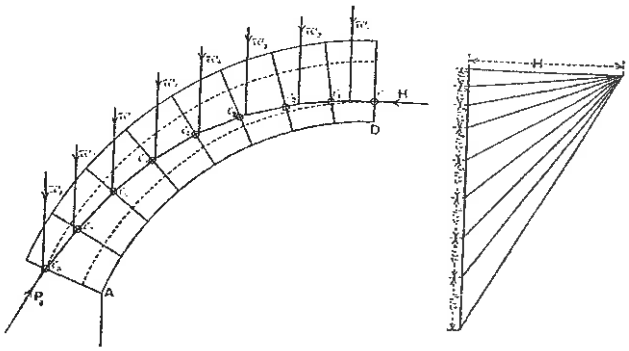

Fig 2(a). Practical graphical method of finding line of resistance of an arch

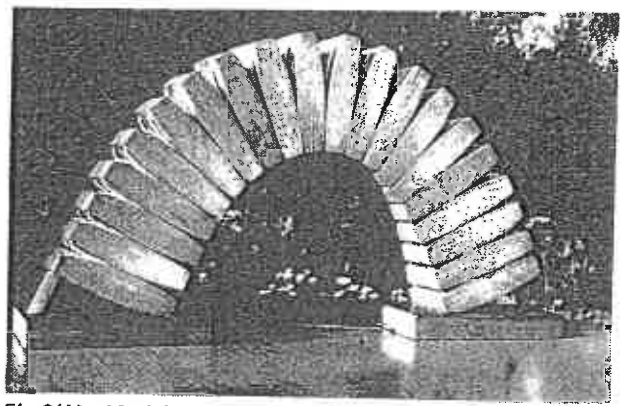

Fig 2(b). Model of arch formed of radiused vousoirs which allow the line of thrust to move in response to point loads. This model was made by Frei Otto to demonstrate the principle of inverting a hanging chain.

the joints, though if the deformations are excessive diagonal ties must be provided.

Professor Otto's first structure of this type was erected for the German Building Exhibition at Essen[4] in 1962 (Fig 4). It was a lattice dome, on a super elliptical base, 15 × 15 m with a height of 5 m at the centre and a mesh size of 0·48 m. It was made with Oregon pine laths of 40 mm × 60 mm cross section and a length of 19 m achieved with finger joints. The laths were connected by bolts. The shape of the dome and lengths of the members were determined by a suspended chain net though, naturally, it was found that the flexural deflection curves of the laths were not exactly those of catenaries. The edge beam was spiked into the ground and erection carried out with a crane with spreader beams, the base being pulled in with diagonal ties.

Later in 1962, at a seminar at the University of California, Berkeley, USA, Professor Otto conducted a series of study projects on suspended catenaries, the definition of a dome by use of a net and, finally, a full-scale erection of a lattice dome made of round steel bars (Fig. 5).

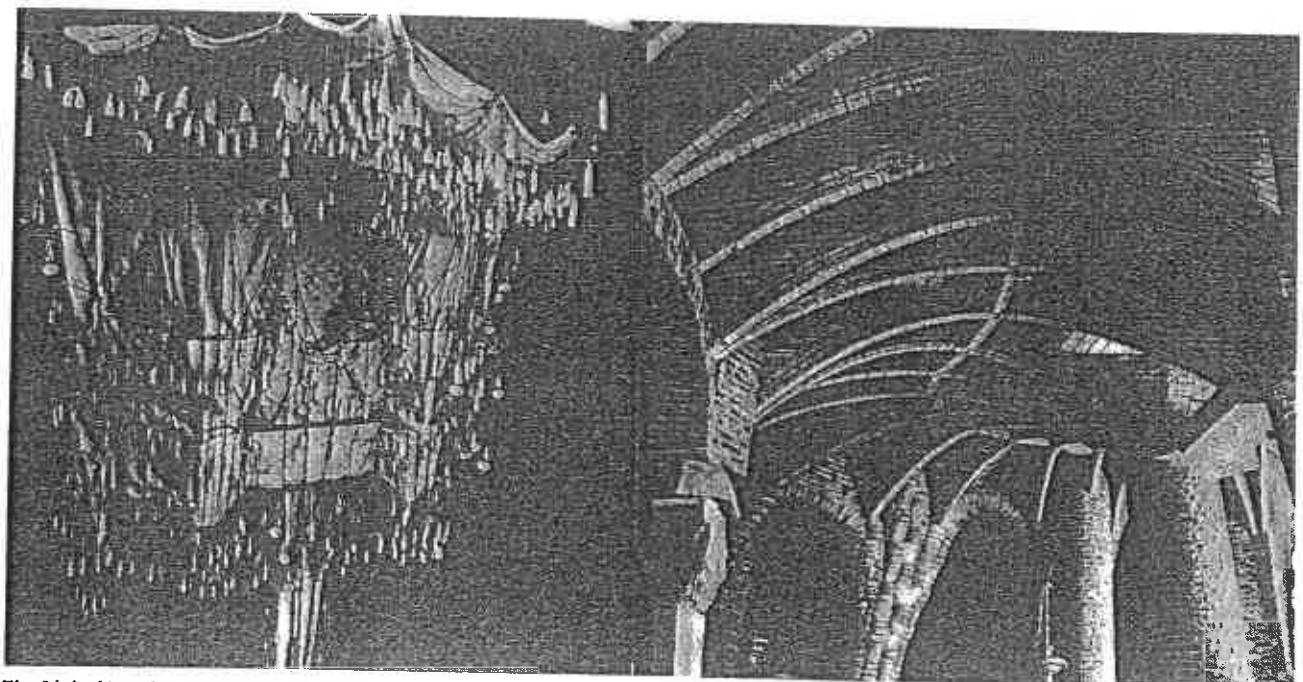

Fig 3(a). Hanging model for Guell Chapel

Fig 3(b). Detail from structure

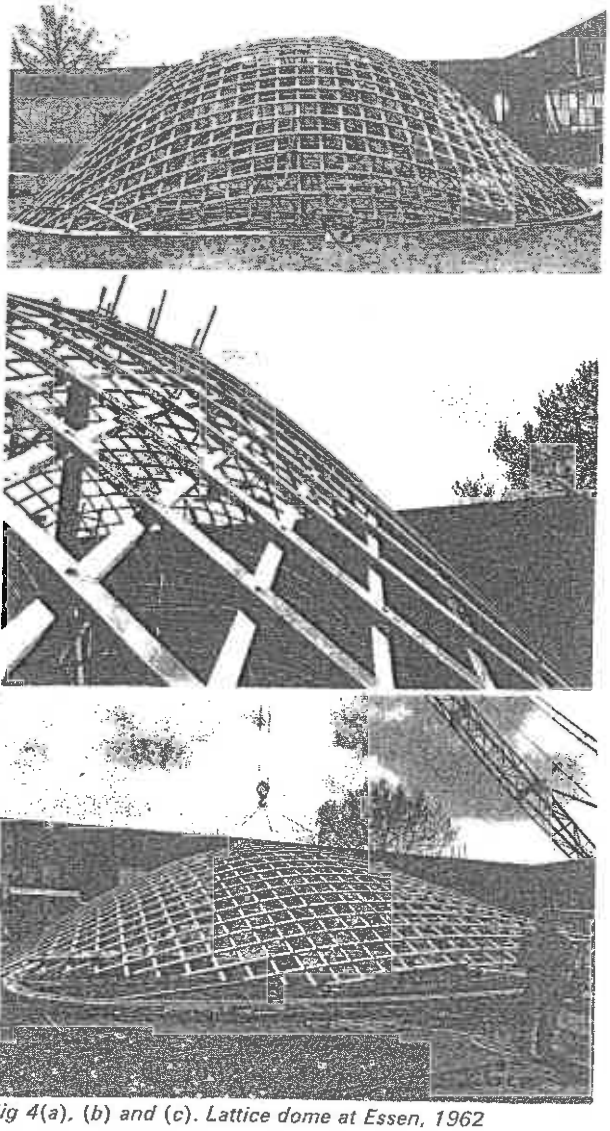

Fig 4(a), (b) and (c). Lattice dome at Essen, 1962

In 1965, in collaboration with Professor Rolf Gutbrod of Stuttgart, he won the competition for the design of the German Federal Pavilion for Expo' 67 at Montreal[5]. The main structure was a large continuous cable net roof but, within the roof, there was an auditorium with its vestibule covered by a timber lattice dome (Fig 6). The plan shape was very irregular, with a re-entrant angle and spans of 17 m × 13 m and 20 m × 4·5 m. For this project a further refinement in the erection method was used when the lattices were pre-fabricated in Germany, collapsed diagonally into narrow

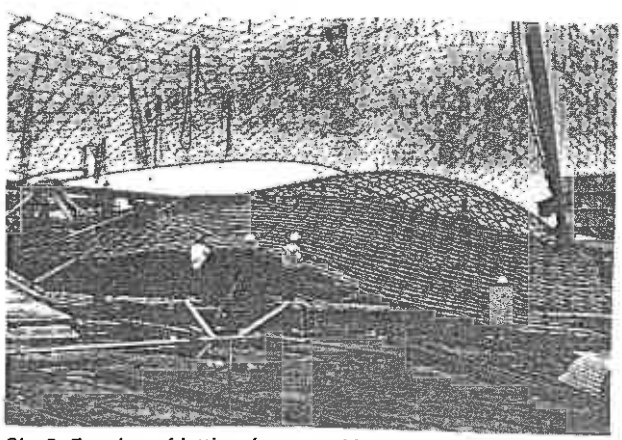

Fig 6. Erection of lattice domes at Montreal

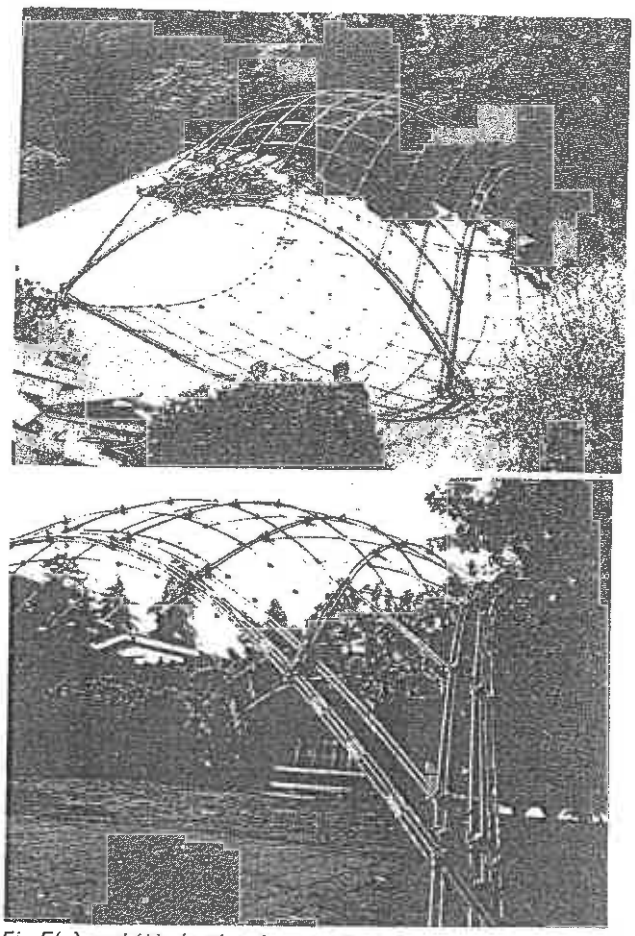

Fig 5(a) and (b). Lattice dome at Berkeley

bundles of strips side by side, transported collapsed to the site in Canada and expanded and erected there.

These three lattice domes are the only ones previously built though several studies have been carried out, including one for a banqueting hall for the Conference Centre in Mecca, Saudi Arabia, where Professor Otto is again in partnership with Professor Gutbrod and Ove Arup & Partners. Within the last two years, however, a rigorous series of shape studies has been carried out with chain nets by a group at the Institut für Leichte Flächentragwerke at the University of Stuttgart[6] (Fig 7).

Nature of the structure

The term lattice shell is used in this paper to describe a doubly curved surface formed from a lattice of timber laths bolted together at uniform spacing in two directions. When flat, the lattice is a mechanism with one degree of freedom. If it were formed of rigid members with frictionless joints, movement of one lath parallel to another would evoke a sympathetic movement of the whole frame causing all the squares to become similar parallelograms. This movement causes changes in length of diagonal lines through the nodes (Fig 8).

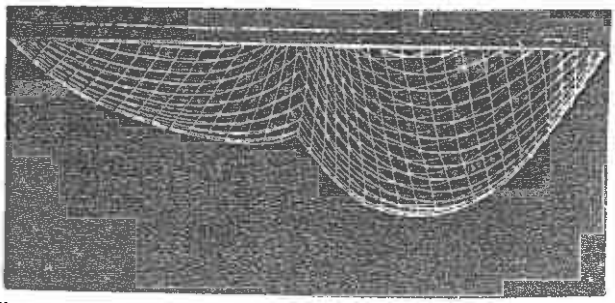

Fig 7. Chain net shape study

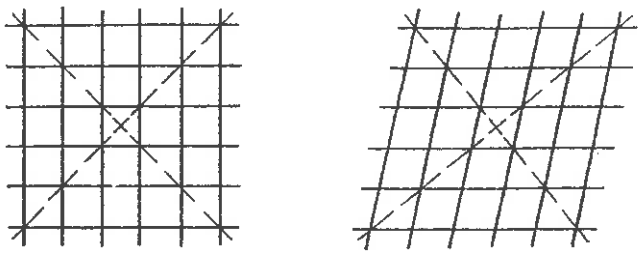

Fig 8. Lattice distortions

It is this property which allows the lattice to be formed into the doubly-curved shape of the shell.

The shape for the shell is established by photogrammatic measurement of a hanging chain model and is funicular. If the shell is loaded with its own weight only, no bending forces result. This is an ideal condition, as in practice the imposed loads on the shell are greater than the self-weight and are not uniformly distributed at the nodes. A funicular shape is an advantage but is not essential.

When the lattice has been curved to the shape of the shell, it is fixed only by its connections to the boundaries. The funicular shape is modified by the effect of bending of the laths and with no loads applied it would be such that the strain energy is minimized.

In this condition the lattice shell resists point loads by bending of the laths. This is acompanied by large movements of the shell and changes in the angles between the laths. These movements indicate that the overall shape of the shell can be easily altered, and to resist these movements diagonal stiffness has to be introduced.

A continuous shell made from an isotropic sheet material has equal properties in all directions. An elemental square on the surface can take direct forces and out-of-plane bending on orthogonal directions (Fig 9). The force/displacement properties are not affected by the orientation of the element. However, an element of a lattice shell consists of a parallelogram of four laths. This element can only resist direct forces in the directions of the laths. It can also resist out-of-plane bending. In its initial pinned condition, it cannot resist diagonal forces. It cannot therefore transmit forces directly from one lath to the next.

Diagonal stiffness can be introduced in various ways:

(a) by making the joints rigid so that shear forces are carried by bending moments around the element ring;

(b) by adding cross ties of cross sectional area considerably less than the laths;

(c) by adding rigid cross bracing of equal area to the laths.

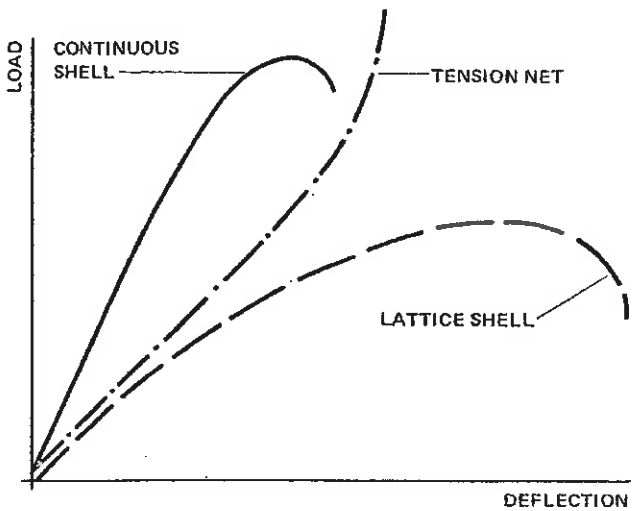

Fig 10

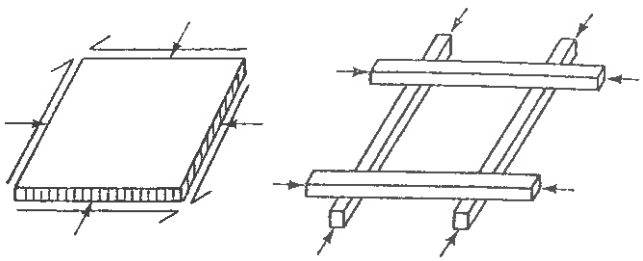

Fig 9. Continuous shell and lattice shell elements

Bracing type (c) would produce a shell which was directly comparable with a continuous shell. Obviously the amount of diagonal stiffness introduced by bracing type (b) can be varied by altering the thickness or material of the ties.

Load carrying behaviour

The loads on a shell can be divided into funicular loads which produce only direct forces in the laths, and disturbing loads which produce bending moments and large deflections. The deflections produced by the disturbing forces change the shape of the shell from its original funicular shape. The direct forces from the funicular loads then produce bending moments which increase the bending moments produced by disturbing loads. As the funicular loads are increased, the stiffness and resistance to disturbing loads is decreased. At a critical funicular load there is no resistance to disturbing loads; a small deflection from the funicular shape causes collapse. This decrease in stiffness to disturbing loads characterizes compression structures. With a tension net the opposite is true; the deflections under load increase the stiffness and resistance to disturbing loads up to the point at which the members break.

With a continuous shell there is an infinite number of funicular loads. Any distribution of load without discontinuities can be carried by direct forces within the shell without the necessity for primary bending moments. This means that deflections will be much smaller than for a lattice shell where disturbing loads are carried by bending of the laths. So the effect of funicular loads in reducing the resistance to disturbing loads is less and the collapse load tends to increase.

Typical load deflection curves of a tension net, a lattice shell and a continuous shell for disturbing loads are shown in Fig 10.

Lattice shells with diagonal stiffness

A pinned lattice shell can only carry disturbing loads by bending of the laths. Under small deflections the structure behaves as a series of inter-connected flexible arches. The bending effects are spread along the whole length of the arch. With large distortions a dimple is formed, and certain of the laths outside the dimple are stretched into tension, preventing further deflection in that zone and causing some increase in stiffness. This behaviour is only possible with low levels of funicular load. With a large funicular load the decrease in stiffness is so great that collapse will occur before the deflections become large.

These large deflections are accompanied by changes in length of diagonal lines through the nodes. In the real structure these changes in length would rupture the covering membrane unless it were made strong enough to resist them. If it is made strong enough then in effect diagonal ties are introduced, the large deflections are controlled and the collapse load is increased. Clearly it is necessary to introduce diagonal stiffness by using the membrane or ties.

Double layer grids

While ties can be used to increase the in-plane stiffness and prevent excessive shear distortion, the only way to increase the out-of-plane bending stiffness is to increase the moment of inertia of the individual members. A double layer grid does

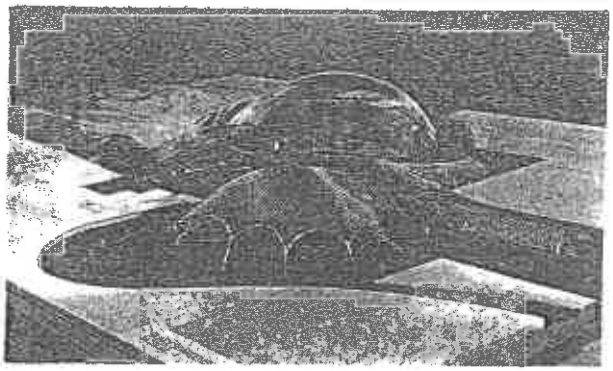

Fig 11. Otto wire mesh model of Mannheim

Fig 12. Links for hanging chain model

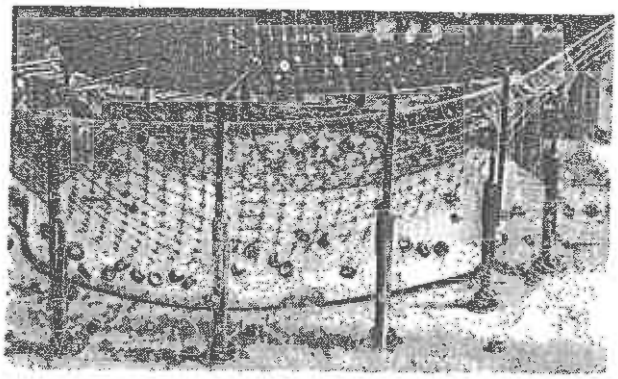

Fig 13. Transferring chain net to supports

this most effectively but introduces other problems; during the bending into shape the two parallel laths along each grid must slide relative to each other. To allow this to happen, one of the layers just have slotted holes. When the final shape is achieved the laths must be prevented from slipping, and even when slipping is prevented the shear stiffness of the composite member is far from ideal.

Architectural design

A federal garden show is held every two years in one of the principal cities in West Germany. The exhibition is open for six months and about four million people visit it. It usually consists of a large park which is landscaped with flowers and shrubs, where growers and nurseries exhibit new and special strains of plants. Playgrounds are included in the landscaping both for children and adults. Special events—concerts, theatre, games and sports—are held on most days.

The garden show is popular among cities because a depressed open area may be re-landscaped with gardens of every kind, paths, lighting, lakes, kiosks and restaurants. The exhibition provides the stimulus to local pride to do this and brings considerable financial help.

The cities of Mannheim and Ludwigshafen (joint population 600 000) were selected in 1970 as the home of the 1975

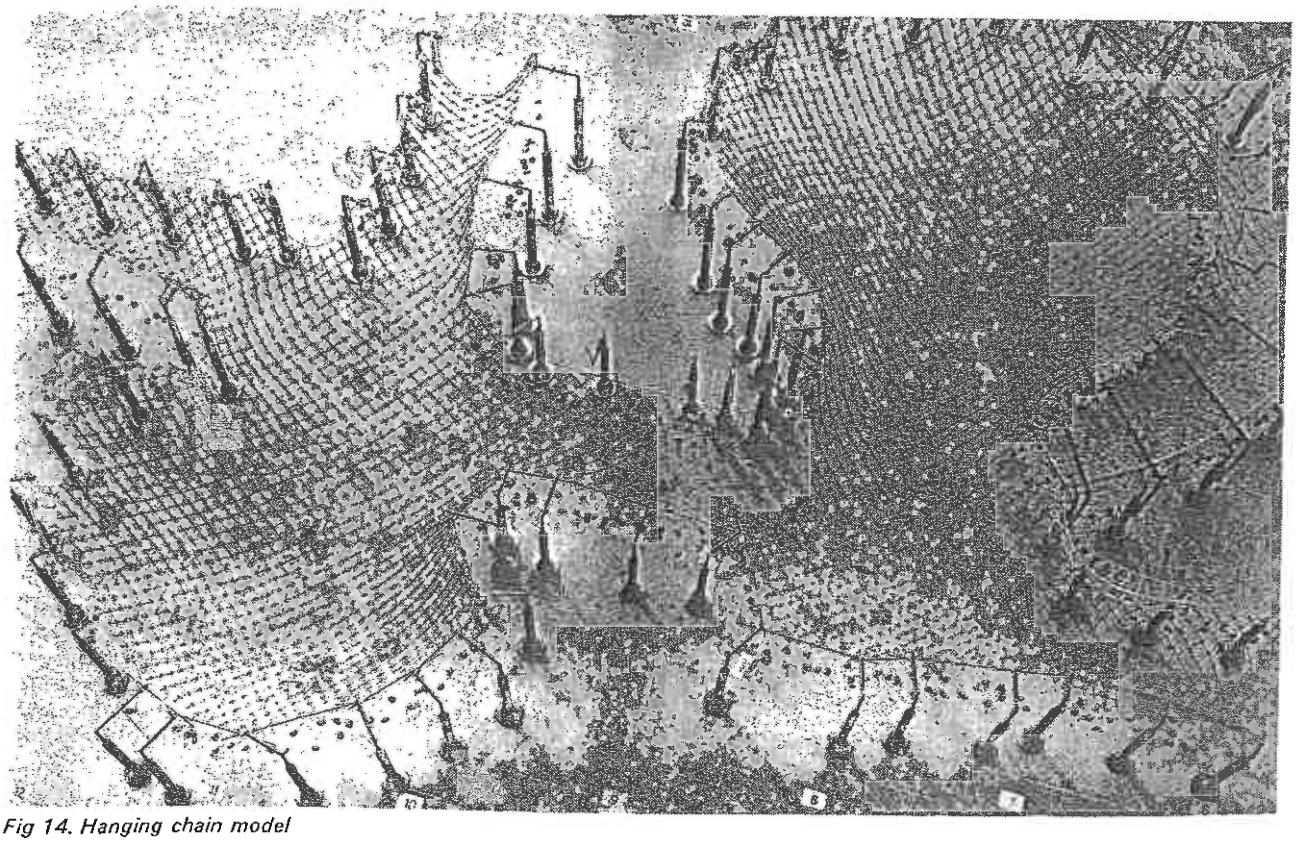

Fig 14. Hanging chain model

exhibition. Two sites, one on either side of the River Neckar, were planned and a cable car transport system has been erected to connect the two entry points.

A Mannheim architectural practice, Mutschler & Partners, was one of the joint winners of a competition held in 1971 to design the parks and was appointed to design the section which included a multi-purpose hall and restaurant. In their competition design the main path of one of the parks led through this complex. For the Multihalle they proposed to use a membrane roof supported by balloons. This scheme was unacceptable to the building authorities, and after some more early thought they asked Professor Otto, who had designed several tent structures for previous garden exhibitions, to help them with a solution.

Together, they investigated various tent and pneumatic solutions. They felt that a free form rounded structure would be most appropriate, as the hall was to be adjacent to the town's newly-created and only hill. Lattice shells were then considered and they evolved a scheme with two principal domes for the Multihalle and the restaurant, connected by tunnels over the walkways. This complex was adjacent to the hill and was surrounded by an artificial canal. Fig 11 shows the final wire mesh model made at Professor Otto's office, Atelier Warmbronn. The lattice was to be covered with a translucent PVC membrane reinforced with open-meshed polyester fabric.

After this model was agreed and accepted, Professor Otto prepared a hanging chain model which was to define the geometry of the roof. This model was made to a scale of 1 :98·9, the node points being small rings connected by rigid links (Fig 12), each 15 mm long to represent every third grid of a 500 mm mesh. The whole mesh was put together by hand and lowered onto a support system prepared on a flat marble slab marked with grid lines (Fig 13). The boundaries were then transferred to the support system and adjusted to find the optimum shape (Fig 14).

A Mannheim engineering practice, Bräuer Spaeh, was appointed to act as structural engineers. Professor Linkwitz and his Institut für Anwendungen der Geodäsie im Bauwesen, of Stuttgart University, were appointed to express the geometry of the chain net model by the photographic and mathematical methods he had developed during the design of the German Federal Pavilion at Montreal and the Munich Olympic stadia.

The responsibility for approving the building for public safety lies with the Board of Surveyors, but for special structures they can appoint a Proof Engineer who approves the calculations and the standard of the finished building. Professor Wenzel of Karlsruhe University was selected for this task.

It was decided to divide the contract into three parts: concrete work, timber and covering. Tender documents were sent out separately during September/October 1973 to three firms for each part. These firms were then put together with their agreement into three groups.

In October 1973 the consulting structural engineer resigned from his appointment and Structures 3, Ove Arup & Partners, were invited to undertake the work. The practice was already aware of the project and knew that there was no previous engineering experience in this field. The roofs were already out to tender and the tenders were due back in three weeks. This period represented the time available to make the preliminary analysis necessary to underwrite the basic sizing. Construction on site had to commence in December 1973 and erection of the lattice shells was to take place in April/June 1974. The building was to be substantially complete in November 1974 and the exhibition was to open on 18 April 1975. This programme is shown in Fig 15.

STRUCTURAL DESIGN

Design process

When Ove Arup & Partners accepted the commission they realised that in order to meet the critical dates for supplying information, shown on the initial programme Fig 15, design decisions would have to be made at the appropriate times based on the information then available. In view of the lack of previous experience they anticipated a design programme which started out on a number of paths simultaneously.

This paper is concerned with the engineering work which evolved as the design developed. It attempts to show how the loads were defined, how the structure was modelled and tested both physically and mathematically and how these models were used to determine the construction details. The flow chart of the design process as it happened is shown in Fig 16.

Initial studies

Tender documents had been sent out previously showing the shells fabricated as a single lattice from 50 × 50 mm timber sizes. As only three weeks were available before the tenders were due in and they had to be accepted only a short time after that, an immediate start was made on

(a) investigations to establish the design loads, and
(b) hand calculations on shell buckling.

As only three lattice shells had been built before and these had been very much smaller, there was not much previous experience available. Rough calculations on the buckling of the shell based on a paper written by Wright[7] indicated that the shell was too thin. 100 × 100 mm laths were required but these could not be bent to shape. It was thought that the strain energy imparted to the laths in the initial bending might improve the buckling performance, although it was realized that this would only be a temporary improvement as the initial stress would creep away. This concept was later demonstrated to be irrelevant.

The building geometry was defined at this time by the hanging chain model at the Atelier Warmbronn. The final geometry was to be defined by computed co-ordinates after Büro Linkwitz had taken stereo photographs of the model and had corrected them to achieve equilibrium of forces in the net, but this was not programmed to take place for two or three months.

To get a graphical representation of the geometry, a contour drawing of the hanging chain model was prepared by Atelier Warmbronn. This drawing also showed the positions of every tenth model grid and the radii at the intersection of these grids, measured by using railway curves.

While waiting for this geometry it was felt essential to gain understanding of the structural behaviour as quickly as possible. So work was started on investigating the properties of timber and, in order to have something real to feel and test, it was decided to make a working model of the Essen shell. This was chosen as the geometrical details were immediately available from Professor Otto. As described under *Model Testing*, page 115, this model was made and tested; scale factors were applied to the results which indicated that the collapse load of the Multihalle shell as proposed was only slightly more than the dead load.

While the Essen model was being made, the tenders were received in Germany and Ove Arup & Partners were formally asked to confirm that the structure would work. The rough calculations had already indicated that the shells were too thin and this was stated. However, the amount and extent of thickening required was uncertain. It was agreed that some provision should be made for extra material and so prices were obtained for areas of doubled laths.

As work on the physical model proceeded, thought was being given to setting up a mathematical model. The ECI 603[8] non-linear space frame programme was thought to be the most suitable. Trial computations on the Essen model were carried out to test the modelling, which predicted a collapse load within 10 per cent of that established by load testing and so established confidence in the computer results.

As a result of these tests, it was realized that the collapse load of the shells had to be improved even though the contract had already been let and the 50 × 50 mm lath size was

agreed. In any case, increasing the lath size would mean that the initial bending stresses would be too great. Doubling the laths one above the other was thought to be the only reasonable way to get adequate bending stiffness, so the decision was taken to do this.

During this stage, work was starting on site and there was pressure to get loads for the foundation design. Using the contour drawing which gave an idea of the curvatures, calculations were made on a coarse grid to establish the direct forces in the laths. These calculations were based on:

$$\text{load} = \frac{\text{force}}{\text{radius}}$$

and on the assumption that the rate of change of force along a lath would be small because of low in-plane shear stiffness. The distribution of forces was estimated by eye and turned out to be close to the Büro Linkwitz distribution. In defining the boundary forces an allowance was made for variations in distribution.

Design loadings

From data obtained from the Weather Office the snowfall in the area is much less than the average for Germany and less than the 75 kgf/m² required as a minimum by the DIN code. Snow was obviously the critical form of loading for a light-weight compression structure. The effects of wind were felt to be less important as the resultant force would be mainly uplift. Nevertheless, there was a possibility of gusting and dynamic effects which had to be investigated.

A 1:200 scale wind tunnel model was made and tests were carried out by the BHRA in the wind tunnel of the Cranfield Institute. Full wind and snowfall records were obtained from the weather service in Karlsruhe and a statistical analysis was performed on them to obtain a design load with a suitable level of probability. The work is described under *Definition of loads*, page 108.

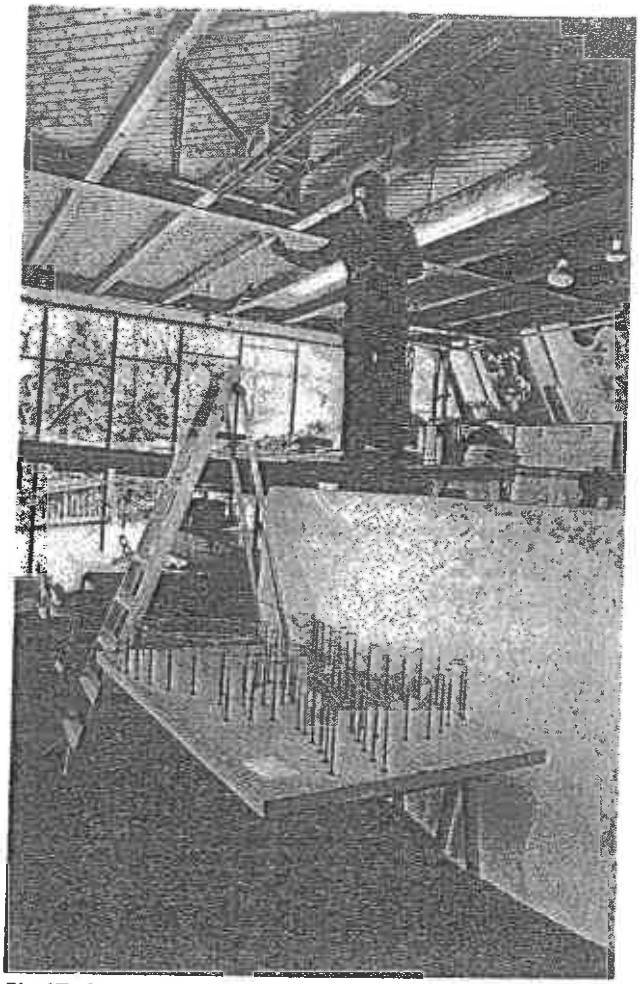

Fig 17. Stereo photography of hanging chain model by IAGB

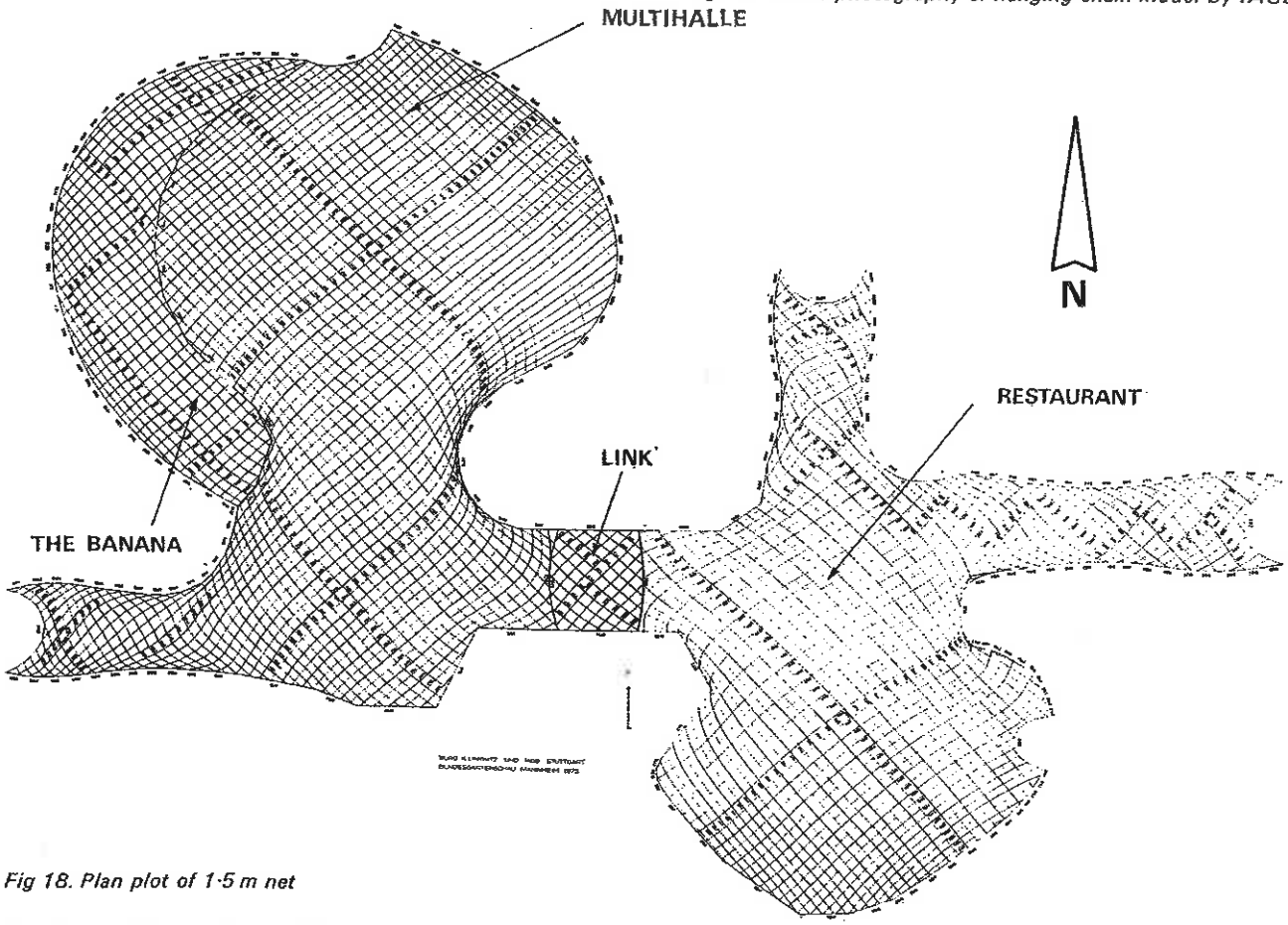

Fig 18. Plan plot of 1·5 m net

Definition of geometry

The geometry of the shells was to be defined for construction by Büro Linkwitz and the Institut für Anwendungen der Geodäsie im Bauwesen at Stuttgart University. This started from the hanging chain model which was photographed using stereo cameras (Fig 17). These photographs were processed to yield an initial set of co-ordinates for the nodes of the hanging chain model. The hanging chain model contaned a number of inaccuracies; for example, the links were not always the proper length of 15 mm, and in places they went into compression. To improve this situation the initial co-ordinates were corrected so that the final set of co-ordinates represented an ideal hanging chain with the distances between the nodes exact and all nodes in equilibrium under self-weight. This processing was done on a CDC 6600 computer using a program prepared by the IAGB[9]. As well as a full set of node co-ordinates, the results of this work included a plan plot of the net and the member forces from the equilibrium calculation (Fig 18).

Modelling

The results were made available to the architect, Atelier Warmbronn, and to Ove Arup & Partners. This marked the start of detailed analysis work on the shells. The co-ordinate system was used to set up the non-linear analysis programs.

The computer plot was used to provide the geometrical information to make a perspex structural model of the Multihalle shell which was then test loaded. The physical modelling work is described under *Model Testing*, page 115. The computations using the non-linear program are described under *Mathematical Modelling*, page 118.

In setting up the input for the Multihalle program, it was necessary to use one member to represent 12 parallel laths. To ensure that such a coarse grid adequately modelled the behaviour of the real structure (made of a material with differing non-linear stress strain properties in three directions) it was necessary to make assumptions about the stiffnesses and to convert these into equivalent member properties for the computer model. The relationships between the behaviour of the computer members and that of the real structure were tested mathematically. The behaviour of the lattice joints was proved by tests described under *Determination of member behaviour*, page 110.

Detailing

The details of the grid were developed in parallel with the computing work, so that the properties of the structure agreed with those of the mathematical model which was finally accepted as having an adequate factor of safety. The boundary details were developed to meet the requirements of the geometry and the erection process, and to have adequate strength to supply the reactions to the lath forces. This work is described under *Development of Details*, page 123.

Definition of loads

The self-weight of the lattice, including an allowance for extra timber and for light fittings, was taken as 20 kgf/m². In addition to the self-weight, the roof must withstand imposed loads arising from construction or maintenance procedures, wind pressure and snowfall. These loads had to be agreed with the proof engineer.

The design load allowance for construction or maintenance was taken as two 70 kg men working close together as well as some equipment making a total of 200 kgf on an area of 3 m². It was felt that loads in excess of this could be controlled, and that this load itself was low compared with the dead weight plus design snowload.

The loads from wind and snow are not controllable, and for a lightweight structure such as this can create pressures two or three times greater than the self weight. The structure had to be designed to resist these loads, and as it was apparent from the outset that it would not be easy to build in a large reserve of strength, it was necessary to define them precisely.

Design wind velocity

The current German code for wind forces, DIN 1055 Blatt 4, calls for all structures to be designed for the same pressure gradient. For structures 20 m high, the stagnation pressure is 80 kgf/m². It is understood that this code is in the process of being revised on a statistical and geographical basis, but for the Mannheim roofs a more accurate estimate of the wind pressure was required at the time.

Wind speed records were obtained from the Mannheim Weather Office and were analysed statistically on the basis that they conform to the extreme value distribution of the first exponential type. This distribution is considered by most authors adequate for defining the distribution of yearly maximum wind velocities and is fully described by Gumbel[10].

In the analysis of the Mannheim wind speeds, the reference height was taken as 20 m, equal to the height of the shell. The return was taken as 20 years, which was considered to be the maximum life of the structure. For structures with dimensions greater than 50 m, the wind gusts have low correlation from point to point over the surface, and so it was considered appropriate to use a 15 second gust speed to allow for the time averaging effect.

Calculated on this basis the reference velocity was 25 m/s which represents a stagnation pressure of 35 kgf/m². The wind rose of relative probability was as Fig 19. Wind speed data were obtained for Darmstadt, Karlsruhe and Freiburg, other Rhine valley towns close to Mannheim[11]. These data were similarly processed and gave results which corresponded well with those for Mannheim.

Determination of wind pressure

Wind pressures on structures are commonly related to the wind stream stagnation pressure, $\frac{1}{2}\rho V^2$, by means of the non-dimensional pressure coefficient Cp. For conventional structures, values of Cp over the surface are well tabulated in Codes of Practice. In general these have been calculated from wind tunnel tests. Little information is available for unusual shapes, and so it was decided to carry out wind tunnel tests to establish the pressure distribution on the Mannheim shells. They were carried out by the British Hydrodynamics Research Association in their low speed wind tunnel at the Cranfield Institute, which has a working section 1·8 m square.

For true modelling of a prototype structure, all parameters should be modelled. To achieve this, the non-dimensional ratios describing the structure and the wind should be constant, and the important parameters should be represented as well. A compromise has to be reached for conventional low speed wind tunnels in that Reynolds number R_N cannot be scaled.[12]

For the lattice shells the dynamic behaviour is uncertain, but it was considered that because of the large length dimension and high structural damping, the wind response would be similar to the effect of an equivalent static pressure. This simplification eased the modelling and allowed the use of a static rather than an aeroelastic model for Cp distribution determination. This same simplification applied to the modelling of the wind and reduced the need to scale the turbulence intensity. An approximation to the velocity distribution near the ground was made to allow one reference velocity V_Z to be used for evaluation of Cp values.

Velocity scaling is then not dependent on the model scale, but on the measuring equipment and other physical limitations in the tunnel. It is rarely possible to scale R_N, however, and as this parameter primarily controls the flow pattern around the structure it is of importance. For flow in a fully developed turbulent boundary layer, such as atmospheric winds, flow pattern is independent of R_N. This type of flow is often ensured by the normal sharp edged wind tunnel models used. Devices such as trip wires or surface roughening are necessary for small rounded models such as the Mannheim lattice shell. By this means flow conditions may be well scaled even though R_N is not identical.

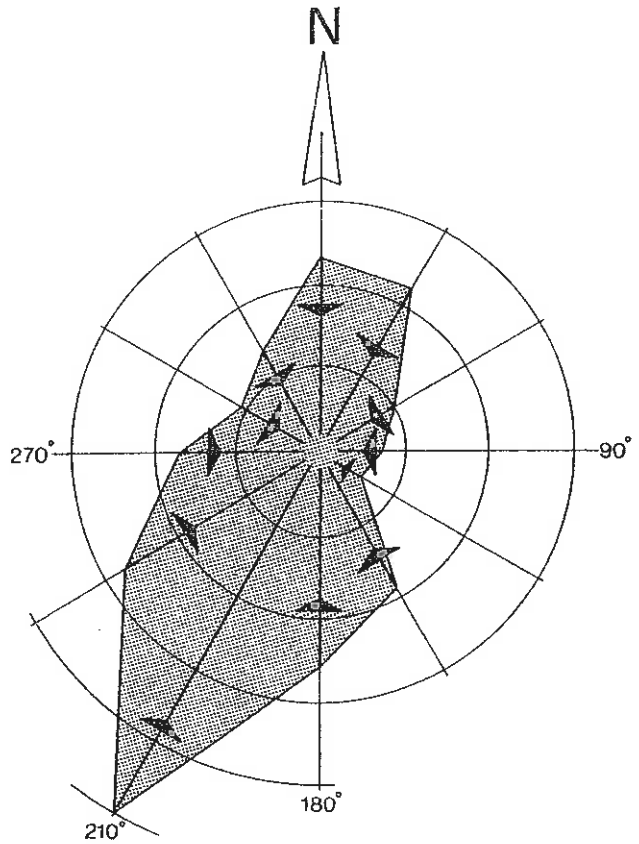

Fig 19. Wind rose of relative probability

These considerations led to the choice of a static rigid hollow model for *Cp* determination for wind-loading calculations.

The model. For convenience the length scale of the model was chosen as 1:200 and the area of surrounding land was determined by the size of the wind tunnel turntable. A rigid model of urethane foam was made by Fairey Surveys from a contour drawing supplied by Professor Otto (Fig 20). From this several clear vacuum-formed models were made with a shell thickness of approximately 2 mm. This produced a rigid model which was transparent and which had openings around the sides as required. The model was firmly attached to a base board and pressure taps were connected to measure relative pressure over the outside and inside surfaces of the model. A large roughened fairing was provided upstream of the model to produce a turbulent boundary layer.

Wind tunnel tests. With regard to flow verification and visualization, to verify the assumption that R_N scaling was not important, a series of runs were made in the tunnel with smoke injected upstream of the model. It was hoped to gain some appreciation of the pattern of air flow over the structure, and to discover any problems of high velocity in the surrounding areas. As was expected, the flow pattern showed no visible change with tunnel speeds of reasonable order and above, and it was concluded that the trips and sharp edge site features were sufficient to ensure that the flow pattern was turbulent and independent of R_N.

No quantitative information was to be gained from smoke tests; however, the following was observed:

(a) Very small flows occurred inside the building. This may underestimate the real condition due to scale effects of small holes; however, it would appear that flow rates inside the building will be low and unlikely to cause discomfort.

(b) The flow around the southern area of the structure appeared to have a high turbulence component from the many trees in the area.

(c) The large tree in the Biergarten near the middle of the structure appeared to reinforce a standing vortex in this area for most wind directions. Velocities here are unlikely to be greater than the natural wind velocity, but on days of high wind speed, some discomfort may be experienced in this area.

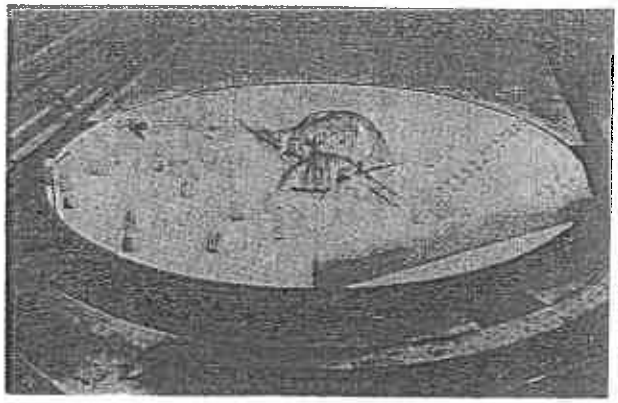

Fig 20. Wind tunnel model

Determination of pressure. The model was instrumented with 150 pressure taps over the surface, including several on the inside. The total pressure at each tap location was measured by manometer. The banks of manometers were photographed for each run.

Prior to any readings a traverse with a calibrated National Physical Laboratory pitostatic tube was carried out upstream and downstream of the model to determine the boundary layer profile. (See Fig 21).

The processing of manometer readings into *Cp* values was done by BHRA. These were then calculated for wind

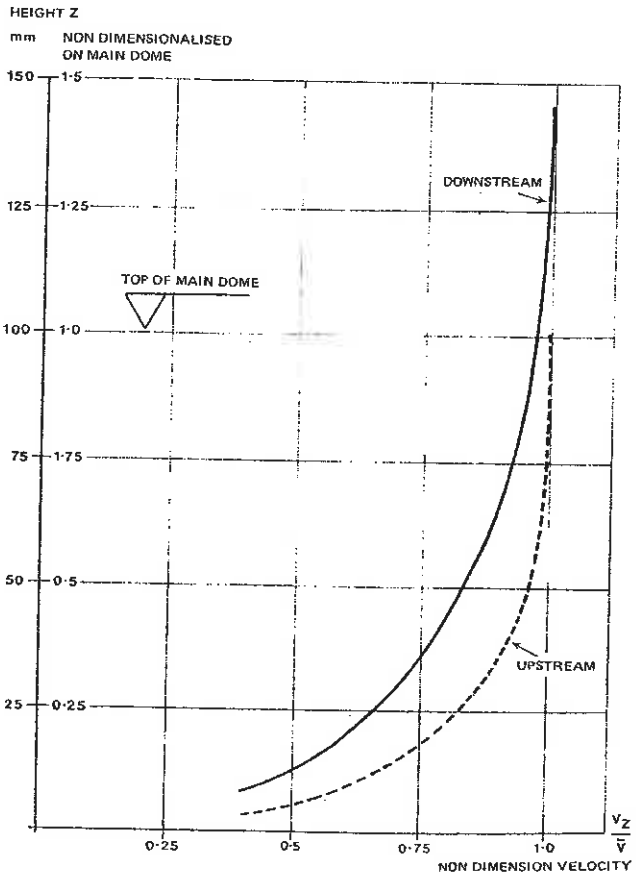

Fig 21. Boundary layer profile

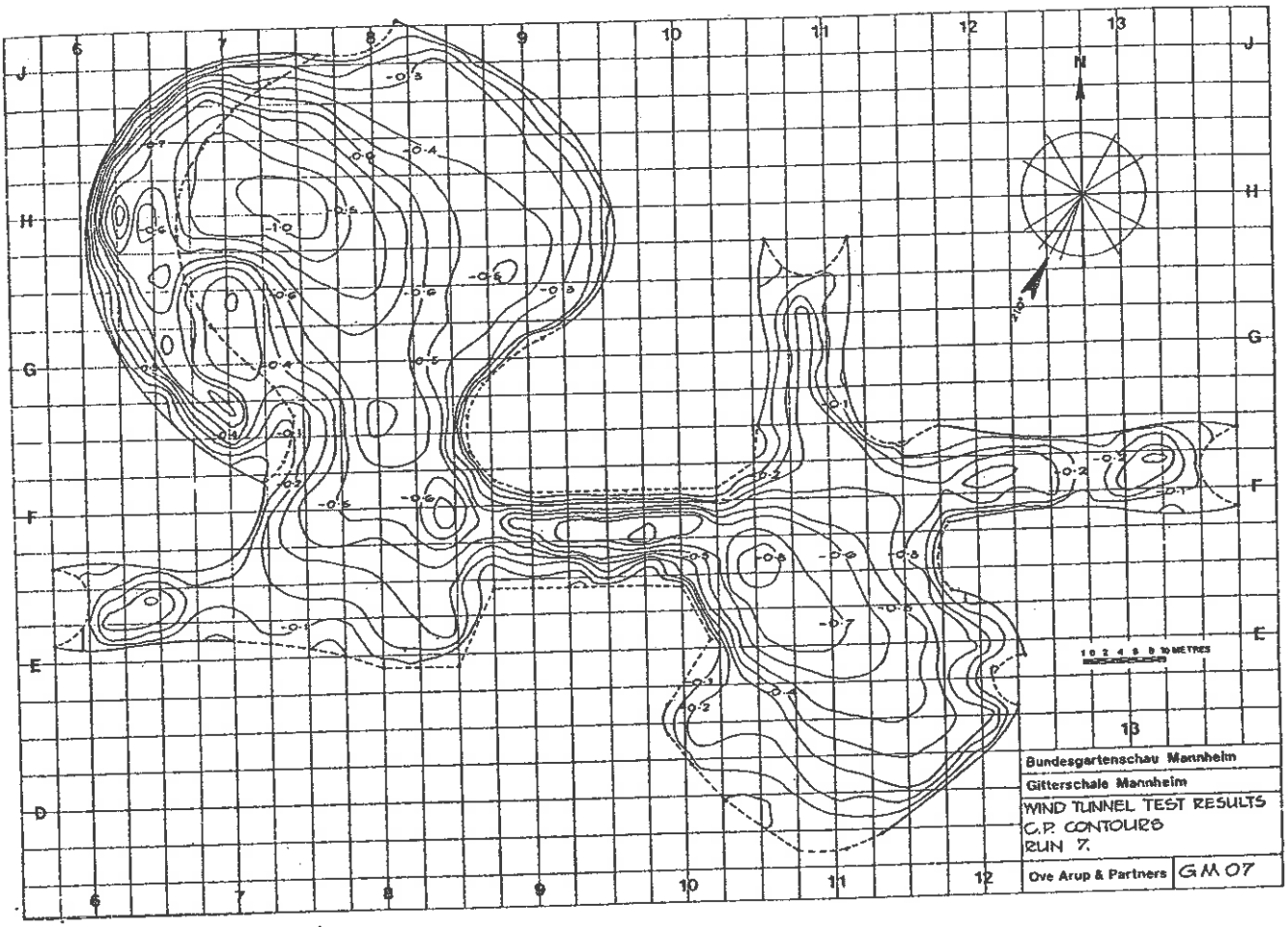

Fig 22. Contour plot of Cp *values*

directions each 30° from North ($\phi = 0°$) with extra readings around the apparently critical wind direction up the Rhine Valley of $\phi = 210°$. Each wind direction has an associated relative probability which may be used to predict the final wind loading on the structure.

In order to present the mass of information in a more useful form, a computer contouring technique was used to produce *Cp* contours for each wind direction. Also the data values were plotted at their measuring locations. The computer plot for *Cp* contours was 'smoothed' by hand to remove the unavoidable anomalies produced by the irregular structural shape. The contours and the data values for wind at 210° are shown in Fig 22.

Design snowfall : different loads

The German code for snow loading DIN 1055 Blatt 5 treats the country geographically with different loads for different areas. Mannheim lies in the area of least snowfall but the DIN code specifies a minimum snow load of 75 kgf/m² which should be applied in this area. This load is nearly four times the self weight and would represent a very severe load case.

As with wind speeds, the snowfall records for the previous 20 years were obtained from the Mannheim Weather Office. These data were processed in the same way as the wind speeds, although the exponential type distribution is not strictly true for snowfall, which can have years in which there is a zero value.

This led to the following results for maximum one day and three days' snowfall with return periods of 20, 50 and 100 years. Observation of the records indicated that a three day period accounted for most of the snowfall in a particular snowy spell. After three days snow weight would be reduced by evaporation.

	20 years	50 years	100 years	
1 day ..	21·0	25·3	28·6	kgf/m²
3 days ..	33·5	40·9	46·5	kgf/m²

The closed part of the Multihalle was equipped with heating plant which it was agreed would be used to melt the snow. For this area a design snow load of 15 kp/m² was taken which, it was felt, was an adequate allowance to provide for a very heavy snowfall rate which overcame the effects of heating, or for a snowfall in the night when there was no one present to turn on the heaters. This is comparable to results from research into snow loads on heated air houses in Scandinavia and West Germany.

The design load for the remainder of the shells was agreed to be 40 kgf/m², and was related to the three day snowfall with a return period of 50 years. With the expected maximum life of 20 years, there was little probability of this load occurring but it was taken because of the importance of snow loading, and because the City of Mannheim did not want to take any clearing action.

Determination of member behaviour

Western hemlock had been chosen by Professor Otto because it was available in long lengths which are normally straight-grained. The tree, *tsuga heterophylla*, is native to the western coast of America from southern Alaska to north California. It reaches a height of 60 m with a bole diameter of 2–2·5 m. The timber is non-resinous pale brown in colour and of even texture. The darker summer wood bands produce a well marked growth ring figure.

Amabilis fir and Grand fir closely resemble Western hemlock, and in some areas they grow together. They are frequently mixed when cut and subsequently exported as commercial Western hemlock. The strength properties of the mixed wood are slightly lower than those for pure Western hemlock.[13]

Timber properties

The structural properties of timber depend on the

direction of the stress in relation to the fibres. They also vary with moisture content and with the duration of load. The strength and stiffness properties of various species of timber have been established by a large number of short-term tests on small clear specimens carried out by several testing authorities. These results show a normal Gaussian distribution of values with a high standard deviation, but have a strong correlation with specific gravity.

For a simple element in bending, these variations in properties do not present a great problem. A design-breaking strength can be established by finding the stress below which only 1 per cent of the results will fall and then applying modification factors to allow for these effects and for additional security. Long term reductions in E will increase deflections, but these can be taken care of by selecting a suitable beam depth.

For constructing lattice shells many of the properties of timber can be advantageous; a low Young's Modulus (E) enables it to be bent and the creep effects cause the initial bending stresses to reduce. For the subsequent behaviour most of these variable properties are disadvantageous and produce structural modelling problems. It was therefore necessary to investigate these properties in depth to be sure of the validity of the structural modelling.

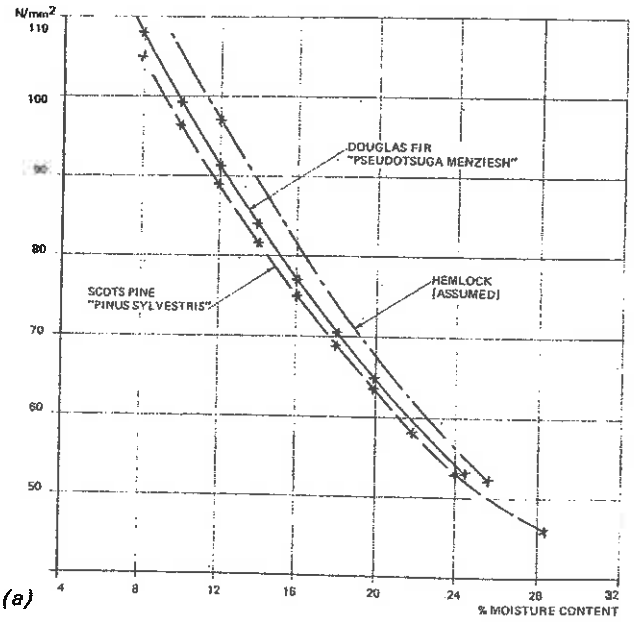

Fig 23(a) and (b). Change of modulus of rupture (a) and change of modulus of elasticity (b) with moisture content

Moisture movement. Hemlock, when green, has a high moisture content and has to be dried with care. The handbook of soft woods[13] gives the following values for initial shrinkage and subsequent movement:

Shrinkage:	
Green to 12 per cent moisture content:	
Tangential	about 4·0 per cent
Radial	about 2·8 per cent
Movement:	
Moisture content in 90 per cent humidity	21 per cent
Moisture content in 60 per cent humidity	13 per cent
Corresponding tangential movement	2 per cent
Corresponding radial movement	1 per cent
Classification	medium movement

The longitudinal shrinkage of timber is not normally quoted. Handbook 72 of the US Department of Agriculture[14] gives the total longitudinal shrinkage as being between 0·1 and 0·3 per cent. Kollman and Côte[15] quote the longitudinal shrinkage as being 0·01 per cent for each 1 per cent change in moisture content, a value which corresponds with the higher value of the previous reference.

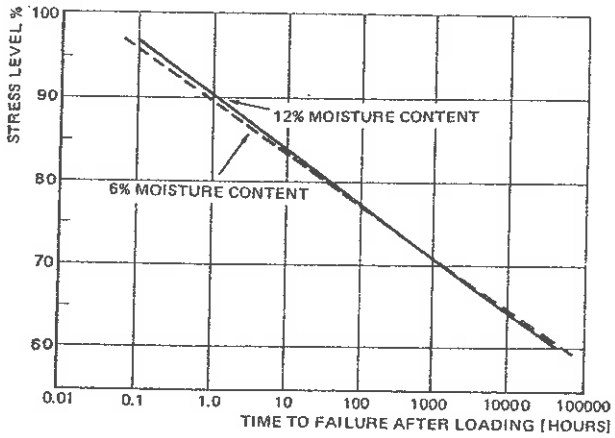

Fig 24. Long term bending strength of small clear Douglas Fir specimens (from data prepared by US Forest Products Laboratory)

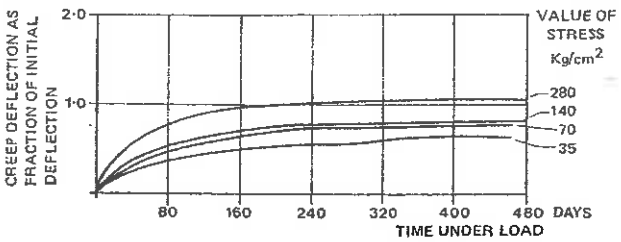

Fig 25. Creep of air-dry beams of mountain ash at 40°C

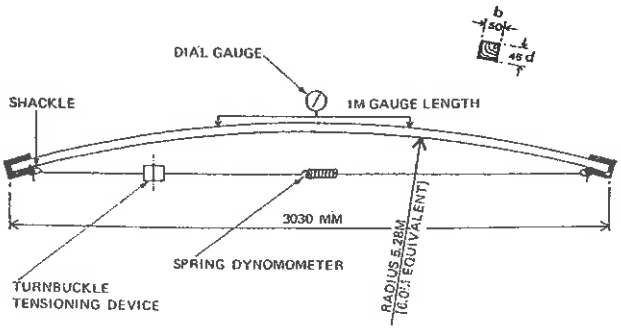

Fig 26. Arrangement for constant strain creep tests

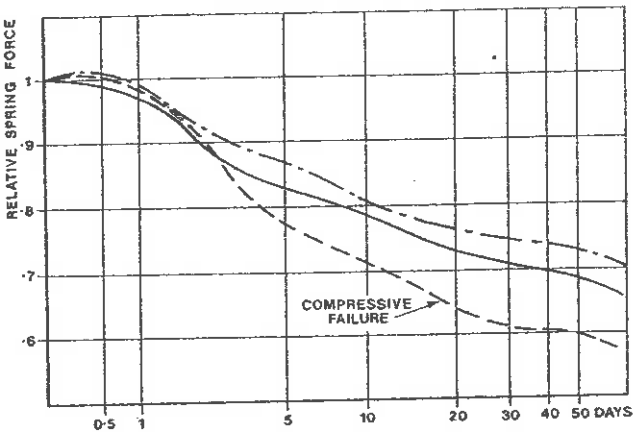

Fig 27. Results of creep tests

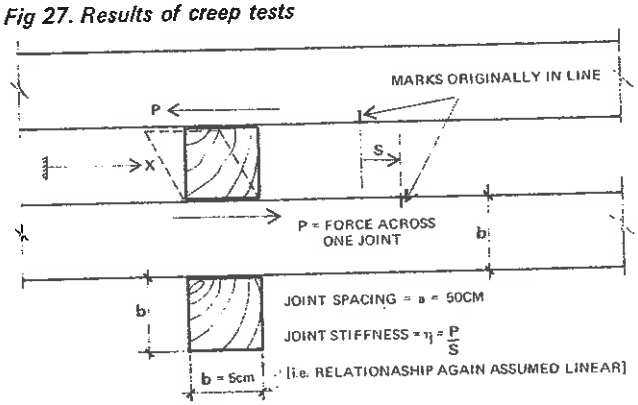

Fig 28. Diagram to illustrate shear deformation at a joint

Strength properties. The Forest Products Research Bulletin 50[16] quotes values of strength properties for a number of timbers based on short term tests on small clear specimens. Those for western hemlock are taken from tests carried out by J. G. Sunley, who in his report[17] shows that they compare well with American and Canadian tests. It therefore seemed reasonable to treat these values as representative and to assume that the timber for Mannheim conformed to this distribution.

The values of bending strength and elastic modulus were as Table 1.

TABLE 1

	Moisture content	Bending strength N/mm²		Modulus of elasticity N/mm²	
		mean	S.D.	mean	S.D.
Green ..	51·0	49·0	10·0	8 700	1430
Air dry ..	12·8	83·0	20·6	10 400	2040

F.P.R. Bulletin 50 gives information from which curves of the change of modulus of rupture and modulus of elasticity with moisture content can be derived. It can be assumed that western hemlock has similar curves. These are plotted in Fig 23(a) and (b).

Duration of load. Booth and Reece[18] give examples of long-term bending tests carried out at the US forest products laboratory on small Douglas fir beams. These results were used to derive the time to failure against stress level curve as Fig 24.

This curve indicates a minimum percentage stress level as 56 per cent for a 50-year load duration and has been used for establishing permissible long-term stresses in CP112.

Creep. Booth and Reece also quote deformation/time curves for mountain ash established by Kingston in 1962. These give creep depth as a fraction of initial deflection (Fig 25).

Fig 29. Rig for shear stiffness tests

These tests were carried out on air dry specimens. Other tests have shown that the creep rate is more or less constant provided that the moisture content is constant but variations accelerate the creep.

These basic properties were used to establish and verify the structure properties of the lattice. However, for some effects where there was uncertainty about the behaviour special tests were carried out. In the case of the lattice joints these tests were carried out in parallel with the buckling load calculations and the development of the details, and was an important part of the design process.

Testing programme

Stress relaxation investigation. For significant areas of the lattice shell, the radius of curvature is relatively small, of the order of 10 m with some areas at 6 m. This curvature results in high bending stresses during erection with the possibility of overstressing the members by the application of service loads. Stresses in timber held to a constant deflection relax, and as a first approximation the reciprocal rule applies. This states that if it takes x days for deflection to increase by a factor of y for constant load-deflection testing, then in the same x days at constant deflection, the stress will reduce by the factor y,

i.e. be $\frac{1}{y}$ times the original stress.

This rule is very approximate but does suggest an order of magnitude. A benefit of this creep-relaxation phenomenon is that the initial high bending stress will relax and reduce to acceptable levels by the time service loads and stresses are applied. To investigate this further, several lengths of hemlock were bent to a predetermined radius of curvature by means of an eccentric calibrated spring as shown in Fig 26.

This radius of curvature was calculated to give the same extreme fibre stress as would exist in 50 mm square timber

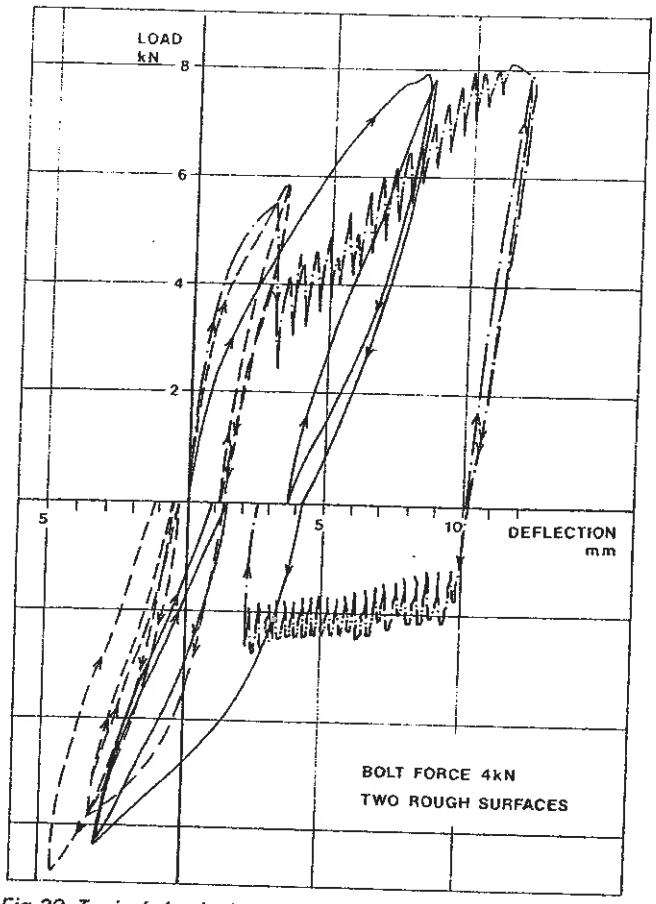

Fig 30. Typical load deflection curves recorded in shear stiffness tests

being bent to 6 or 12 m radius of curvature. The curvature was noted as 6 or 12 m equivalent radius.

The radius of curvature was maintained constant and the reducing spring force was measured over a substantial period of time. The effect of compressive stress due to the load application method is small, and the stresses can be considered to be purely bending for the purpose of calculation of stress relaxation.

The results of these tests are presented in Fig 27, non-dimensionalized and plotted to a logarithmic time scale. The tests were useful in that they demonstrated that the high initial bending stresses relaxed quite quickly, although they were carried out in internal conditions where the relative humidity would not vary as much as outside, and this could alter the creep behaviour.

Shear tests on node joints. The development of the standard node is described in the section *Development of details* on page 123. The shear stiffness of the node joints η is given by $\frac{P}{S}$ where P is the force transferred between the upper and lower laths at a joint and S is the relative movement (Fig 28). The value of η controls the out of plane shear stiffness of the lattice. The problems associated with the shear stiffness of the joint are described in the section on *Mathematical modelling* on page 118. In order to justify the values of shear stiffness used in the collapse load computation a series of tests was carried out.

At first, it was thought that the interface slip would be the main problem and so tests were carried out to investigate this. A test rig was set up as Fig 29, a large spring of known stiffness being used to control the clamping force. This was tested on an Avery Dennison Universal testing machine and a continuous load-deflection plot was made. Fig 30 is a typical set of results for a joint loaded several times cyclically; the slip points can be clearly seen. If the joint did not slip the piece of lath in the middle would start to roll round. The joint could then be taken up to a high load without slipping. These tests indicated a shear stiffness at low loads of up to 150 kgf at 1000 kgf/cm, and this value was used for the computation.

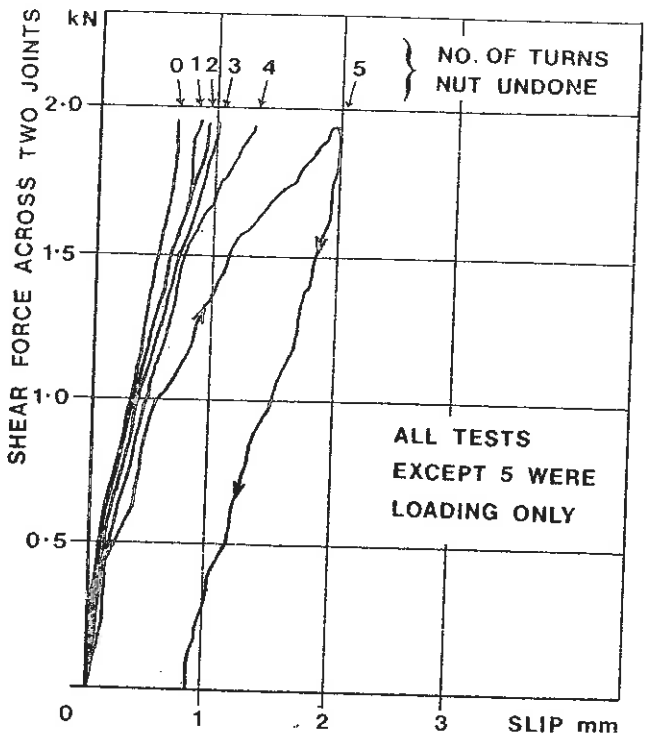

Fig 31. Typical load deflection curves for test using disc springs

After some computer runs had been made it became apparent that the shear stiffness was more critical to the collapse load than envisaged. It also appeared possible that the long spring could influence the shear stiffness and so when the washers for the real joint became available a further series of tests was made. These were carried out with the disc springs in various stages of compression. Fig 31 shows a typical set of load/deflection curves. These indicate that the curves are linear for a range of bolt loads from 500 down to 350 kgf (four turns undone) with an η of 1000 kgf/cm. This can only mean that the deflections are controlled by the shear deformation of the middle piece of timber and local deformations of the contact points. A check calculation on this basis gave a shear stiffness of a similar order of magnitude.

Tests on boundary connection. The maximum lath force is around 750 kgf and is transferred to the boundary by bolts in shear. The minimum edge distance allowed by DIN 1052 is 3 d, which means that the maximum permissible diameter of bolt should be 8 mm. The allowable bolt loads from DIN 1052 and from BS112 are shown in Table 2.

TABLE 2

ϕ	DIN 1052	ϕ	BS112	Short term and load sharing
8	110			
10	170	9·5	150	194
12	240	12·5	230	343

To take the maximum lath force in single shear would require seven 8 mm diameter bolts and the rules for spacing would not allow these to fit on the edge board. It was necessary to go outside the DIN rules to make the boundary connections and so it was proposed to carry out tests to prove the strength of 10 mm and 12 mm bolted joints.

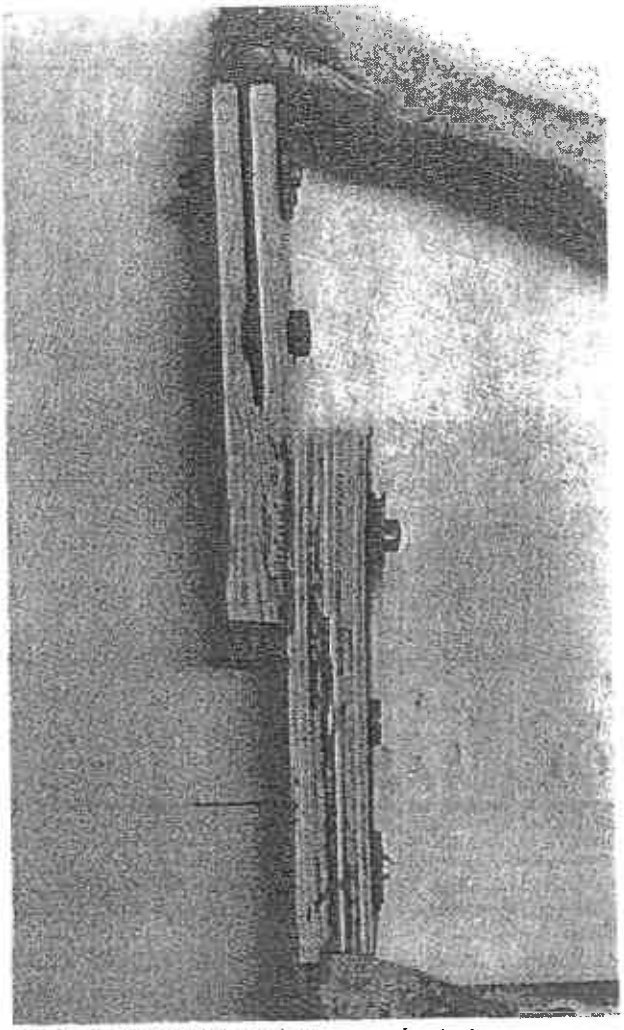

Fig 32. Assembly for boundary connection tests

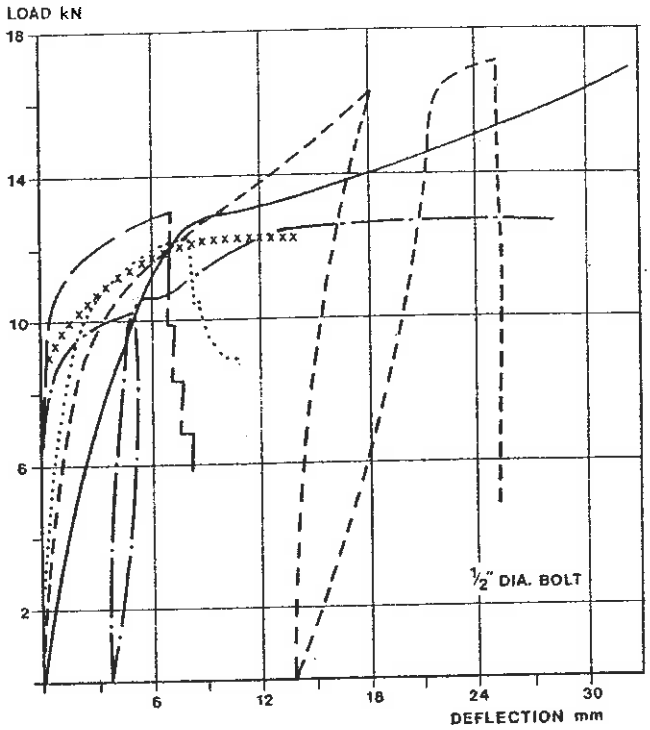

Fig 33. Results of boundary connection tests

A test assembly as Fig 32 was arranged using 12 mm and 20 mm bolts in accurately drilled holes. The end clearance was 50 mm. The assembly was tested in tension and load deflection curves as Fig 33 were obtained.

On the basis of these tests, bolt loads of 200 kgf and 400 kgf were agreed for the 10 mm and 12 mm bolts.

Rotation of lattice joint. The model testing work indicated that it was necessary to develop some in-plane shear stiffness in the lattice either by ties or by making the node joints rigid against rotation. The typical node joint, Fig 50, incorporates spring washers to obtain a clamping force. This force gives the node joint some resistance to rotation.

In order to evaluate this shear resistance, simple rotation tests were carried out. A joint was assembled as Fig 34, and loads were applied to the cantilever part by hanging a weight at varying radius. Deflections were measured using a dial gauge. Tests were done with virgin surfaces and after polishing by repeated rotations. A plot of the moment/rotation curves for polished surfaces is given in Fig 35.

Effect of fire-proofing salts

The hemlock laths had to be treated with flame proofing salts to satisfy the requirements of the fire officer. A sample panel complete with covering membrane was tested by lighting a fire beneath it to see if the fire spread. This test was considered to be satisfactory.

In the impregnation process 6 to 8 per cent of salts were absorbed into the timber in a water solution. The timber was then dried to a moisture content of around 10 per cent for glueing. In this drying process the salts combine with the walls of the cellulose fibres. This can reduce the strength of the timber, especially if the drying schedule is too severe, as is now admitted by some suppliers of salts.

As generally the strength and stiffness properties of timber vary in proportion, this discovery caused considerable anxiety lest the elastic modulus be reduced as well. To check on this a

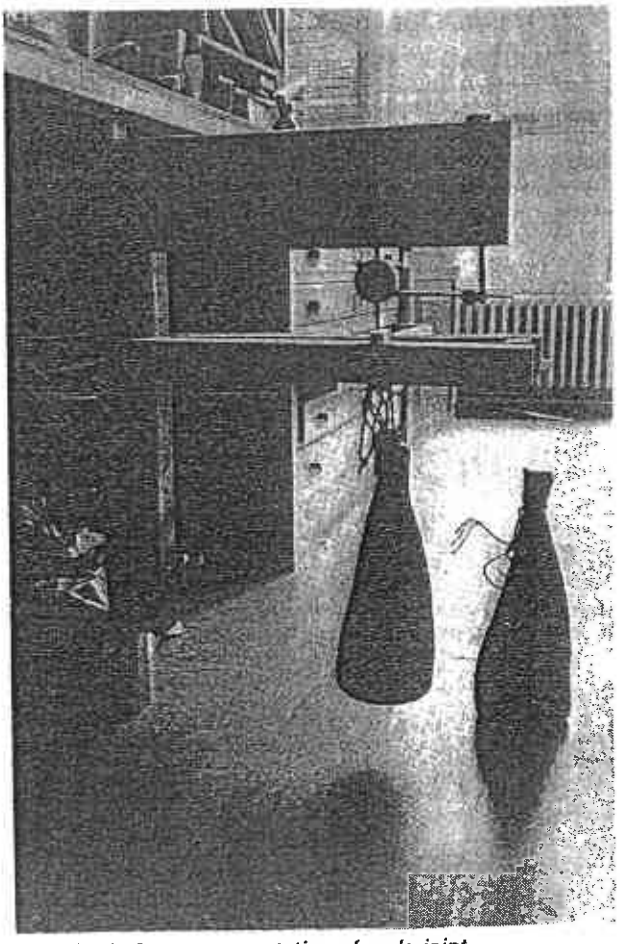

Fig 34. Rig for tests on rotation of node joint

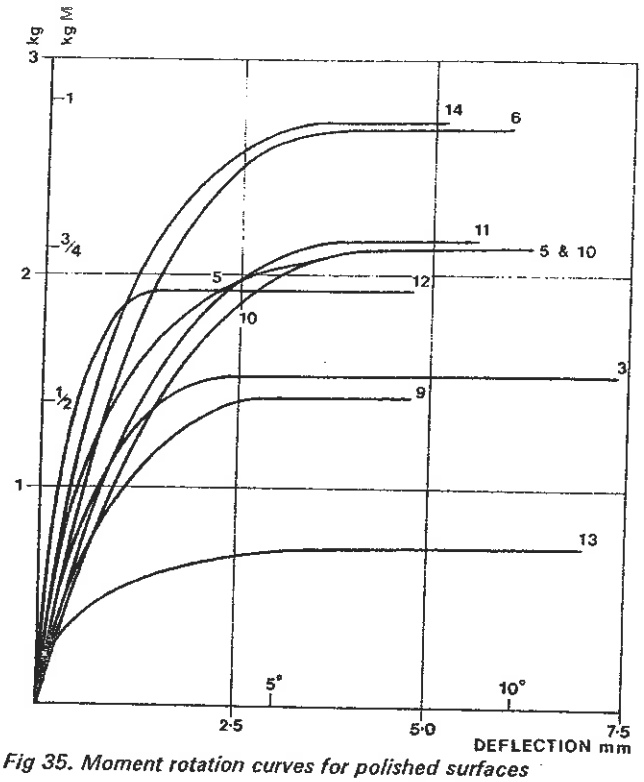

Fig 35. Moment rotation curves for polished surfaces

series of 4-point bending tests was carried out at the contractor's factory on treated and untreated timber. In these tests the central deflection was measured with a dial gauge and used to calculate the elastic modulus. The tests indicated that there was a 20 per cent drop in bending strength but it appeared that the elastic modulus increased by 10 per cent.

Model testing

Essen model

As soon as structural design was started, it was decided to make a 1/16 scale model of the 15 m span Essen dome to help gain some understanding of the behaviour of lattice shells. It was also decided to make the laths as thin and flexible as possible so that the structural properties resembled those of the Mannheim Multihalle shell. The most suitable material for the model laths was perspex strip which had a Young's modulus ¼ of that of timber. It was also easily worked and jointed.

The basic lattice for the model consisted of 3 × 1·7 mm laths at 50 mm centres. The dimensions of the model were as Fig 36. The joints were made by drilling small holes in the members at 50 mm centres and then passing small pins through the holes. The pins were then bent over to complete the joint. The laths were cut to length using the cutting pattern obtained from Atelier Warmbronn and were tied down with adhesive tape to a preformed base board (Fig 37).

The model was loaded by hanging bundled 100 mm nails at the nodes, the average weight of each nail being 12·5 g. Each load case consisted of a uniformly distributed load plus a point load at one of three points denoted as centre, side and corner. With the UDL constant the point load was increased and its deflection measured. This enabled the failing load to be determined. The UDL was then increased and the same procedure repeated. The failing point loads were then plotted against the UDL to establish the critical UDL.

Four sets of tests were carried out with different conditions of diagonal restraint. These were:

(A) pinned joints;

(B) glued joints, i.e. no rotation at the joints;

(C) pinned with loose ties;

(D) glued with nylon ties at all nodes.

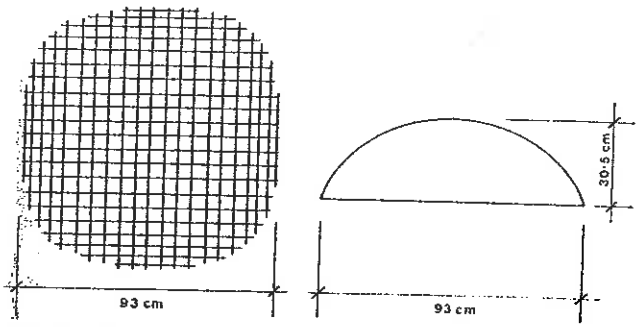

Fig 36. Dimensions of Essen model

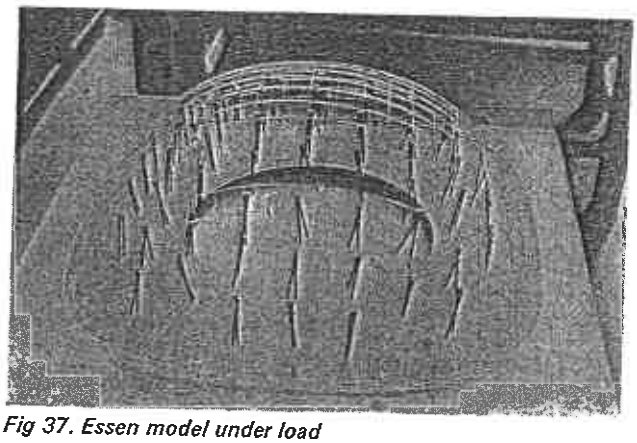
Fig 37. Essen model under load

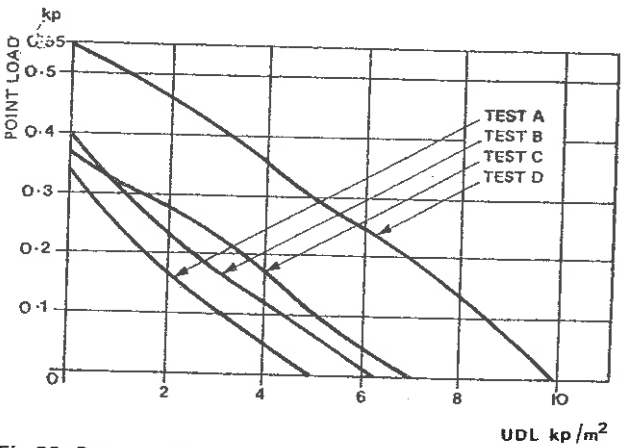

Fig 38. Essen model tests. Graph of centre point load against uniformly distributed load

Interpretation of results

For test case A the 'corner' point gave the lowest failing load. With this case the geometry of the structure allowed large sway movements to take place which greatly reduced the failing load. This mode of failure was prevented by the addition of some diagonal stiffness, and with ties this point became the strongest. The addition of diagonal stiffness increased the collapse loads and decreased the deflections prior to collapse, thus making the collapse far more sudden.

The centre point gave the most consistent failing loads. In the graph, Fig 38, the maximum centre point load is plotted against UDL to predict the critical UDL for each of the four sets of tests.

Scale factors

Dimensional analysis[19] was used to compare the properties and behaviour of the model to that of the real Essen shell and also to try to predict the failure loads of the Mannheim shells.

The properties of the structure which define and control its behaviour are listed as follows:

S = Span
If the model is geometrically scaled then its size can be represented by a typical dimension, say the span

$\frac{EI_{xx}}{a}$ = The out of plane bending stiffness of the surface per unit length (a = spacing of laths)

$\frac{E\,I_{yy}}{a^3}$ = is proportional to the contribution of the timber members to diagonal stiffness, if the joints between timber members are rigid

$\frac{EA}{a}$ = is the axial stiffness along the timber members per unit length

$\frac{E'A'}{ka}$ = is proportional to the contribution of the ties to the diagonal stiffness (A = area of ties, ka = tie spacing)

The collpase load q_{cr} is defined as a function of $S, \frac{E\,I_{xx}}{a}, \frac{E\,I_{yy}}{a^3}, \frac{EA}{a}, \frac{E'A'}{a}$.

As there are six terms involved including q_{cr} and two dimensions, force and length, four independent non-dimensional groups can be formed such as:

$$\text{I} = \frac{q_{cr}}{\frac{E\,I_{xx}}{a\,S^3}} = \frac{q_{cr}}{\frac{E\,I_{xx}}{a}} \times \frac{1}{S^3}$$

$$\text{II} = \frac{S^2\,I_{yy}}{a^2\,I_{xx}} = S^2 \times \frac{E\,I_{yy}}{a^3} \times \frac{1}{\frac{E\,I_{xx}}{a}}$$

$$\text{III} = \frac{S^2\,A}{I_{xx}} = S^2 \times \frac{EA}{a} \times \frac{1}{\frac{E\,I_{xx}}{a}}$$

$$\text{IV} = \frac{S^2\,E'A'}{k\,E\,I_{xx}} = S^2 \times \frac{E'A'}{ka} \times \frac{1}{\frac{E\,I_{xx}}{a}}$$

It is possible to form other non-dimensional groups such as $\frac{a^2\,A}{I_{yy}}$, but these further groups are only combinations of I to IV above. Hence:

$$\frac{q_{cr}}{\frac{E\,I_{xx}}{a\,S^3}} = f\left[\frac{s^2\,I_{yy}}{a^2\,I_{xx}}, \frac{s^2\,A}{I_{xx}}, \frac{s^2\,E'A'}{k\,E\,I_{xx}}\right] \quad \ldots . (1)$$

Equation 1 shows that non-dimensional group I is a function of II, III and IV only. Hence, if the model is constructed so that the numerical values of the groups II, III and IV are the same as on the full size structure, then the group I will also have the same value on model and full size structure. If group I has the same value for the model and the full size structure, then the collapse load on the structure can be found from the collapse load on the model, since $\frac{E\,I_{xx}}{a\,S^3}$ is known for both.

The deformation of the grid shell is mainly due to out-of-plane bending and diagonal distortions of the grid squares. If the diagonal stiffness is much less than the axial stiffness then the influence of the group III properties can be ignored. The diagonal stiffness is made up of the in-plane bending stiffness, group II and the tie stiffness, group IV. If the ties have a greater stiffness than the in-plane bending then group IV will overshadow group II. In this case, group I will be the same for the model and full scale structure provided that the tie stiffness is correctly scaled.

Therefore, to scale up the critical load from structure 1 to structure 2, this expression is used:

$$\frac{q_{cr}\ (1)}{q_{cr}\ (2)} = \frac{\left[\frac{E\,I_{xx}}{a\,S^3}\right](1)}{\left[\frac{E\,I_{xx}}{a\,S^3}\right](2)}$$

Prediction of collapse loads

In Table 3 the results from the Essen model testing are scaled up to predict failing loads for the Essen shell and for the Mannheim shells with both double and single grids. The Mannheim shells are not geometrically similar, and so an average value of the radius over the large area of the dome was taken as the controlling dimension (S) and compared with a similar dimension for the Essen model.

TABLE 3

	Collapse load including structure own weight in kgf/m²	
	Rigid joints	Rigid joints with ties
Essen shell (single layer) ..	150	—*
Mannheim Multihalle (single layer)	3·8	—*
Mannheim Multihalle (double layer)	100	160
Mannheim restaurant shell (single layer)	5·8	—*
Mannheim restaurant shell (double layer)	150	240

*Model results cannot be meaningfully scaled as the ratio of tie stiffness to out of plane bending is not correct.

The results demonstrated quite clearly the low buckling capacity of a single layer grid for the Mannheim shells. They also indicated the advantages of having a double layer grid with ties, and on the basis of the tests the decision was taken to double the grid.

Unfortunately, the model tests for a single layer grid cannot accurately predict the behaviour of a double layer grid, as the out-of-plane shear stiffness becomes important and cannot be modelled. The importance of this effect was not fully realized until after a Multihalle model had been made and tested, and the results compared with the computer model. It is discussed under *Comparison with computer results*, page 117.

Details of Multihalle model

A model of the Multihalle was constructed in a similar way to the Essen model described. It is to a scale of 1:60 and consists of 1·40 mm deep by 2·60 mm wide perspex members in a single layer with a joint spacing of 50 mm. One perspex member therefore represents $60 \times 5/50 = 6$ double layer members on the full scale structure.

The joints were not glued since the tests of the full scale joint showed that a single bolt connection does not provide sufficient stiffness to prevent relative rotation of the member in the plane of the lattice. However, the tests on the Essen

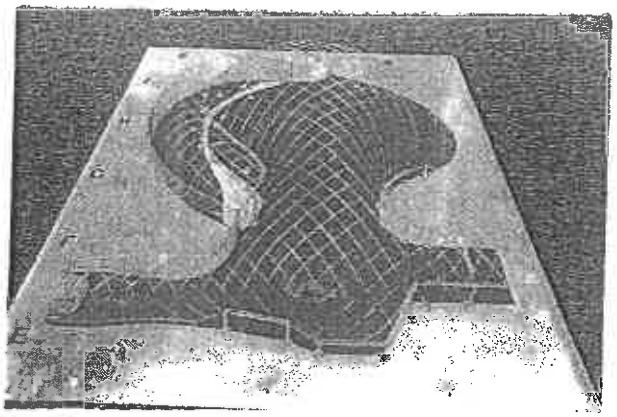

Fig 39. Multihalle model

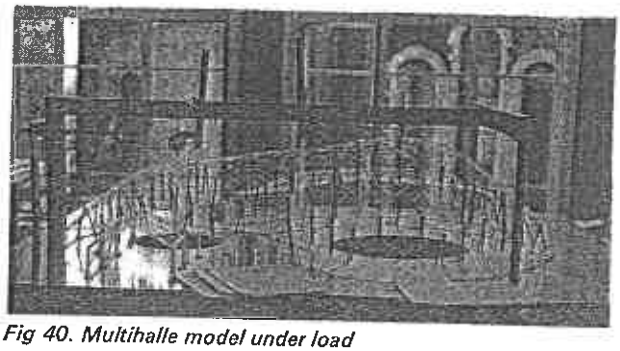

Fig 40. Multihalle model under load

model showed that the effect of glueing the joints is slight. The effect is further reduced if ties are present.

The model was built on a timber base board with perspex rod and sheet to represent the supporting columns, beams, arches, and concrete walls. No attempt was made to scale the stiffness of the supporting structure except for the arch in the Multihalle. This is because the deflections of the boundaries will not be large enough significantly to affect the behaviour of the shell.

Some of the tests were performed with diagonal ties consisting of stout linen thread added to the model. The ties were at a spacing corresponding to $3\sqrt{2}$ m on the full scale structure, and were attached to the nodes by wrapping the thread around the pins and then adding a drop of glue.

Photographs of the model are shown in Figs 39 and 40.

Test procedure

The model was tested using a similar procedure to that employed for testing the Essen model. A distributed load was first applied to the model and then a point load at various locations in turn. At each location the deflection of the structure was recorded as the point load was increased. The test locations are shown in Fig 41.

The procedure was adopted since it is possible to predict the collapse load from the load-deflection curves without actually collapsing the model. There was reluctance to collapse the model since once started, the collapse is difficult to stop and would result in considerable damage. This is especially so when the model has ties, due to the higher load carrying capacity, and this was demonstrated in the final Essen model test.

The load was again applied using 100 mm nails each weighing 12·5 g. The deflection of the structure under a point load was measured, using a dial gauge for the first experiments. Later, a lever arrangement was fabricated out of fine wire to avoid the friction inherent in a dial gauge, and this enabled readings to be obtained using smaller point loads. This meant that the stiffness of the structure could be evaluated without affecting it by gross local deformations.

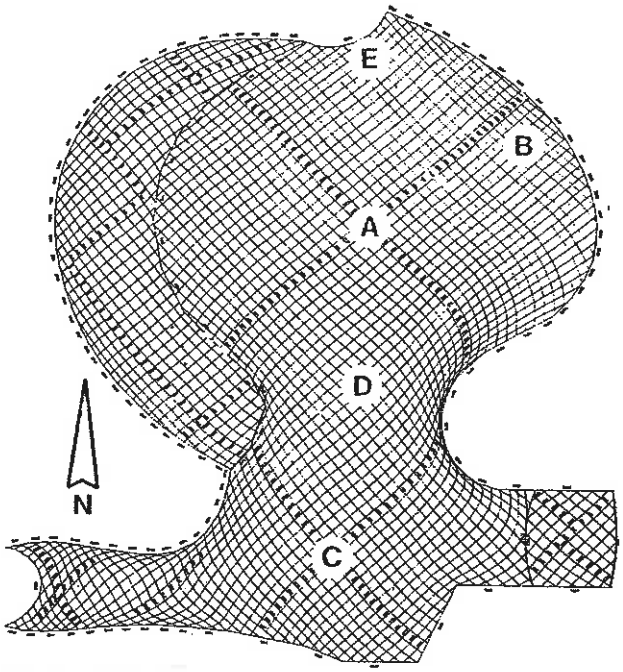

Fig 41. Multihalle plan with test load points

Test results

The load/deflection curves for point A without and with ties is given in Fig 42(a) and (b). Each curve represents the load/deflection behaviour with a constant distributed load.

The applied UDL is given by the ringed number adjacent to each curve. This number has to be multiplied by 0·625 to give the UDL in kgf/m².

Fig 43 shows how the point load/deflection behaviour varies with the UDL. These curves can be extrapolated to give the collapse UDL. In each case the curve which predicts the lowest collapse UDL should be used. The collapse UDL for the model can, therefore, be taken as:

4·5 × 0·625 = 2·8 kgf/m² with no ties

20 × 0·625 = 12·5 kgf/m² with ties

Scaling of results

As with the Essen model tests, the results were scaled using the non-dimensional group

$$\frac{q_{crit}}{\frac{I_{xx}}{a\,S^3}}$$

Scaled up in this way, the collapse load of the Multihalle shell was predicted as 63 kgf/m² with no ties and 280 kgf/m² with ties, and consequently ties were adopted for the real structure.

Comparison with computer results

The computer model with additional out-of-plane shear introduced in highly stressed areas predicted a collapse load of slightly more than 100 kgf/m² under uniform loading (see *Multihalle results*, page 123). The difference between this and the 280 kgf/m² predicted by the model tests occurs because the perspex model does not scale the shear deformation of the double layer members of the full scale structure. This is largely controlled by the slip/unit force 'η' of the individual node joints. The values of η are discussed in the section on mathematical modelling and tests to establish η are described in the section on timber testing.

A suitable non-dimensional group, including η, can be added to those on page 116,

which would be $\frac{\eta\, S^2}{ab^2E}$.

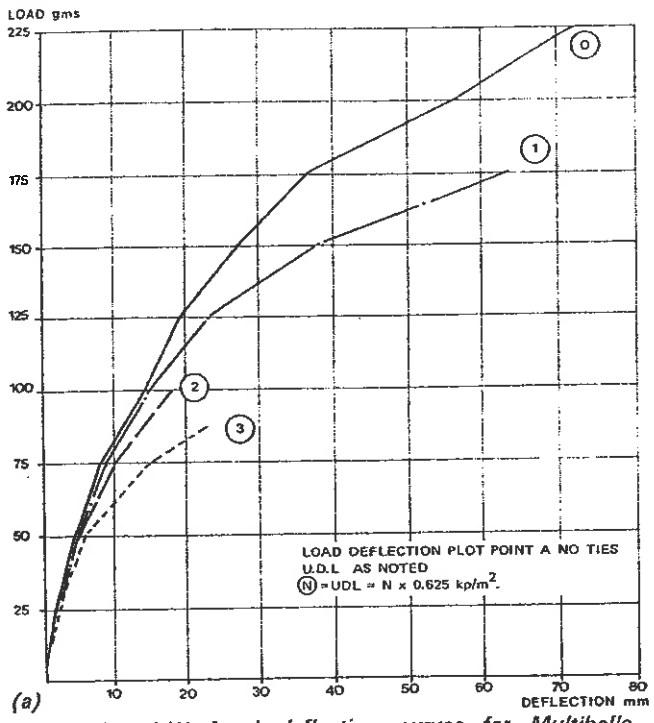

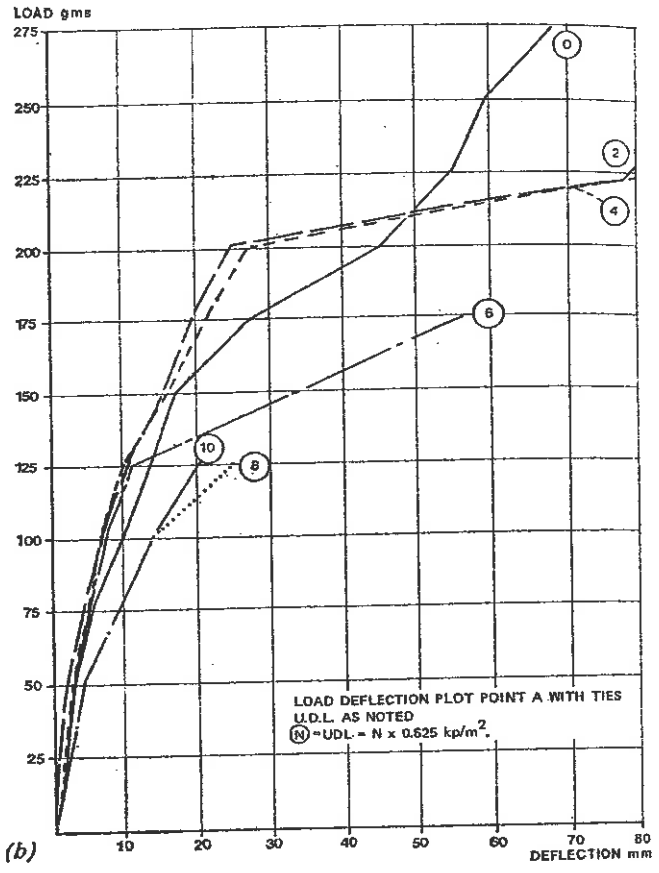

Fig 42 (a) and (b). Load deflection curves for Multihalle model

It would not be possible to construct a model in which both this group and group III $\frac{(S^2A)}{I_{xx}}$ are scaled if η is low and varying using a single layer model. The perspex model corresponds to a full scale structure with a very high value of joint stiffness and therefore predicts a higher collapse load than the computer model in which realistic values of η were used.

In spite of this drawback, the model was useful in providing qualitative data showing the type of buckling failure to be expected and the critical areas of the structure.

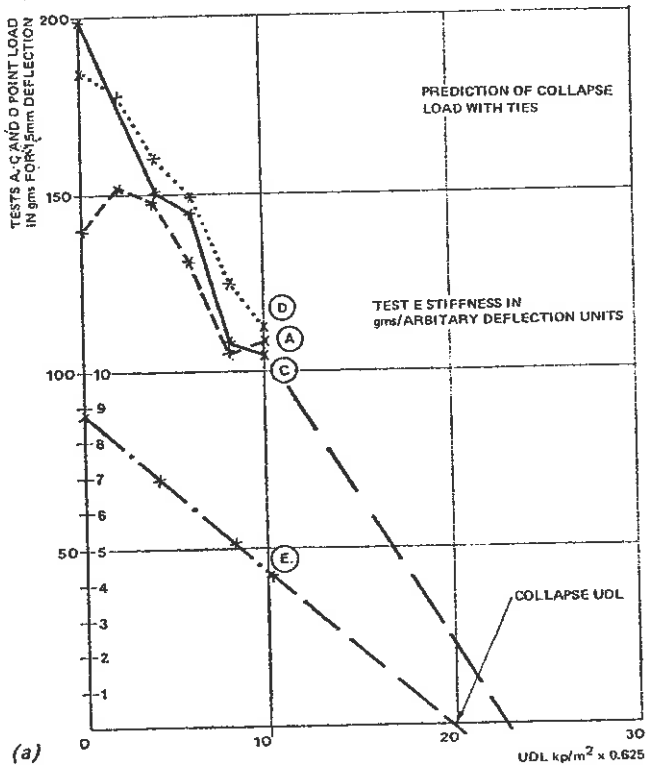

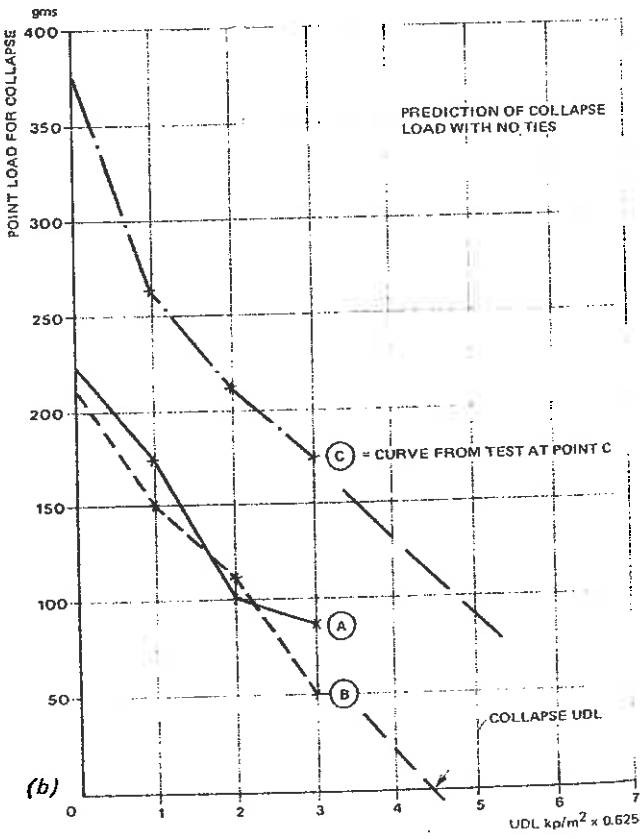

Fig 43 (a) and (b). Graphs of point load against uniformly distributed load

Mathematical modelling

The most crucial part of the analysis of the shells was the evaluation of the collapse load under various load distributions. This involved an analysis to predict the buckling behaviour and also to investigate stresses in the shells which greatly increase as the buckling load is approached.

The most interesting aspects of this analysis are not so much the intricacies of the methods employed, which have all been used before to various extents, but the ways it was necessary to idealize the structure in order to perform the analysis. This is, of course, a problem common to all structural analysis; however, in the case of the Mannheim shells, the complexity of the structural behaviour and the novel method of construction made it especially difficult.

There is always some degree of uncertainty in buckling calculations, partly due to approximations in the calculations themselves and partly due to the influence of constructional inaccuracies and other effects. Safety factors are therefore of great importance and these are discussed on page 123.

Analytical techniques

When the computer analysis of the shells was first considered, two alternatives were available; either to use an 'off the shelf' program or to write one specially. The second alternative held and still holds many attractions since there were certain phenomena—for example, the shear stiffness of the double layer grid—which required special study. It was felt that it should be possible to write a program which was economical in computer time and storage if the regular nature of the grid were utilized. This last point is important since the principal of superposition cannot be used in a situation where buckling is being investigated, and thus many more computer runs are necessary than is usually the case. However, it was decided that there was insufficient time to develop a program, and also the development costs could be prohibitive.

Standard linear structural analysis programs are based on the assumption that the equations relating the nodal forces to the nodal displacements are linear. In other words

$$P_i = \sum_{j=1}^{N} K_{ij}\, d_j \qquad \ldots . (1)$$

where P_i is the load or moment corresponding to the i^{th} degree of freedom of a structure, d_j is the displacement or rotation corresponding to the j^{th} degree of freedom, K_{ij} is a stiffness term and N is the total number of degrees of freedom. There would be N such equations and most programs then simply rearrange the equations to get

$$d_i = \sum_{j=1}^{N} F_{ij}\, P_j \qquad \ldots . (2)$$

where F_{ij} is a flexibility term. The deflections corresponding to loads $P_1, P_2 \ldots P_j \ldots P_N$ can now be found by substituting into these equations.

In the case of buckling or any non-linear behaviour, the nodal forces can again be related to the nodal displacements:

$$P_i = \phi i\ (d_1, d_2, \ldots, d_j, \ldots, d_N) \qquad \ldots . (3)$$

where this time ϕ_i is a non-linear function and would contain such terms as d_1^2 and $d_1 d_2$. It would be nice to solve these equations and get a solution of the form

$$d_i = \theta_i\ (P_1, P_2, \ldots, P_j, \ldots, P_N) \qquad \ldots . (4)$$

Once this is done for a particular structure, it would only be necessary to feed in the values of P_1 to P_N for any particular load to find the displacements and hence strains and stresses. Unfortunately, this is generally not possible and instead the set of equations (3) has to be solved numerically.

First program type

Two programs were investigated in detail. The first program predicts the buckling load of a structure by making assumptions which yield the following equation:

$$\lambda P_o = [K - \lambda G]\, d$$

where λP_o is the external load vector
- λ being the load factor
- d is the displacement vector
- K is the normal linear stiffness matrix
- G is a matrix whose terms depend solely on the geometry of the structure and a linear combination of the internal forces within the structure under a given load P_o. These internal forces are found by performing a purely linear analysis.

The structure is considered to have failed when the load factor is such that the displacements tend to infinity.

This corresponds to the matrix $[K - \lambda G]$ being singular or the determinant of this matrix being zero. This leads to a polynomial in λ, the lowest root of which gives the load factor at collapse.

The assumptions made in this method generally result in the collapse load being overestimated except for the case of the loading being funicular, when the 'exact' solution is obtained. The method is analogous to the 'classical' methods of analysing columns, arches and shells, and these also tend to overestimate collapse loads.

These thoughts are confirmed by Tezcan and Ovunc[20] who give further examples of structures where the method yields optimistic results.

In the case of the Mannheim shells, although the structure is designed to be funicular for self weight, there was concern as to the effect of non-funicular snow loads and imperfections and for this reason the method was rejected.

The method does, however, present certain advantages for structures where it is possible to estimate the degree of error in the result and adjust the safety factor accordingly. One advantage is the relative efficiency in terms of computer time, and a second advantage is that the load factors and deformation patterns can be found for a number of modes of collapse from only one computer run. This would be useful in a structure where it is possible to suppress the primary mode by some method and hence make other modes critical.

Program adopted

The second program examined uses the method described in Tezcan and Ovunc[20] and was written by Electronic Calculus Inc. The program was found to be more suitable and was used on a Univac 1108 computer with augmented core storage.

The method solves the set of non-linear simultaneous equations

$$P_i = \phi_i\ (d_1, d_2 \ldots d_j \ldots d_N) \quad (1) \text{ (Equation (3).}$$

using a technique based on the Newton-Raphson iteration scheme. The method involves the repeated solving of sets of linear equations to obtain successive approximations to the solution. The calculation is terminated when a sufficient degree of accuracy has been obtained.

The set of equations to be solved to find the $(r+1)^{th}$ approximation to the solution can be written as follows:

$$P_i - (P_i)_r = \left(\frac{\partial \phi_i}{\partial d_1}\right)_r ((d_1)_{r+1} - (d_1)_r) + \left(\frac{\partial \phi_i}{\partial d_2}\right)_r ((d_2)_{r+1} - (d_2)_r) + \ldots + \left(\frac{\partial \phi_i}{\partial d_j}\right)_r ((dj)_{r+1} - (d_j)_r) + \ldots + \left(\frac{\partial \phi_i}{\partial d_N}\right)_r ((d_N)_{r+1} - (d_N)_r) \qquad \ldots . (2)$$

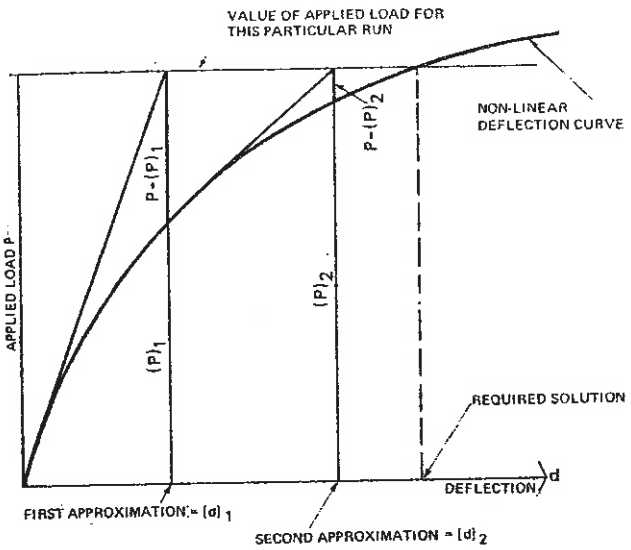

Fig 44. Graphical representation of solution technique

The values $(P_i)_r$ and the partial derivatives $\left(\frac{\partial \phi_i}{\partial d_j}\right)_r$ are found using equation (1) and the values of displacement $(d_1)_r \ldots (d_N)_r$ obtained from the previous iteration. The set of equations is linear in $(d_1)_{r+1} \ldots (d_N)_{r+1}$ and can be solved using standard methods involving matrix algebra.

This procedure is repeated replacing r by $r+1$ until the error represented by $P_i - (P_i)_r$ is within acceptable limits. The first set of displacements $(d_1)_1 \ldots (d_N)_1$ are calculated assuming $(d_1)_o = (d_2)_o = \ldots (d_N)_o = 0$ and the results from the first iteration will therefore be identical to those obtained from a purely linear analysis.

It should be noted that the solution obtained will apply to only one load distribution and load factor. The whole analysis will have to be repeated for each separate loading condition.

This procedure can be expressed graphically for a structure with only one degree of freedom (Fig 44).

If the load imposed on the structure is greater than the buckling load, then no solution can be found. Thus bounds can be obtained for the buckling load—the lower bound being the highest load at which the program converges and the upper bound the lowest load for no solution.

Further technical details of the method can be found in a paper by Tezcan and Mahapatra[21], which goes into more detail than the paper by Tezcan and Ovunc quoted at the start of this section.

Input data and derivation of member properties

Having decided on a suitable program, the next problem was to form a mathematical model of the structure suitable for analysis by the program. Ideally the model should contain the same number of nodes as the true structure, have curved members and have loads applied along the members. There would be nine degrees of freedom at each node (see *Out-of-plane bending and shear* and *In plane forces*, page 121) and the ties would be represented by members which are removed when they are in compression. Additionally, the stress/strain relation of the timber would be non-linear and would also be time dependent to represent creep.

The program chosen did not fulfil any of these requirements. It used straight beam elements between nodes with six degrees of freedom. To reduce computer time with the iterative solution technique the program had been written to operate entirely in core and there was therefore a limit to the number of nodes which could be used.

For the Multihalle one computer node represented 144 nodes of the real structure and for the restaurant 81. The input data had to be selected so that this coarse grid of beam elements would model the behaviour of the real structure.

The member properties for the true structure were derived assuming linear stress/strain behaviour and the data obtained from the timber tests. They were then modified for the computer model where one straight member represents a number of curved double layer members of the true structure.

The relevant co-ordinates of the structure were selected from computer output produced by Büro Linkwitz and IAGB.

Out-of-plane bending and shear. If the members and joints of the structure are assumed to have linear load/displacement properties then the bending behaviour of a member out of the plane of the lattice will be dependent upon three properties:

(a) the value of Young's Modulus, E;

(b) the geometric properties of the section;

(c) the stiffness of the joints in the structure in taking horizontal shear forces.

For the arrangement shown in Fig 28, the force P can be related to the moment M and curvature K by considering longitudinal equilibrium:

$$P = -\frac{ab^2}{2}\frac{d}{dx}\left(\frac{M}{b^3} - \frac{1}{6} b\, EK\right)$$

The slip S can be found by compatibility of displacements:

$$\frac{ds}{dx} = \frac{1}{E}\left(\frac{13\, bEK}{6} - \frac{M}{2b^3}\right)$$

Hence, using the relation $\frac{P}{s} = \eta$:

$$\frac{d^2}{dx^2}\left(M - \frac{1}{6} b^4\, EK\right) = -\frac{2}{ab^2}\frac{\eta}{E}\left(\frac{13}{6} b^4\, EK - M\right) \quad \ldots . (1)$$

Equation (1) is the governing equation for out-of-plane bending of a member.

As a check, it can be seen that if η is infinite, $M = \frac{13}{6} b^4\, EK$, and if $\eta = 0$ then $M = \frac{1}{6} b^4\, EK$. This is as one would expect, since $\frac{13}{6} b^4$ is the value of the full composite second moment of area, whereas $\frac{1}{6} b^4$ is the sum of the individual second moments of area of the two laths.

It is possible to represent such a structure in a computer analysis. However, to do so it is necessary to introduce an extra degree of freedom at each end of a member, or two degrees of freedom per node, one for the members in each direction. A suitable degree of freedom would be the slip, S.

If no extra degree of freedom is introduced, then the nearest member equation which can be found is

$$\frac{12}{13}\frac{d^2M}{dx^2} = \frac{-2\eta}{ab^2E}\left(\frac{13}{6} b^4\, EK - M\right) \quad \ldots . (2)$$

The behaviour of a member obeying equation (2) can be compared with a member on the true structure obeying equation (1) by considering the following simple examples:

EXAMPLE OF BUCKLING LOAD OF PIN-ENDED COLUMN

If the length of the column is L, the buckling load, Pcr, using equation (1) above is given by

$$P_{cr} = \frac{26}{12} b^4 \frac{E\pi^2}{L^2} \frac{\left(1 + \frac{1}{26}\frac{E\pi^2 ab^2}{L^2\eta}\right)}{\left(1 + \frac{1}{2}\frac{E\pi^2 ab^2}{L^2\eta}\right)}$$

and if η is large

$$P_{cr} = \frac{26}{12} b^4 \frac{E\pi^2}{L^2} \frac{1}{\left(1 + \frac{12}{26}\frac{E\pi^2 ab^2}{L^2\eta} - \frac{12}{26^2}\left[\frac{E\pi^2 ab^2}{L^2\eta}\right]^2 + \ldots\right)}$$

Equation (2) gives:

$$P_{cr} = \frac{26}{12} b^4 \frac{E\pi^2}{L^2} \frac{1}{\left(\frac{12}{26}\frac{E\pi^2 ab^2}{L^2\eta}\right)}$$

EXAMPLE OF SIMPLY SUPPORTED BEAM WITH UNIFORM LOAD

For the true model of a beam span L with a load W/unit length, the midspan deflection δ is given by

$$= \frac{WL^4}{\frac{26}{12} b^4 E}\left[\frac{5}{384} + \frac{3}{8\theta}\left[1 + \frac{2}{\theta}\left(\frac{1}{\cosh\sqrt{\theta}} - 1\right)\right]\right]$$

where $\theta = \frac{26\eta L^2}{4ab^2 E}$

For the computer model, the beam can be replaced by a string of N shorter beams loaded at the nodes by loads equal to $\frac{WL}{N}$. If N is even the midspan deflection is given by:

$$\delta = \frac{WL^4}{\frac{26}{12} b^4 E}\left[\frac{5}{384}\left(1 - \frac{4}{5N^2}\right) + \frac{3}{8\theta}\right]$$

$$= \frac{WL^4}{\frac{26}{12} b^4 E}\left[\frac{5}{384} + \frac{3}{8\theta}\right] \text{ if } N \text{ is large}$$

Again, where $\theta = \frac{26\eta L^2}{4ab^2 E}$

It can be seen in both examples that if η is large, the deflection due to joint flexibility is identical for both computer and true models. In addition it can be seen that if η is reduced, the computer *underestimates* the true member stiffness. The approximation is therefore safe.

Equation (2) is represented in the computer in the following form:

$$\frac{d^2M}{dx^2} = \frac{A}{\lambda_y I_{xx} 2(1+\nu)}(M - EI_{xx}K) \quad \ldots . (3)$$

where I_{xx} = full composite second moment of area
A = member area
ν = Poissons ratio (used to determine shear modulus, G)
λ_y = area shape factor

To bring equation (3) into the same form as equation (2), λ_y must be given by the relationship

$$\lambda_y = \frac{E}{2(1+\nu)} \times \frac{72}{169} \times \frac{a}{\eta}$$

Since one member in the computer analysis represents a number of members on the true structure, the values of A and I_{xx} in the computer model are chosen such that A/L and I_{xx}/L are constant for the computer and true models, where L is the member spacing which equals the member length. ν and λ_y are independent of L.

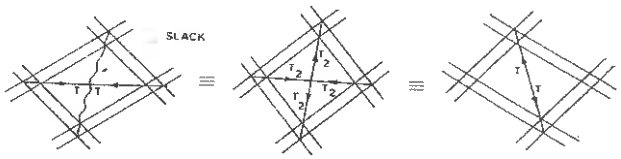

Fig 45

In plane forces. In plane forces are taken in three distinct ways:

(a) axial forces in the timber members;
(b) axial tensions in the tie members;
(c) shear forces in the timber members;

The axial stiffness of the timber and tie members depend solely on their cross-sectional areas and the values of Young's modulus. The ties can only transmit tensile forces, but in the computer model the ties can also transmit compressive loads. However, the axial stiffness of the ties is low compared to that of the timber members and also the timber members cross approximately at right angles. It can be seen, therefore, that one tie in tension is equivalent to one tie in compression or two ties of one half the stiffness, one in tension and one in compression. (See Fig 45).

The tie areas in the program are therefore taken as:

(Tie area on true structure) × ½AB if computer model has ties in two directions

or (Tie area on true structure) × AB if computer model has ties in only one direction.

$$\text{Where A} = \frac{\text{Tie spacing on true structure}}{\text{Tie spacing on computer model}}$$

$$\text{B} = \frac{\text{Tie Young's Modulus}}{\text{Timber Young's Modulus}}$$

The last term is necessary since the program assumes that all members have the same material properties. The area of the timber members is taken simply as their actual area multiplied by the ratio of member spacing of computer to true model.

Shear forces in the timber members act in conjunction with the ties in resisting forces in the lattice in the directions of the ties. The behaviour of the members in taking shear forces is dependent on the following three factors:

(a) their bending stiffness about an axis normal to the lattice;
(b) the member spacing;
(c) the stiffness of the joints on the structure.

The relative rotation of the timber members in each direction at the joints represents an additional degree of freedom at each node. The introduction of an extra degree of freedom can be avoided by making the assumption that the moments at the ends of each member are approximately equal. If this assumption is made, then the joint flexibility can be represented as a member shear flexibility.

If the lattice in Fig 46 is subject to strains ϵ_{11}, ϵ_{22} and γ_{12}, then the contribution of member shear forces to σ_{11}, σ_{22} and σ_{12} is given by

$$\frac{(\sigma_{22}\cos^2\alpha - \sigma_{11}\sin^2\alpha)}{\cos\alpha\sin\alpha} =$$

$$\frac{12EI_{yy}}{L^3}\left(\frac{1}{1 + \frac{12EI_{yy}}{2KL}}\right)(\epsilon_{22} - \epsilon_{11})$$

where K = joint stiffness, M/θ, as described on page 114.

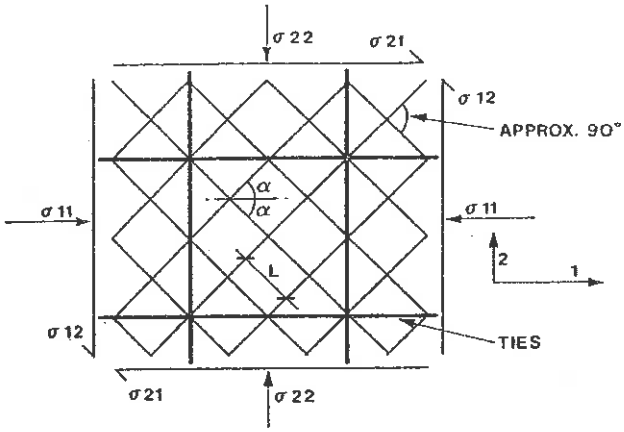

Fig 46

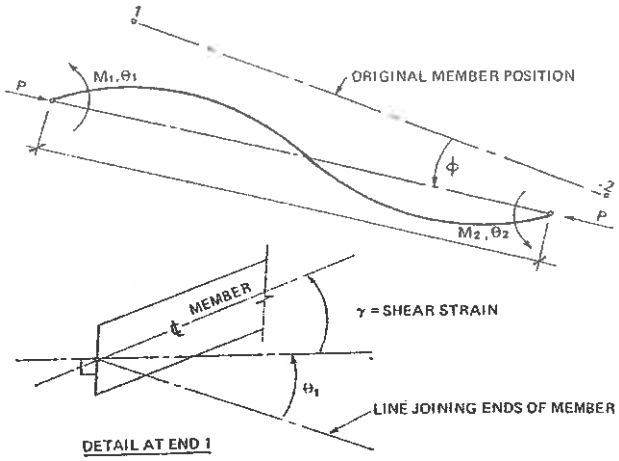

Fig 47

The joint stiffness K can be replaced by a member shear stiffness such that

$$K = \frac{L\,A\,E}{4(1+\nu)\lambda_x}$$

Where ν = Poisson's ratio

λ_x = Area shape factor for in-plane shear forces

i.e. $\dfrac{(\sigma_{22}\cos^2\alpha - \sigma_{11}\sin^2\alpha)}{\cos\alpha\sin\alpha} =$

$$\frac{12EI_{yy}}{L^3}\left(\frac{1}{1+\dfrac{24\lambda_x(1+\nu)I_{yy}}{L^2A}}\right)(\epsilon_{22}-\epsilon_{11})$$

The term $\left(\dfrac{1}{1+\dfrac{24\lambda_x(1+\nu)I_{yy}}{L^2A}}\right)$ is

equal to the drop in member stiffness due to shear flexibility if the member axial loads are relatively low and the moments at the ends of the member are equal. This can be seen by examining the member stiffness equations given below.

Therefore, the value of I_{yy} in the computer model is chosen such that I_{yy}/L^3 is the same for computer and true models. As mentioned previously the member area A is chosen such that A/L is constant. Therefore, λ_x is taken as the same value in the computer model as in the true model.

Reduction in member stiffness by axial forces. The presence of axial force in the timber members alters their shear and bending stiffness. If the force is compressive then the stiffness is reduced, if tensile it is increased. In order to handle members with high shear flexibility, the program had to be amended so that the member stiffness equations were as follows:

If M, θ, ϕ and P are defined as in Fig 47 and θ_2 corresponds to the degree of freedom common to all members meeting at joint 1, then

$$M_1 = \frac{4EI}{L}\left[\epsilon\left(\frac{S_1}{2}+\frac{S_2}{4}\right)+\left(\frac{S_1}{2}-\frac{S_2}{4}\right)\right](\theta_1-\phi)$$

$$+\frac{2EI}{L}\left[\epsilon\left(S_1+\frac{S_2}{2}\right)-\left(S_1-\frac{S_2}{2}\right)\right](\theta_2-\phi) \quad \ldots\ldots(1)$$

Where S_1 and S_2 are non-dimensional stability functions:

$$S_1 = \frac{(1-2\mu\cot 2\mu)\mu}{4(\tan\mu-\mu)} \quad \text{(Compression)}$$

$$= \frac{(1-2\mu\coth 2\mu)\mu}{4(\tanh\mu-\mu)} \quad \text{(Tension)}$$

$$S_2 = \frac{\mu(2\mu\,\mathrm{cosec}\,2\mu-1)}{2(\tanh\mu-\mu)} \quad \text{(Compression)}$$

$$= \frac{\mu(2\mu\,\mathrm{cosech}\,2\mu-1)}{2(\tanh\mu-\mu)} \quad \text{(Tension)}$$

$$\mu = \left(\frac{PL^2}{4\left(E-\dfrac{\lambda 2(1+\nu)P)\,I}{A}\right)}\right)^{1/2} \quad \text{(Compression)}$$

$$= \left(\frac{-PL^2}{4\left(E-\dfrac{\lambda 2(1+\nu)P)\,I}{A}\right)}\right)^{1/2} \quad \text{(Tension)}$$

$$\text{and } 1/\epsilon = \frac{1+\lambda 8\,(2S_1+S_2)\,(1+\nu)\,I}{L^2A}$$

E, I, A, ν and λ are as previously defined. When $I = I_{xx}$, $\lambda = \lambda_y$ and when $I = I_{yy}$, $\lambda = \lambda_x$.

In the case of a member with high shear stiffness, $\epsilon = 1$ and equation (1) reduces to the form

$$M_1 = \frac{4EI}{L}S_1(\theta_1-\phi) + \frac{2EI}{L}S_2(\theta_2-\phi)$$

This is identical to the equation quoted by Horne and Merchant[22] if the stability functions S_1 and S_2 are replaced by s and c such that:

$$s = 4S_1$$

$$\text{and } c = \frac{S_2}{2S_1}$$

The member stiffness described by equation (1) is very different from that of a member with high shear stiffness. For example, in the special case $P = O$, both S_1 and S_2 are equal to 1·0 and equation (1) reduces to:

$$M_1 = \frac{4EI}{L}(0{\cdot}75\epsilon + 0{\cdot}25)(\theta_1-\phi)$$

$$+\frac{2EI}{L}(1{\cdot}5\epsilon - 0{\cdot}5)(\theta_2-\phi)$$

If the shear stiffness is high, $\epsilon = 1{\cdot}0$, but as the shear stiffness is reduced ϵ also reduces. Thus at some point the term $(1{\cdot}5\epsilon - 0{\cdot}5)$ will be zero and will then become negative. The physical meaning of this can be seen in Fig 48.

If end A of the beam is rotated by the angle θ, the resulting moment at the fixed end B is given by

$$M = \frac{2EI}{L}(1{\cdot}5\epsilon - 0{\cdot}5)\theta$$

If $\epsilon = 1{\cdot}0$, the standard result $M = \dfrac{2EI}{L}\theta$ is obtained.

If $\epsilon = 0$, a moment of opposite sign is produced: $M = -\dfrac{EI}{L}\theta$.

This can be seen physically by considering Fig 49.

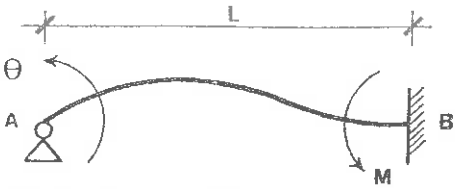

Fig 48. (Diagram for shear stiffness example)

$$M = -F\,h$$

$$\theta = \frac{F\,L}{\left(\frac{h}{2}\right) \times \left(\frac{2I}{h^2}\right) E} = \frac{F\,L\,h}{E\,I}$$

$$\text{i.e. } M = \frac{E\,I}{L}\,\theta$$

Boundary conditions. The boundary conditions of the true structure correspond to elastic supports. However, it was decided that except for arches and cables, it would be sufficient to provide fixed 'pinned' supports for the computer model. This is because the translational stiffness of the supports is high and the effect of edge rotation is small except in the immediate region of the boundary. The effect of the pinned supports, if any, would be to reduce the buckling load. A small number of boundary nodes were fixed in rotation; this was necessary to reduce the half bandwidth of the structure stiffness matrix to enable the computer model to be analysed with the core storage available.

The arch and cable boundaries were modelled by introducing members to represent the arches and cables.

The program handles only one load distribution and one load factor per run. This is due to the fact that superposition of loads cannot be used since the load/deflection relationship is non-linear.

Multihalle results

The Multihalle model had 192 nodes, 297 main members representing the lattice, 254 ties and four members representing a boundary area. A total of 14 runs was carried out for varying load cases and member properties. The first four of these runs were invalid as it was discovered that the program was not able to accept members with very low shear stiffness. The program was altered before the fifth run to include the member stiffness equations given previously.

The ninth run with a UD load of 105 kgf/m² failed to converge, but in a way that indicated that only a small reduction in load was necessary. The shear stiffness of the nodes for this run was taken as 2540 kgf/cm. Subsequent modifications to the tie connection details altered this value and further tests on the typical node confirmed that the value should be 1000 kgf/cm. Runs with this value of shear stiffness and a UD load had failed, so it was known that the shear stiffness had to be increased in certain areas. Hand calculations were carried out to test the effect of shear flexibility on an equivalent column section, and these indicated that the laths with high axial forces needed extra shear stiffness. The computer model was altered so that certain members had shear stiffness values of 2540 and 5000 kgf/cm depending on the axial load and run 12 with this pattern converged with a UD load of 100 kgf/m² (load factor = 2·85).

Runs were also carried out with a heavier load on the unheated area and run 13 with the same varying values of shear stiffness converged with loads of 150 and 87·5 kgf/m² on the unheated and heated areas respectively. (Load factor = 2·5.)

Restaurant

Having discovered the problems with the shear stiffness for the Multihalle, the runs for the restaurant were carried out with the intention of finding how much stiffness was

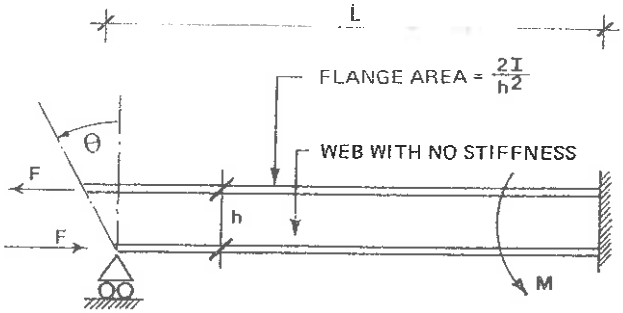

Fig 49

necessary. The computer model had 224 nodes, 318 lattice members, 155 ties, 20 arch members and 15 cable boundary members. It was possible to include more nodes than in the Multihalle model, since ties were only added in one direction instead of two. This effectively decreased the band width of the stiffness matrix.

The first three runs were carried out with a deliberately high load to test the program and to obtain a pattern of forces. After this, the shear stiffness of the members was increased in areas of high force. Some problems were encountered with the arches due to shear flexibility since the program assumes that all members have the same value of ν, λ_x and λ_y.

Run 7 converged after 8 cycles at a load of 150 kgf/m² (load factor 2·5). This run was particularly interesting as the structure was on the point of collapse and had developed large deflections in critical areas.

It was felt that the flat area by the river was particularly susceptible to non-uniform loading and so further runs were tried with an additional load in this region. These indicated that additional bending stiffness was required and so additional laths were inserted. Run 10 converged with loads of 110 kgf/m² generally and a load of 150 kgf/m² on the flat area.

Safety factors

For normal beam elements it is conventional to calculate the moments applied to the beam by the loads and compare these to the breaking strength of the beam. For such a simple example, it does not matter whether the safety factors are applied to the loads or to the stresses. The current philosophy is now changing from factored stresses to factored loads.

Buckling problems have never been treated so simply. For timber and iron columns, it has been known for a long time that Euler's theoretical buckling load cannot be achieved, because the load is never concentric. Early investigators, particularly Hodgkinson[23] and Claxton Fidler[24] devised rules to cover these errors which were expressed as tables of ultimate stress against values of length divided by diameter or radius of gyration. The same approach is currently applied to steelwork but using the Perry Robertson formula[25]. This makes allowances for initial curvature and secondary moments at the ends and includes a factor of safety of 1·7. An additional allowance for imperfect fixing of the ends is made when selecting the effective lengths.

For timber lattice shells the problem is more complex. As well as a factor for the probability of the load being exceeded, the overall factor of safety must take into account variations in member properties, accuracy of shape, load distribution and the accuracy of the computer model. It is useful to consider these partial factors along the lines suggested by ISO 2394[26] as in Table 4.

Development of details

The work of detailing the grid shell can be broken down into a series of design decisions. The details of the grid, typical node point, ties, blocking pieces are related to the non-linear analysis and involve stiffness. The details at the boundaries were calculated on a strength basis with normal factors of safety, but were influenced by geometrical requirements.

TABLE 4

Partial factor from ISO 2394	Property or factor or particular application	Comments	Value
γ_{m_1}	Variations in E	It is reasonable to assume that all the timber member properties are directly related to E. The shear stiffness tests have indicated that these are linear provided the bolts do not become excessively slack. This must be checked by inspections. The collapse load is essentially directly proportional to E.	
		A mean short term value of 111×10^3 kg/cm² has been taken for timber. Some allowance must therefore be made for the probability of the E value of the laths being less than this.	1·2
		This mean value is taken at 12 per cent moisture content and would reduce by about 10 per cent if the moisture content increased to 18 per cent.	1·1
		With long term effects the E could drop to 60 per cent of this value but the dead load stresses are much lower than the stresses near collapse and although creep could take place at this stress level the higher value of E would still apply for short term disturbing loads. For long term disturbing loads there would be considerable warning of collapse and so this value should be looked at in conjunction with γ_{c_1}.	1·2
γ_{m_2}	Accuracy of shape of shell	Computer model with 6 m straight members has poor shape. Excessive deformation will be eliminated by site checking.	1·2
γ_{s_1}	Variations in loading	See report on loads of short duration. It is presumed that snow on Multihalle will be cleared by heating.	1·4
		(For the case of a 10 kgf/m² imposed load equal to a once in 50 years' snowfall this factor can be less.)	(1·2)
γ_{s_2}	Not applicable		
γ_{s_3}	Accuracy of computer model and assumptions	Can be broken down into effect of: (a) Straight members 6 m long representing parallel laths. Pessimistic in that effect of double curvature on out-plane bending and shear is neglected. Pessimistic in that shape is bad (already taken into account in γ m²). Pessimistic in that member buckling can take place within the plane of the lattice. (b) Representation of low out of plane shear stiffness: pessimistic, see Fig 00. (c) Effect of rotational stiffness: pessimistic, see *in plane forces*. (Pessimistic means that computed collapse load would be lower than actual).	1/1·2
γ_{c_1}	Nature and significance of buckling collapse	Little warning and total collapse. Therefore use 1·3 where short term E applies. If a longer term E was used this would imply a slow failure and a lower value could be used.	1·3
γ_{c_2}	Consequences of failure	If the Hall is closed when the snow load exceeds the design load, the consequences of failure will be small in terms of loss of life. At other times this factor can be accounted for by γ_{s_1}.	1·0

OVERALL FACTOR OF SAFETY (PRODUCT) = 2·85

For the restaurant shell and unheated areas, a load of 60 kgf/m² has been taken. This includes a snow load of 40 kgf/m² which represents a one-day snowfall with a return period of 100 years, or a three-day snowfall with a return period of 50 years. As the design life of the building is 20 years, this represents an extreme value and in this case it is acceptable to use a value of $\gamma_{si} = 1{\cdot}2$. This results in an overall factor of safety of 2·45.

The decisions leading to the selection of 50 × 50 mm laths and the doubling of the grid layers have already been explained

The typical node joint

In order to take advantage of the increased stiffness of the double layer lattice it is necessary to transmit shear at each node joint, but during erection one layer has to slip over the other. This implies that mechanical connectors cannot be utilised to generate shear in the finished joint, and so friction between the timber surfaces must be used. To achieve adequate friction there has to be a clamping force which must be maintained when the timber shrinks. This can be effected with a bolt and spring if the range and stiffness of the spring is adequate.

Some years ago, the Timber Research and Development Association conducted some experiments on a friction grip timber joint to be used in house construction. This joint used Bellville spring washers both as a means of applying a known tension to the bolt and as a means of reducing the effect of creep on bolt tension. Their reports suggested a co-efficient of friction of 0·47 with the timber stressed to its allowable bearing stress.

Initial calculations indicated that a shear force of 150 kg would be required, which meant that a clamping force of 400 kg would be suitable. This force gave a bearing pressure at about the same level as the allowable stress quoted in CP112. At this level, creep was not thought to be a problem. It was anticipated that the movement of the timber between 21 per cent and 13 per cent moisture content would be around 2 per cent. (See *Testing programme*, page 113). It was therefore necessary to find a spring system which could maintain a force of 400 kg after 5 mm shrinkage. The final joint, Fig 50, has four 35 mm diameter disc springs which, in series, gave a load deflection curve as Fig 51.

The spring washers were separated from the timber by a flat washer 55 mm in diameter and 1 mm thick. This thickness was chosen so that it would spread the load and thus prevent local crushing and yet be flexible.

As explained this typical node was tested at TRADA to establish its shear stiffness.

Ties

The model tests on the Essen and Multihalle shell demonstrated that the addition of ties to increase the diagonal stiffness of the lattice increased the collapse load and

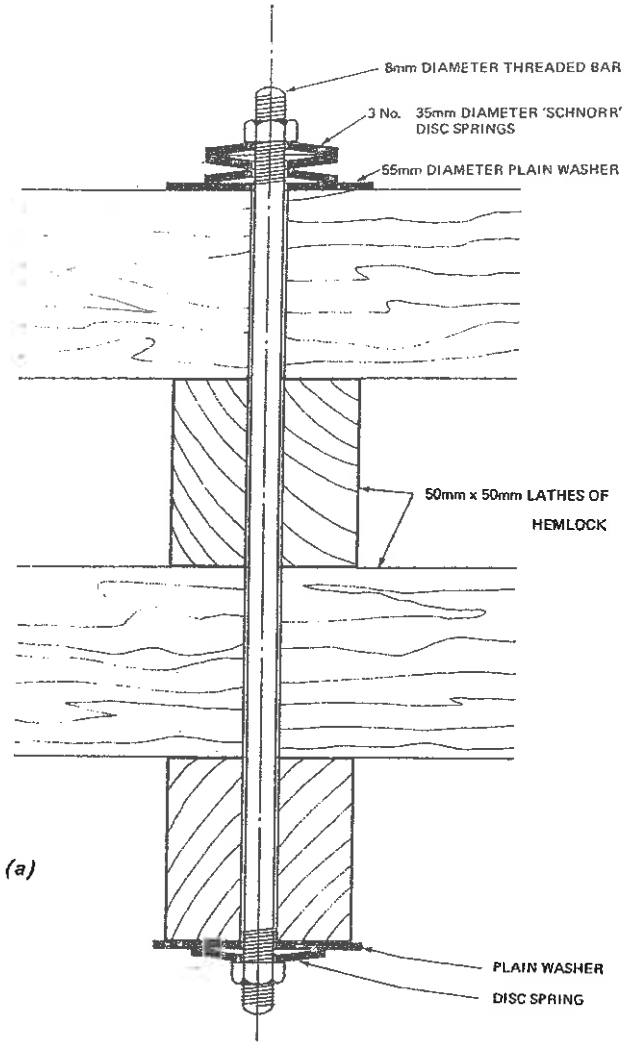

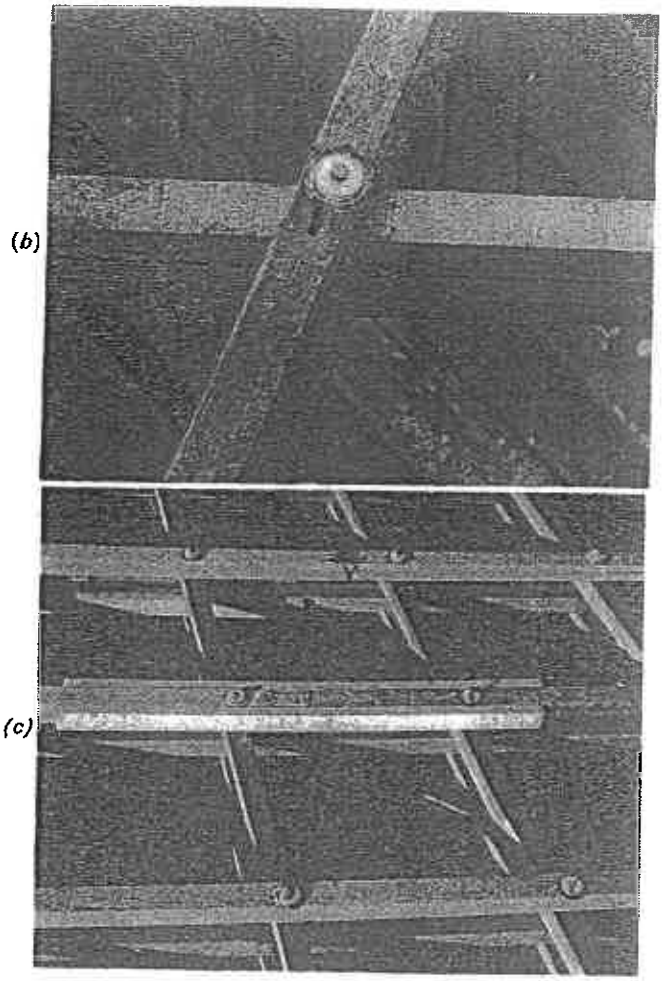

Fig 50(a), (b) and (c). Node joints

reduced the size of the buckle. With ties the shell under uniform loading became more brittle and collapse was sudden. The Mannheim shells are irregular in shape and subject to natural loads which are non-uniform; for such effects diagonal stiffness is essential to the load-carrying behaviour and prevents certain modes of gross deformation. The tests on the rotational stiffness of the joints indicated that this was low. Investigations into using the Trevira-reinforced PVC skin as diagonal stiffening showed that the elasticity of this material was too low to be effective, and it was subject to creep and deterioration in ultra-violet light. Steel wire ties were selected as having the necessary properties of strength and stiffness.

By this time, some successful runs of the non-linear programme for the Multihalle had been carried out. This showed that a pair of 6 mm diameter 19 wire strand ties at 4·5 m c/c, through every sixth node in each direction, would provide suitable stiffness.

It was hoped to fix the ties inside the grid at their intersection points, but it was difficult to achieve an adequate simple fixing able to transfer 1·0 tonne from any one pair of cables to the laths.

The alternative fixing arrangement was to fix the ties on the outside of the shell at each lattice node. With the slotted holes on the outer layer, there was no room for fixings additional to the node bolts, so these had to be used to attach the ties as well. Some small aluminium cable clamps were found which are used in electrical engineering and which use two 8 mm tightening bolts. One half of the clamp is threaded and can be used to replace the top nut on the standard node. The loose part of the clamp could be placed later and secured with another nut. A loose bolt could be used in the second hole of the clamp. (See Fig 52).

There was thus no problem to grip the wire and to transfer the forces to the bolt. However, with the slotted holes in the top layer of laths, the bolt would not bear on the timber and some form of shear connector was required. Standard bulldog connectors have 12 mm holes and were not suitable. It was thought that normal flat washers with the spring washers would have sufficient friction but simple tests proved that this was not so. Eventually the contractor was persuaded to order 50 mm diameter bulldog connectors with 8 mm holes, which were the ideal connection.

The same aluminium clamp was used in groups of three for the end connection of the ties connected to strips of steel, which were bolted to the edge members in various ways according to type.

Blocking pieces

The later runs of the non-linear programmes indicated that lack of shear stiffness of the composite members was initiating

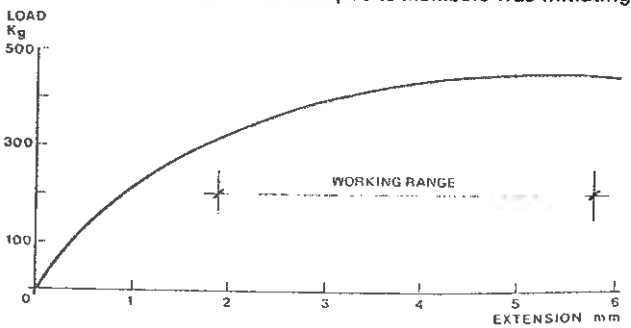

Fig 51. Load deflection curves for disc springs

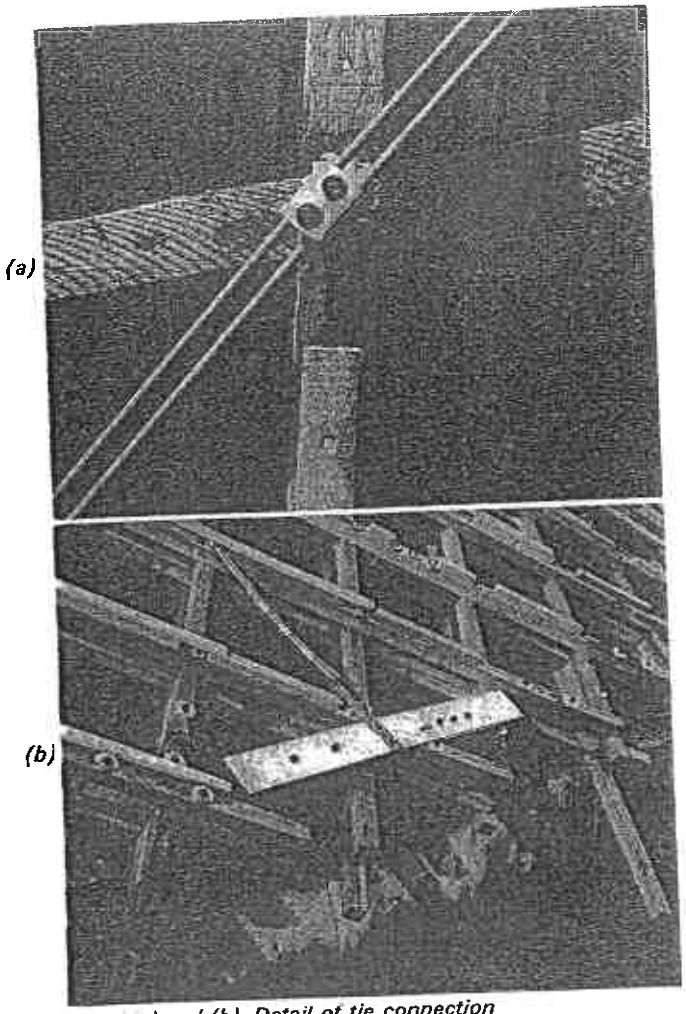

Fig 52(a) and (b). Detail of tie connection

buckling. Further tests on the actual joint confirmed the correctness of the stiffness value which had been used. It seemed clear from these tests that the load deflection behaviour was controlled by shear deformation of the laths at right angles to and between the loaded members. The stiffness could not therefore be increased by altering the bolt arrangement.

To obtain an adequate and consistent factor of safety over the whole of the shell, it was necessary to increase the stiffness in members which had a high axial load. This was done in the computer model and led to satisfactory load carrying behaviour. It was then necessary to find a way of increasing the out-of-plane shear stiffness in the real structure.

Blocking pieces between the laths with bolts right through at a suitable spacing were the obvious solution. The problem was to find a rigid connection. Bolts and dowels in pre-drilled holes were controlled by the stiffness of the bolt in bending and bearing. An arrangement which gave no slip at the interfaces was required and this meant glueing or friction grip bolting.

Glueing on site has many problems. First there was that of tolerance; the gap between the laths varied in width. There was also the problem of glue: Resorcinal was the most suitable, but this would take 10–14 days to set at 10°C and by then the shell was to be erected in the winter. During the setting period the glue line pressure would have to be maintained for the curing period without movement, and it was felt that walking on the laths would cause movement.

Because of these problems, glueing was abandoned and a friction system investigated. Tolerance was still a problem but this was overcome by using wedges. Three 8 mm bolts with the standard spring washers were then used to clamp the laths and wedges tight. (See Fig 53).

Extra strengthening

The part of the restaurant shell by the concrete boundary adjacent to the river is very flat. The direct forces in the laths normal to this boundary are the largest in both shells and the area is susceptible to snow drifting. It was therefore thought prudent to try a computer run with a concentrated load in this area. It was found that if the load in the remainder of the shell was reduced the collapse load was also reduced. From consideration of the shell as an arch in the direction of the high lath forces, it was apparent that the additional load above the uniform load was causing bending in the flat area of the laths rather than arch forces. The bending moments which were proportional to the difference in load were causing deflections which initiated buckling. It was considered reasonable to limit the difference in loading to 40 kgf/m² equal to the design snow load and to strengthen the shell for that case. To do this it was necessary to increase the bending stiffness by 50 per cent by adding extra double laths in that area. These were laid up loosely in the grid and the bolts drilled and fixed after erection.

Joints in laths

The laths were made up in the Poppensieker factory into lengths 30 to 40 m long by finger jointing. The finger joints used were only 20 mm long with a 6 mm root, a profile chosen by the contractors to suit their machines. It was one which would be more suitable for joining laminating boards than for this special use, and quite a number of finger joints broke on site during handling and erection.

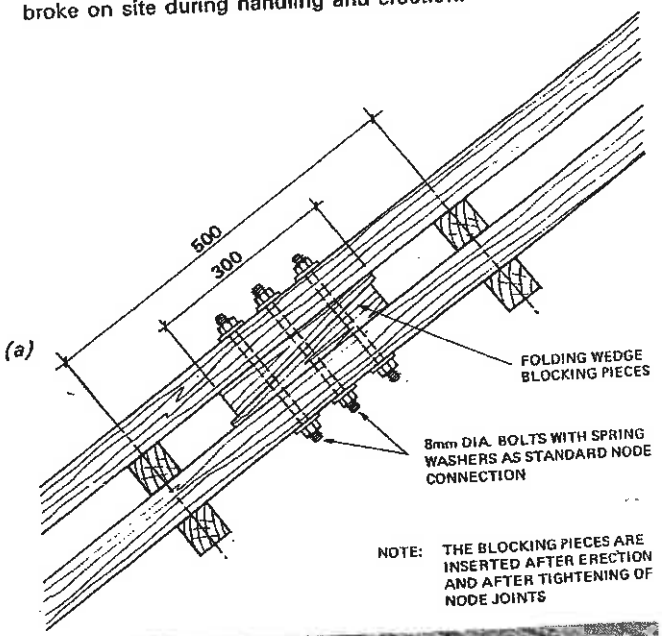

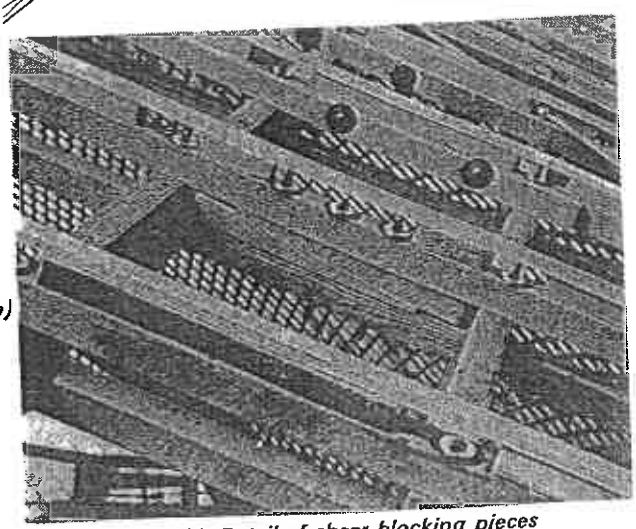

Fig 53(a) and (b). Detail of shear blocking pieces

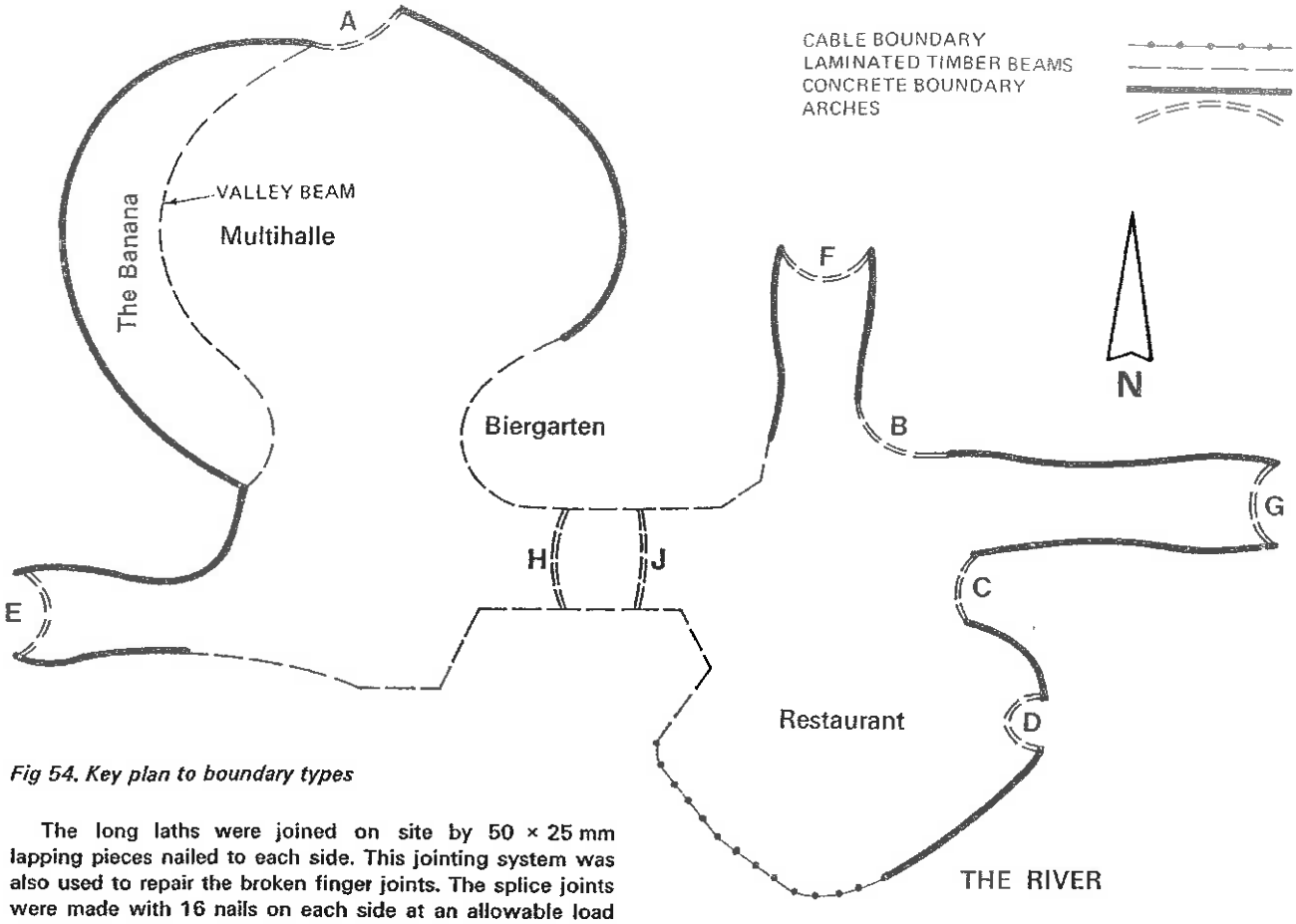

Fig 54. Key plan to boundary types

The long laths were joined on site by 50 × 25 mm lapping pieces nailed to each side. This jointing system was also used to repair the broken finger joints. The splice joints were made with 16 nails on each side at an allowable load of 30 kgf/nail. However, following the experiences with the stiffness of the blocking pieces, it was thought necessary to check on the stiffness of the nailed joints and a reference was found.[27] Calculations on a pair of laths bent to uniform curvature showed that the low stiffness of the nailed joints caused loss of bending moment which, with the low shear stiffness of the standard node, extended a considerable distance from the joint. The overall effect of joints and breaks would have been a loss of out-of-plane bending stiffness in the order of 30 per cent. To stiffen up these joints and make them rigid, the standard spring washers were used to generate friction, two on each side of the joint.

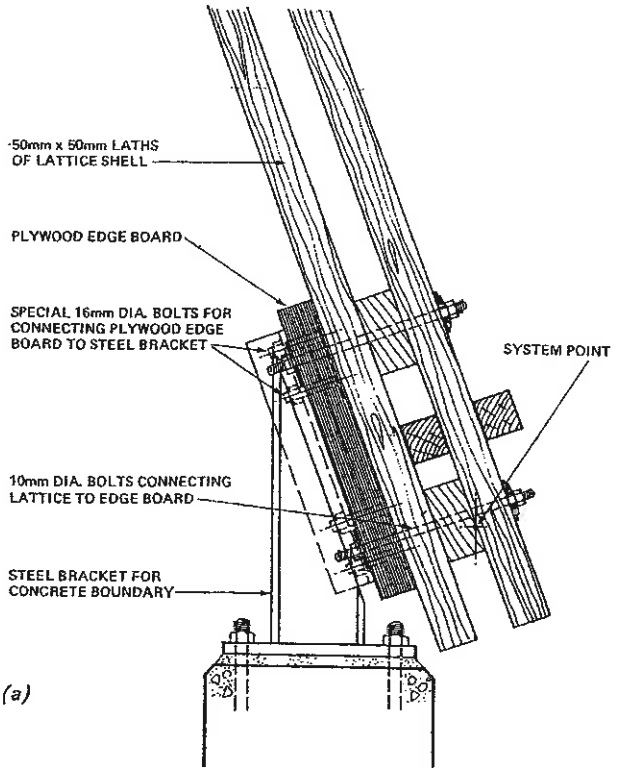

Fig 55(a) and (b). Arrangement at concrete boundary

Boundary details

A key plan to the boundary types is shown on Fig 54.

Concrete boundaries

Some simple calculations for the connection to the concrete walls showed that the forces which had to be transferred from the laths were larger than had been supposed, at first, and with the double layer grid the eccentricity was increased and this created moments at the boundaries. A detail using a 400 × 50 mm plywood board attached to the concrete wall with steel brackets and bolts was suggested. The plywood board allowed the laths to be bolted to it with two or three bolts which seemed to be the right number to take the forces. The board could be bolted to the bracket and the bracket bolted down to the concrete.

The problem of the varying angle could be solved by having a bracket which rotated; however, this would require expensive fabrication and friction grip bolts were necessary to take the moments. The detail shown in Fig 55 was therefore adopted, and it was decided that each bracket should be individually fabricated to the correct angle.

Valley beam boundary

Atelier Warmbronn had proposed for the valley beams a circular timber beam 500 mm in diameter with the grid shell attached by steel straps. Calculations proved that the 500 mm diameter beam was nicely sized, but there were problems with the connection of the laths. The final detail followed that of the concrete boundary; the laths were bolted to a 400 × 50 mm plywood board, attached to the round beam by steel brackets and coach screws. In this case coach screws had to be used, as bolts were impossible, but the steel brackets for the main shell and for the Banana were jointed by a loose steel strap so that they formed a complete ring. This would prevent the coach screws from having to work in tension and they were satisfactory in shear. (Fig 56).

The valley beams were supported by horizontal or suitably sloped plates on top of steel columns. Horizontal forces on the plates were taken by timber connectors. The columns were designed to take the horizontal forces as vertical cantilevers.

Cable and beam boundaries

Originally, all the external boundaries supported on columns were intended by Professor Otto to be cable boundaries. In a region of a grid shell where the boundary forces are fairly constant along the edge and where the change in angle of the boundary system line at the columns is not so great as to cause excessive reaction, cable boundaries are perfectly feasible. Part of the restaurant shell boundary met these conditions and has been made with cables.

The remainder of the cables were badly conditioned; spans varied widely along a run of cables as did the load conditions. These would have required a change of cable force at the column heads, and there were some severe angle changes at the columns which would produce large resultant forces from the cable. In some areas the grid shell twisted around the system line by as much as 10 or 20 degrees/m. It was decided that these factors made the use of cable boundaries in this area impractical.

Alternatives in the form of beams were examined. Possibilities which were considered were:

(a) round timber beams similar to the valley beam;
(b) thick laminated timber beams, beneath the lattice;
(c) thin laminated timber beams on either side of the lattice with a core of a steel tube which would stiffen the beams against out of plane bending and torsion;
(d) thin laminated timber beams 60 mm thick on either side of the lattice.

It was decided to adopt thin laminated timber beams because they provide the correct amount of resistance to the

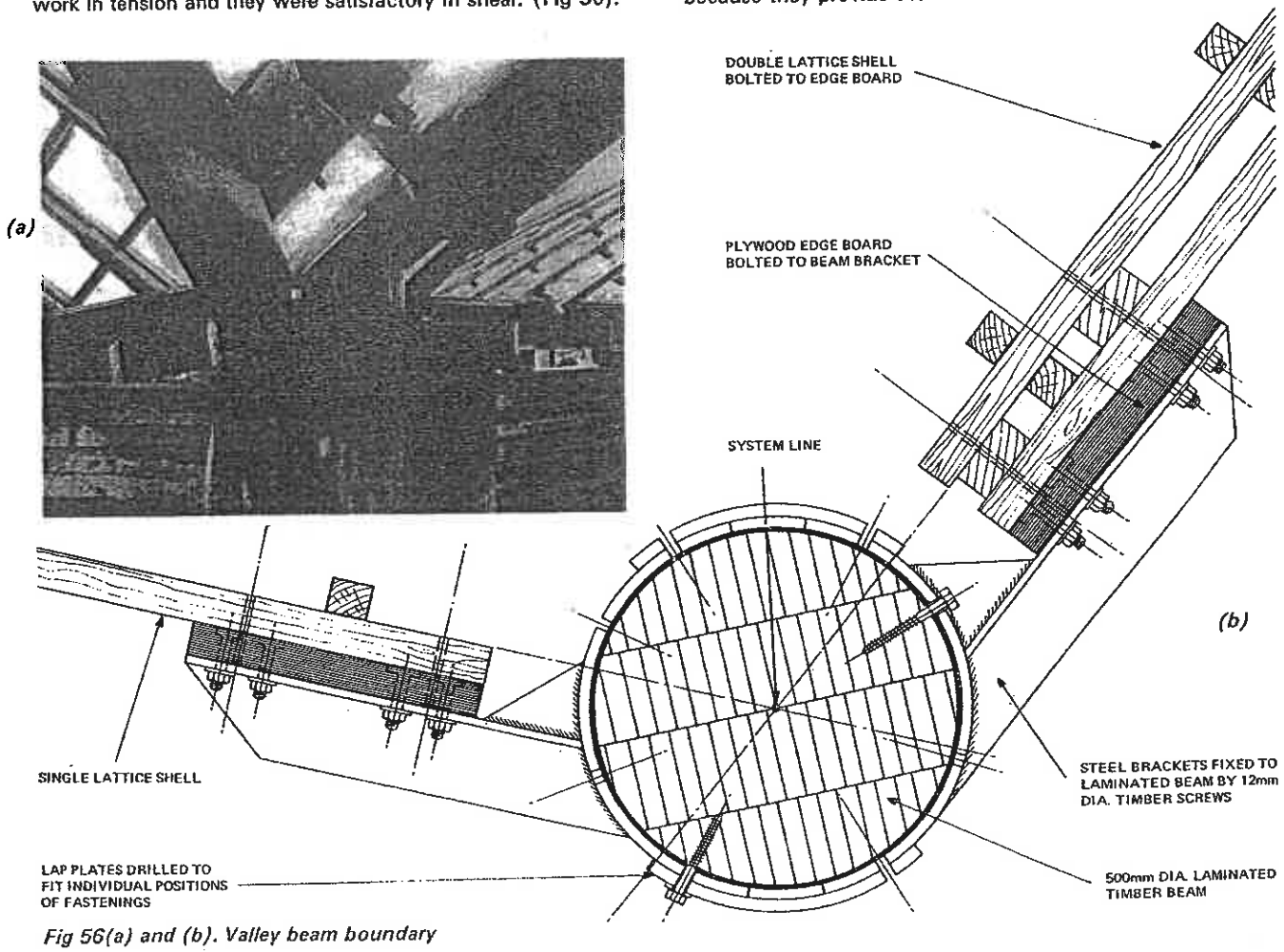

Fig 56(a) and (b). Valley beam boundary

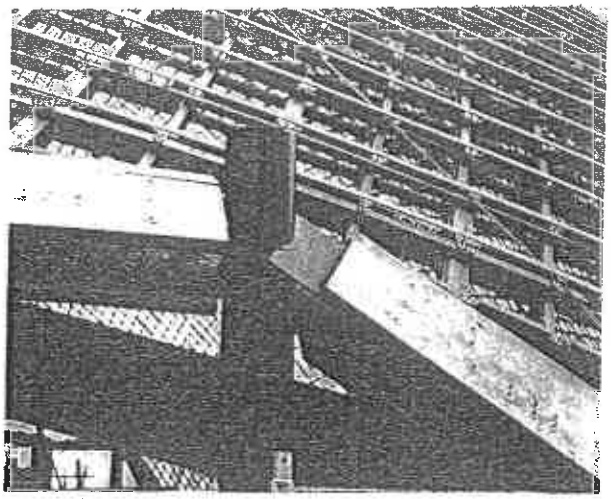

Fig 57. Laminated beams

lath force with the minimum increase in edge thickness. The simplest way to connect the beams to the columns was to connect the beams to parallel steel plates with timber connectors, and to weld the plates to the top of the columns (Fig 57). Although the connection was simple the geometry was not; every beam/column connection had different angles of fine and twist. It was realised that the plates would have to be accurately cut to profile and accurately positioned on the columns and that there would be no way of checking the accuracy of the resulting work except by offering up the beams. Ove Arup & Partners reluctantly undertook to define the profiles and the marking system for the plates. They also undertook to supply the contractor with the exact lengths of the beams to fit the plates.

To calculate the plate profiles a geometrical program for the Hewlett Packard desk computer was written. The input for this program was the system point of the column head, the bottom of the column, the system point at the other end of the beam and a point in the lattice. The program took a week or so to prepare and because of the difficulty of checking the output a second program was written.

Having got confirmation that the programs were giving the correct answers, work started on plotting the profiles full size on pre-prepared drawings. As this work proceeded it was realised that there were inconsistencies in the Linkwitz grid in the region of boundaries which met at an angle. It also seemed that some beams had to be twisted through 90° in 5 m so that the grid would fit. To overcome these difficulties it was necessary to select the grid points with care, and in some places the points were adjusted to ensure an even slope of the boundary. Where the laths were prevented from being bolted to the beams by the column connection plates or because the angle of the beam was incorrect, they were cut and additional laths inserted as reinforcement.

Details for cable boundary

It was necessary to devise details for the part of the restaurant shell which was to be supported on cables. When uniformly loaded in their plane, cables behave in a similar way to beams except that the compression force is made up by the end reactions. The difference is that the cable profile and the end reactions must be compatible with the load distribution.

For a grid shell standing on a cable, the cable profile should be defined by the distribution of forces in the laths, but conversely, the forces in the laths could be defined by the cable profile. It is the interaction that is important and it was thought that if the cable and associated region of shell were well conditioned there would not be a problem. The Linkwitz forces were taken as being suitable for defining the cable profile but in each span the forces were averaged out and treated as uniform so that the cable profile was taken to be a parabola.

The cable boundary is divided into five spans by columns. These columns are not stiff enough to change the force in the direction of the cable by a significant amount so the cable tension has to be considered constant. The spans are 5, 6.5, 10, 6·5, 5 m. The loads and slopes also vary in each span. The influence of the cable tension on the deflection was studied to try and optimise it for all spans and finally a cable tension of 12·5 tonnef was selected.

To connect the grid shell to the cable it was decided to stick to the principle of first connecting the laths to a plywood

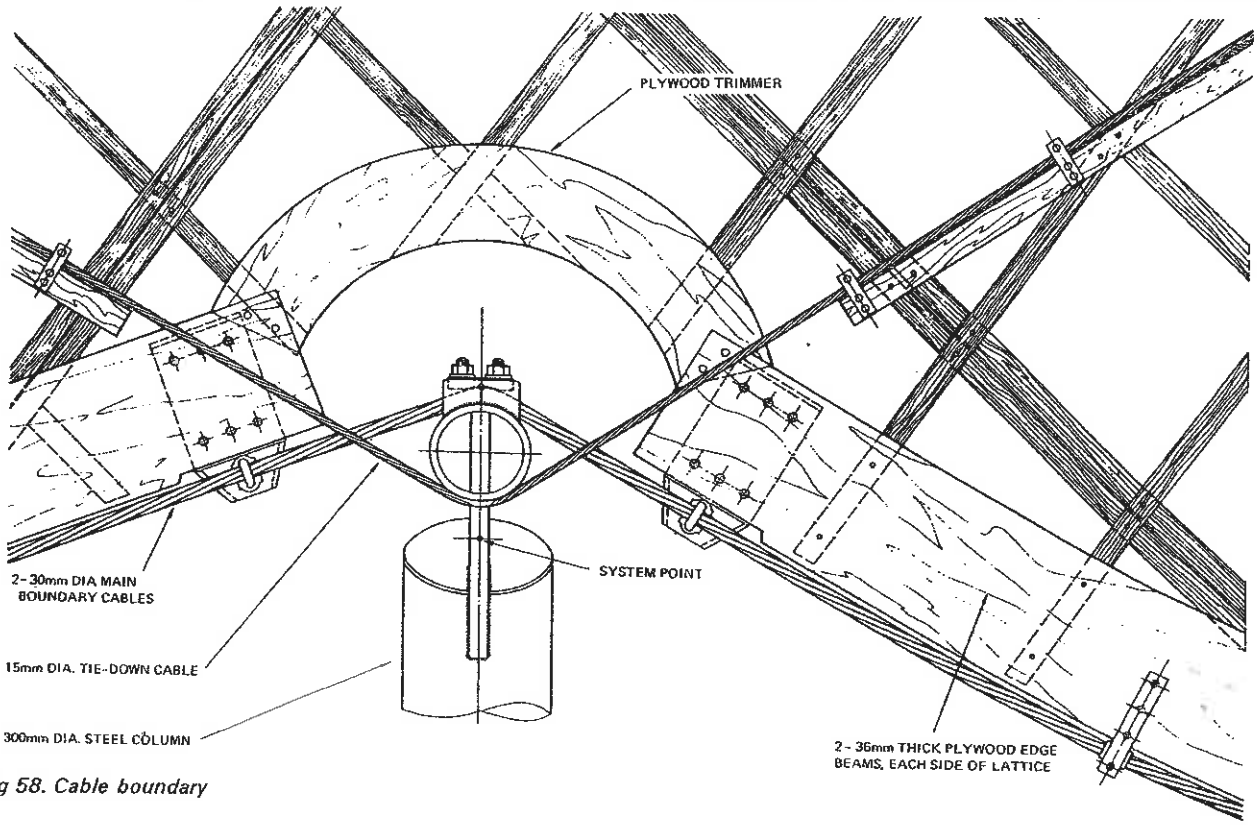

Fig 58. Cable boundary

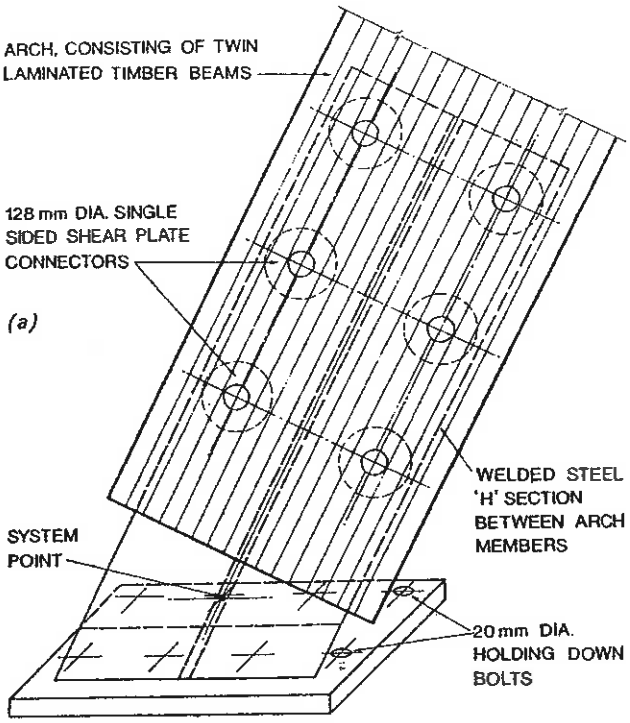

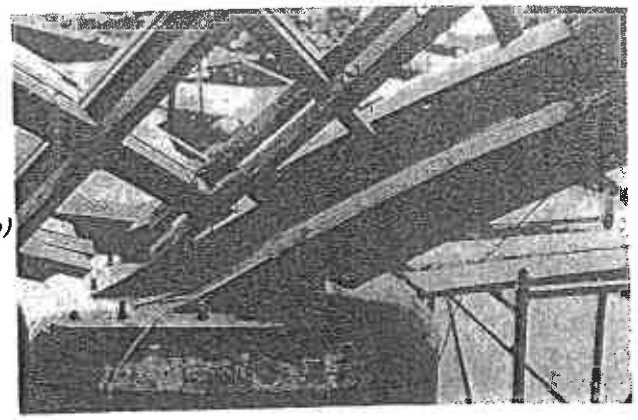

Fig 59(a) and (b). Arch foot point

board and then connecting the board to the cable. (See Fig 58). This system was chosen as more than one bolt was required to transfer the forces from the laths. In addition, the plywood would give some bending stiffness which would help cope with the difference between the lath force distribution and the cable profile. It would also provide the out-of-plane stiffness which the system required and could be used to define the cable profile.

At the columns the cables were brought together. This was done partly to overcome problems with the angle of the column head and partly to provide resistance to out of plane shear forces.

Arches

As with the beams, the arches were designed in laminated timber 60 × 500 mm on either side of the grid. Again the geometry was a problem because the arches had to lie flat on the surface of the shell. It was possible to make the arch for the Multihalle in laminated timber but all the other arches twisted so much that they had to be laminated from thin ply which was cut to the developed surface. Once again the engineers found themselves writing geometrical programs to produce the fabrication drawings.

The arches had to be connected to concrete bases using special steel brackets. The laminated timber was connected to parallel steel plates which fitted between the two layers with timber connectors and these steel plates were welded to a horizontal plate which was held down with bolts to the concrete. (See Fig 59). Drawings were prepared which gave cutting dimensions of the plates so that when assembled, the plates would be in the same plane as the arches. Achieving the necessary standard of accuracy proved to be very difficult as the same points had to be used for both the arch development program and for the plate angles. Point *E* of arch *A* proved to be the most difficult as at this point the arch, the valley beam and the boundary of the Banana all met. There were many possible sources of error and three of them were found by experience.

Issue of drawings

The drawings which were finally prepared for the beams and arches were fully dimensioned so that the contractor could fabricate directly from them. At the start it was believed that this work was to be done by the contractor and it was not allowed for in the programme. The difficulties involved in the geometrical calculations were also underestimated and this had a further delaying effect. In spite of this, as can be seen in the progress chart (Fig 16), the drawings were just issued in time for construction as the concrete work was in delay.

As the contractor was not involved in preparing the drawings he did not fully understand the system of defining the geometry and this led to some errors. Producing such drawings is a process of communicating the construction requirements to the contractor who must understand them in order to build from them. In the authors' view this communication is more satisfactorily achieved if the fabrication drawings are prepared by the contractor and checked by the engineers.

ERECTION

Principles

The lattice shell system can be thought of as construction technique which is related to the form finding process of using hanging chain nets. During erection the laths which have been laid out flat are lifted into shape, then fixed at the boundaries and the node bolts tightened. For a single layer lattice such as those built at Essen and Montreal, the stiffness of the lattice during erection is almost the same as that of the finished structure and so the shell can be expected to stand as soon as the boundaries are fixed. It can also be expected to adjust its shape so that the strain energy of the bent laths is minimized. This means that bumps induced in the surface by the initial lifting process will be re-distributed.

With double layer shells, stiffness is added by tightening the node bolts so that the two layers act compositely and by installing the ties. In its unbolted condition the collapse load of the Multihalle is about equal to its self-weight, so after just fixing the laths at the boundaries the shell would not take up a stable shape. In addition, during lifting the laths deflect in bending between the lifting points and unless a large number is used the shape will not be good.

Crane systems and model simulation

The lattice shells built at Essen and Montreal had been lifted into shape with cranes. In the tender documents for Mannheim a similar system of lifting had been proposed and the contractor had priced for this. As the boundary details were developed, the engineers became concerned about this system of lifting. Realizing that very large cranes would be required to lift the grid at that radius and that these would have to remain on site for a few weeks until bolting up was completed, they asked the contractor to consider alternatives in terms of scaffold towers and jacks. The contractors felt that cranes would be quicker and safer and were reluctant to change from that which they had priced.

The engineers were therefore asked to find suitable lifting points which would fit the cranes and spreaders and which would produce a good shape for the shell. It appeared to be very

difficult to calculate the effect of the lifting points on the shape, and it was thought that a model which scaled the weight and stiffness of the two unbolted single layer grids would provide the most information and would allow for experimenting with different spreader arrangements.

A suitable woven wire mesh was found in a builders' merchants, the weight and stiffness of which was found by measurement and proved by measuring the period of a vibrating wire. Applying scale factors indicated that if the weight of the mesh was increased to five times the self weight the properties would be correctly scaled for a 1:60 model. 10 mm lead fishing weights were used to achieve the necessary increase in weight and a model was made from the Linkwitz cutting pattern (Fig 60). This model was taken to Mannheim and was used in discussions with the contractor to find the best lifting arrangement and to define with him the step by step sequence of operations. The crane loads were measured by weighing the model with a small spring balance. This work demonstrated that it was necessary to have cranes which could lift 16 tonnef at 40 m radius.

In addition to the main cranes, extra supports around the edges were required to get the correct shape in this area and the contractor proposed to use 10 m timber poles and winches for these. The contractor was now faced with having four 200 tonne cranes on site for about three weeks at an alarming cost. At this time, when the Multihalle lattice was half laid out they investigated a proprietary system of scaffolding which formed towers 1 m square, stable to 17 m height, and which had sections 1·33 m, and 1·00 m and 0·33 m in height. They proposed to use these instead of the cranes and to push up the lattice from below (Fig 61).

Lifting with scaffolding towers

This change involved a complete redesign of the lifting points. With the support point now below there was a basic instability of both the towers and the spreaders which had to be taken into account. An H-shaped system of spreader beams was proposed, supported at the centre, which had to be designed to transmit forces in the plane of the lattice as well as normal forces. The connection between the main beam of the spreader and the scaffold towers had to accommodate rotations in any direction. A ball joint was ideal and the contractor found a suitable ball from a caravan tow attachment and fabricated a socket from tube and plate. The joint between the main spreader beam and the two secondaries had to be designed for rotations about a normal axis to allow for the angle change of the lattice. The shear at this point and at the centre point was transmitted by Bulldog shear connectors.

To minimize the cost of scaffolding, it was necessary to have the widest possible spacing between the towers but this was obviously dependent on the bending strength of the lattice and the deflection between the towers. The spacing could be increased if larger spreaders were used but these would become unmanageable if too large. A tower spacing of 9 m was selected with 3·5 × 2·5 m timber spreaders (Fig 62). In designing this system the engineers worked in close collaboration with the contractors to ensure that the system was stable, giving design assistance where necessary. The first tower and spreader was installed three weeks after the system was proposed.

Lifting

At first the contractors intended to jack up the towers using lorry jacks, each tower being jacked up 33 cm at a time and a new section added. As the towers were lifted some of them had to be moved horizontally to allow for the change of shape of the lattice. This gave the contractor the idea of using fork lift trucks which would be heavy enough to control the base of the towers without restraint and which could carry out both lifting and moving quickly (Fig 63). During the lifting and traversing process the lattice was anchored with cables at

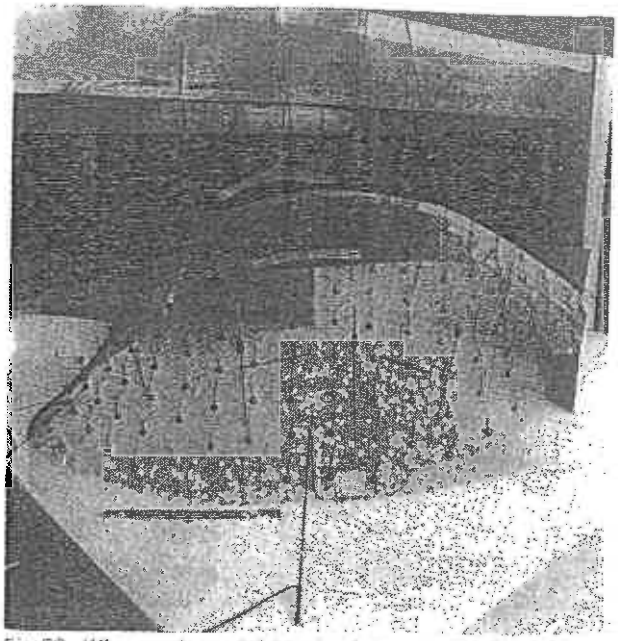

Fig 60. Wire mesh model to simulate self weight deformations of unbolted lattice

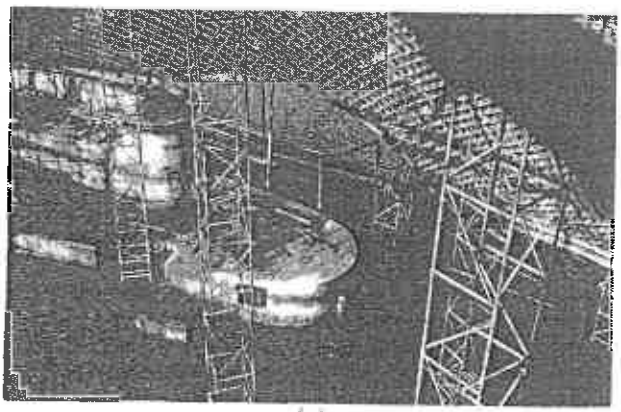

(a)

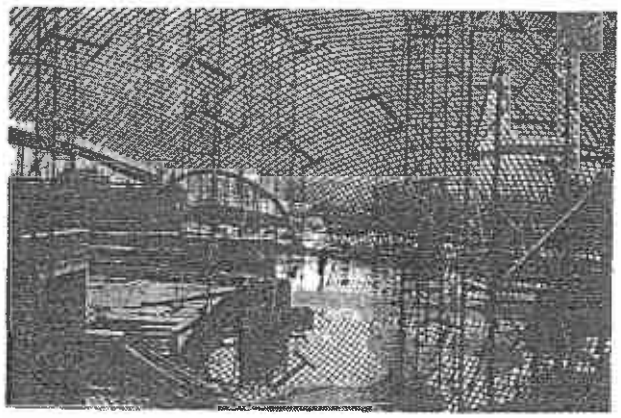

Fig 61(a) and (b). Scaffold towers *(b)*

certain key points to prevent collapse. The towers were stable to a height of about 17 m so the ones that were higher than this had additional bracing cables to ensure their stability. The towers which were on the raised areas inaccessible to the fork lift truck were lifted using a specially-designed frame.

Shape adjustment and bolting up

When all the towers of a shell were close to the right height and position, there was about 200 mm deflection between the tower points and the centre points and as the tower spacing was close to the buckling wavelength of the dome

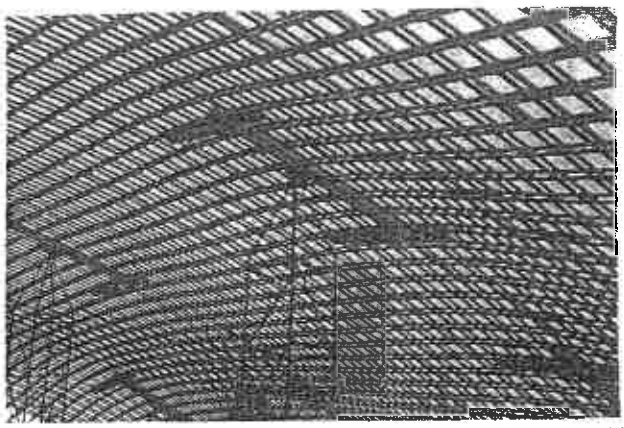

Fig 62. Detail of spreader and ball joint at top of scaffold towers

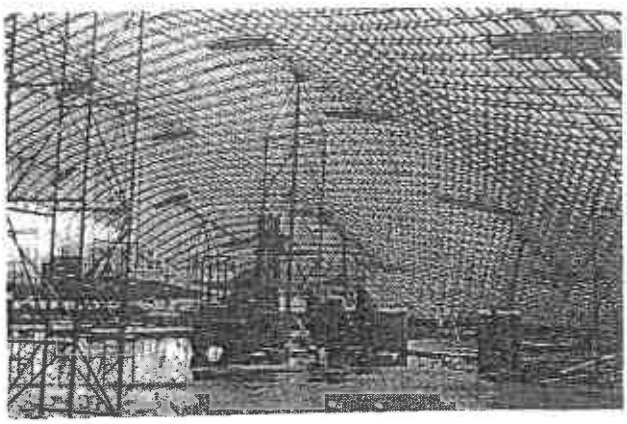

Fig 63. Fork lift truck being used to raise a tower

it was important to reduce this error. Hand calculations indicated that a tolerance from the Linkwitz shape of ±50 mm over this length would be acceptable. It was therefore necessary to try bolting up the middle strips between the towers and then adjusting the tower heights to eliminate the bumps.

The properties of the square grid of laths is such that with the boundaries in their correct positions it is only necessary to determine the heights of the node points for these to be in a unique position. Additional checks can be made on the horizontal positions and on selected diagonal lengths. However, using these methods together would result in redundant information and could lead to confusion when adjusting the shape of the shell. The heights of the nodes were therefore taken as the controlling dimension with checks on the horizontal position of a few central points and on some diagonal lengths near the boundary. The curvature of the laths was checked for smoothness by eye.

For the Multihalle, two middle strips on a NE to SW diameter across the large dome were adjusted and bolted up first. The towers between these strips were then lowered so that the bumps were smoothed out and these were bolted up. In lowering the towers the strips already bolted up tended to move, and to eliminate the bumps it was often necessary to lower the towers more than was required, and to rejack the shell into the correct shape after the area was tightened. It is important to work out from the centre to the boundary which is bolted up only when the whole strip is correct, otherwise errors could be built in.

After this first diameter strip was fixed, work proceeded on strips at right angles running in a NW direction but always working from the centre outwards. When the whole of the NE half was fixed, work progressed southwards towards the Biergarten and the area over the walkways.

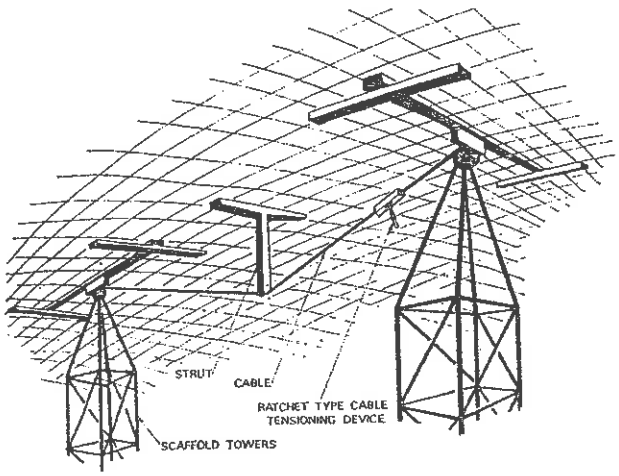

Fig 64. Diagram of flying strut used to eliminate low areas

Where difficulties were experienced with flat areas between the towers or with bumps at the towers which would not come out, then flying struts were introduced, supported on cables stretched between the towers (Fig 64), which could apply an additional load to the shell.

It was anticipated that there would be difficulties with bringing the Biergarten area of the shell into its correct shape where it slopes outwards at the beams. As described already, the slope of the beams in this area had been adjusted from that predicted by the Linkwitz coordinates, and it was found on site that the shell could be pulled into this shape without problems and it fitted the boundary well for most of its length. At one column where the change in angle was largest, it was necessary to cut the laths and allow them to separate so that the grid could be pulled into the corner.

At the beam and arch boundaries, the laths were first bolted to the inner member with a few bolts; the bolt holes were then drilled through the laths and inner member. The outer member was then fitted into place and connected at the ends. The bolt holes were drilled through from inside and the bolts fitted and tightened.

When the erection system was considered in the design stage it was thought that there would be snags with the laths not slipping smoothly or with the bolts jamming in the holes. This latter problem did occur if the slotted holes had not been correctly set out, but apart from that the lifting proceeded smoothly and quietly, and by using the scaffold towers the lifting process was slow enough to allow time for these points to be checked. The lifting and bending to shape of the single layer areas proved more troublesome. Because of the tight curvature more breakages were experienced and with fewer laths to redistribute the load these tended to spread.

Load test

At a fairly early date in the design process the proof engineer had stated that he felt that it was necessary to proof load the structure to satisfy all parties that it would carry the snow loads and it was agreed that building permission would be dependant on this test. As the structure had to be finished before the test load was applied, a formula had to be worked out whereby the permission to start erection could be given on the basis of the engineering calculations.

Ove Arup & Partners maintained that the load testing was unnecessary and that it should be possible to verify the assumptions made in the calculations on the basis of the work carried out. However, the political benefits were obvious and it was agreed that it would be interesting to apply this ultimate check on the computer calculations. Accordingly an area for loading of about 500 m² on the Multihalle was selected by the proof engineer who requested that it should be loaded to 1·7 times the design load. This meant that a load of 40 kgf/m², equal to 2·5 times the imposed load, had to be applied.

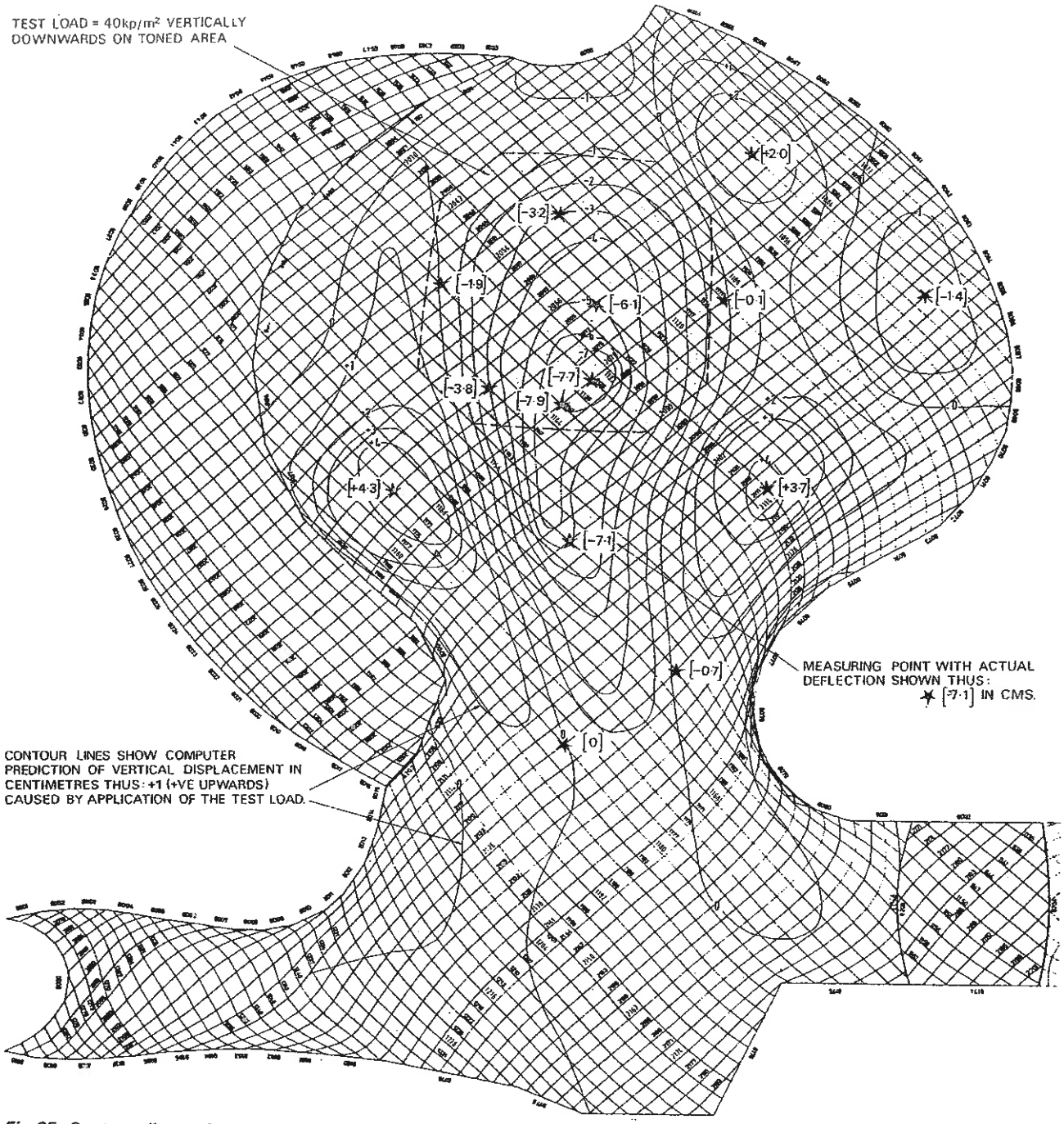

Fig 65. Contour lines of vertical deflections predicted by computer for test load case with measured deflections superimposed

The non-linear program was run with this load case and the resulting deflections were plotted (Fig 65). The results were examined to check for any areas of over stress which could be damaged.

A system for applying the load was devised (Fig 66) using dustbins borrowed from the city of Mannheim, filled with water so that each weighed 90 kg. These were to be hung from every ninth node using iron wire. The dustbins would be placed on concrete blocks and the load would then be applied by lifting them and removing the blocks. The load was to be applied in four stages, measurements of vertical deflections being made at 14 selected points using hanging weights.

Additional measurements were to be made by Professor Otto and the staff of the IL, using double exposure photographic techniques, and by the staff of the IAGB, using a theodolite fitted with an infra-red tacheometer measuring to prisms attached to the shell.

It seemed that the load test was going to be a major event with a large number of visitors from the city present as well as most of the people who had worked on the structure, and so it was thought to be prudent to carry out a preliminary test with a quarter of the load. This enabled the various systems and procedures to be tested, and boundaries checked, and had the addtional advantage of taking up some of the slack in the structure. The results of this preliminary test looked promising.

In the full load test the resulting deflections, plotted in Fig 65, agreed very well with those predicted by the computer program. The loading and unloading curves for the central point are plotted in Fig 67 as well as the deflection for the linear cycle of the computer program. The non-linear effects and the change in stiffness as the load is applied can be clearly seen from this diagram.

It is interesting to note that the timber was very wet at the time of testing and so the value of Young's Modulus would be about 10 per cent low and the deflections should have been

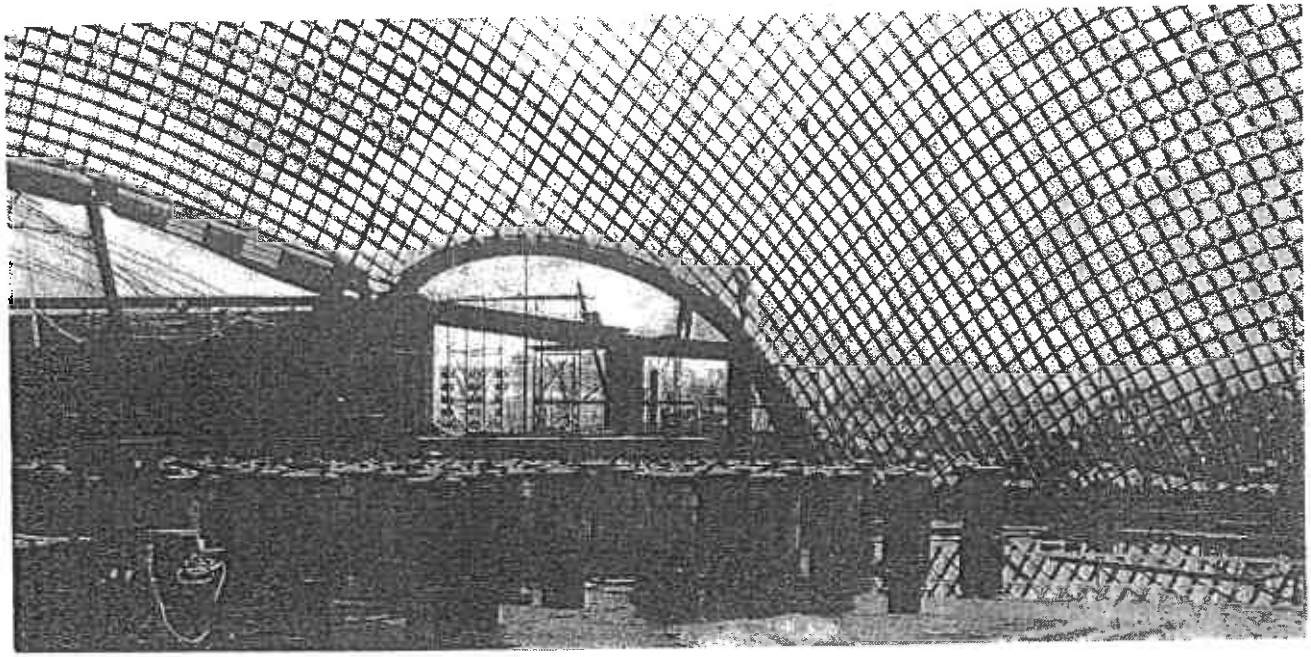

Fig 66. Test loading in progress

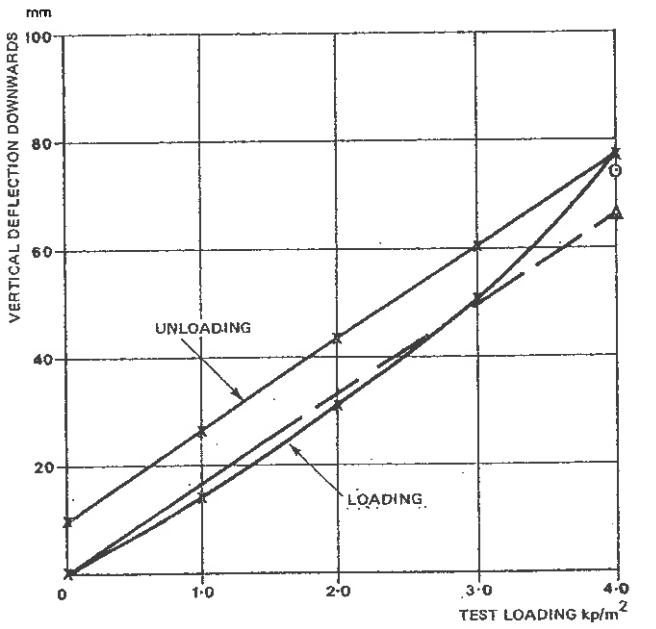

Fig 67. Loading and unloading curves for central point

correspondingly high. The agreement of the measured deflections with those computed confirms the statement made in the section on *Safety factors*, page 124, that the assumptions made in the mathematical modelling were pessimistic.

Conclusions

The authors feel that this is an extremely interesting form of construction though probably more economic for shorter spans with simpler boundaries. Not only is such a structure easy to erect but it enables almost any plan shape to be simply covered.

Regarding the problems of working in Germany, the authors would like to stress the lack of nationalistic prejudices in those they worked with. They wonder if a German firm working in Britain would have been welcomed and helped quite so openly. There appears to be a harder interface in Germany between architects and their structural engineers and the latter have more status in the public's eye, more power with the clients and often less integration in the design development. Professional practices are smaller and headed by strong individuals. At first the authors were slightly disconcerted by this individuality though it turned out to be more apparent than real. The practices are not as centralized as in Britain and if this had not turned out to be a very specialized building it would have been entirely designed by Mannheim engineers.

There was no evidence that the workers on site worked any harder than they do in England but perhaps due to the lack of centralization in the country and the absence of quantity surveyors, there was a much more direct approach to both design and contract management. In the field of materials supply it was much simpler to get deliveries than it ever appears to be in Britain and one seemed able to get special parts or special pieces of steelwork made, galvanized and delivered in a short time.

Unlike some excursions abroad, this has been almost wholly delightful, especially since the authors were never suspected of having local interest and their advice was probably taken as being entirely unbiased, because it was thought that they stood to lose the most or gain the least according to the success of the building.

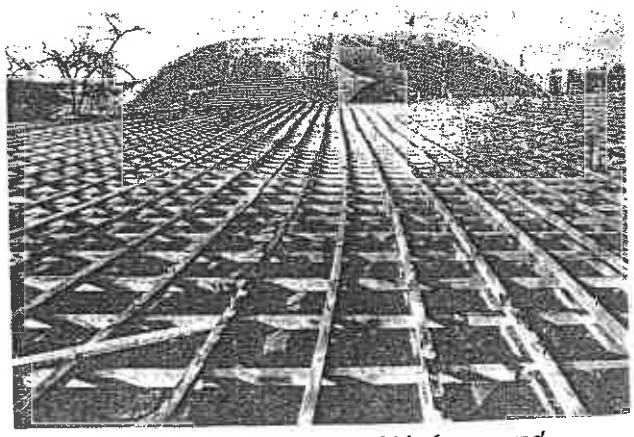

Fig 68. Multihalle with restaurant grid in foreground

The authors would especially like to thank the architects—Carlfried Mutschler, Joachim Langner and Winfried Langner; the roof consultants—Professor Frei Otto and Ewald Bubner; their collaborating engineer—H. Spaeh; the proof engineer—Professor Wenzel and his associates, K. Oertling and B. Frese; Professor K. Linkwitz and H. D. Preuss, who carried out the photogrammetry; the timber contractors—Firma W. Poppensieker; and the engineer in charge of the work on site—W. Toll.

In presenting such a paper, the authors represent the efforts of many. All these they thank but they particularly wish to acknowledge their colleagues:

John Howell: Aerodynamics and timber testing
Chris Williams: Mathematical interpretations and justifications; analysis of the Multihalle
Joachim Schock: Analysis of restaurant
Rod Macdonald: Geometry of boundaries
Frank Pyle: Detailing and production of drawings
Michael Dickson: Site planning
Terry Ealey: Site control
Robert Pearson: Advice with analysis and checking of calculations

They also thank Dr. John Simper of the BHRA for assistance with wind tunnel testing, and Harold Burgess and George Weller of TRADA for their help with timber testing.

References

1. Rankine, W. J. MacQuorn. *A Manual of Applied Mechanics*, 1858. In fact, this property of using the analogy of inverted chains to analyse arches was first put forward by Phillipe de la Hire in 1695.
2. Otto, Frei. *Tensile Structures*, Vols. 1 & 2, MIT Press, 1967.
3. Sweeney, J. J. and Sert, J. L. *Antoni Gaudi*, Architectural Press, 1970.
4. Roland, Conrad. *The Work of Frei Otto*, Longman, 1970. This gives a description of both the Essen and the Berkeley lattice shells.
5. 'Report on the German Pavilion for the Montreal Expo' 1967' (*unpublished*). *Institut für Leichte Flächentragwerke.*
6. 'IL 10, A Report on Gridshells' (to be published shortly), *Institut für Leichte Flächentragwerke.*
7. Wright, D. T. 'Membrane forces and buckling in reticulated shells', *Journal of the Structural Division, ASCE*, Vol. 91, No. ST 1, February 1965.
8. 'Non-linear static analysis of space frames, space trusses and plane grids', *Electronic Calculus Inc. Program 603.*
9. For description of *Institut für Anwendungen der Geodäsie im Bauwesen* work, see paper 'Analytical form finding and analysis of prestressed cable networks', *International Conference on Tension Roof Structures PCL*, April 1974. Also references quoted at the end.
10. Gumbel, E. J. *Statistics of extremes*, Columbia University Press, 1967. See also Davenport, A. G. 'The application of statistical concepts to the wind loading of structures', *Proc. ICE*, Vol. 19, Paper 6480, 1961.
11. Anon. 'Wind in Western Europe', *Laboratoria Nacional de Engenharia Civil*, Lisbon, 1963.
12. Several Authors. 'Wind effects on buildings and structures', *Symposium 1b, The National Physical Laboratory*, HMSO, June 1963. See paper no. 1 by C. Scruton and paper no. 21 by R. E. Whitbread.
13. *Handbook of Soft Woods*, HMSO, 1960.
14. *Wood Handbook No. 72*, US Department of Agriculture, US Government Printing Office, 1955.
15. Kollmann, F. P. and Côte, W. A. *The Principles of Wood Science and Technology—Solid Wood.*
16. 'Bulletin No. 50—The strength properties of timber', *Ministry of Technology, Forest Products Research*, HMSO, 1969.
17. Sunley, J. G. 'Strength properties of Western hemlock', *Forest Products Research Laboratory*, May 1959.
18. Booth, L. G. and Reece, P. O. *The structural use of timber*, Spon Ltd, London, 1967.
19. Buckingham, E. 'On physically similar systems', *Physical Review*, 1914.
20. Tezcan, S. S. and Ovunc, G. 'An iteration method for the non-linear buckling of framed structures', chapter 45 of *The International Conference on Space Structures, University of Surrey*, September, 1966, ed. by R. M. Davies, Blackwell Scientific Publications, 1967.
21. Tezcan, S. S. and Mahapatra, B. C. 'Tangent stiffness matrix for space frame members', *Journal of the Structural Division, ASCE*, Vol. 95, No. ST 6, June 1969.
22. Horne, M. R., and Merchant, W. *The Stability of Frames*, Pergamon Press, 1965.
23. See 'Report of Commissioners into the use of iron in railway structures', 1853. Hodgkinson carried out a number of tests on columns and derived an empirical formula.
His work was used by Lewis Gordon to derive a better formula. See Rankine, W. J. MacQuorn, *A Manual of Applied Mechanics*, 1858.
24. Fidler, Professor Claxton. *Proc. ICE*, Vol. LXXXVI, 1886.
25. Mills, G. M. *Theory of Structures*, Macmillan, 1965.
26. 'General principles for the verification of the safety of structures'. *International Standard ISO 2394*, 1973.
27. 'Bulletin No. 41—The strength of nailed joints'. *Forest Products Research*, HMSO, 1957.